Stratigraphy, petrology, and geochemistry of the North Touak-Cape Dyer volcanic belt, and implications for the tectonic setting of the Paleoproterozoic Hoare Bay group, eastern Baffin Island

By
Rae Dawn Keim

A Thesis Submitted to the College of
Graduate Studies and Research
in Partial Fulfillment of the Requirements
for the Degree of Master of Science
in the Department of Geological Sciences
University of Saskatchewan
Saskatoon

PERMISSION TO USE

In presenting this thesis in partial fulfillment of the requirements for a Masters of Science (M. Sc.) degree from the University of Saskatchewan, I, Rae Keim, agree that the libraries of the University of Saskatchewan may make it freely available for inspection. I further agree that permission for the copying of this thesis in any manner, in whole or in part, for scholarly purposes may be granted by the professor who supervised my thesis work (Dr. Kevin Ansdell) or, in his absence, by the Head of the Department of Geological Sciences, or the Dean of the College of Graduate Studies and Research. It is understood that any copy or publication or use of this thesis or parts thereof for financial gain shall not be allowed without my written permission. It is also understood that due recognition shall be given to me and to the University of Saskatchewan in any use which may be made of any material in my thesis.

Requests for permission to copy or make use of the material in this thesis, in whole or in part, should be made to:

Department Head
Department of Geological Sciences
University of Saskatchewan
114 Science Place
Saskatoon, Saskatchewan
S7N 5E2

ABSTRACT

During the Geological Survey of Canada's Cumberland Peninsula Integrated Geoscience project a ~150km long NE-SW trending volcanic belt, now termed the North Touak-Cape Dyer volcanic belt, was mapped.

The volcanic rocks that comprise the belt are dominantly green weathering komatiitic rocks with some black weathering tholeiitic occurrences. Given the similar stratigraphic position, textures, mineralogy, and geochemical characteristics of the volcanic rocks throughout the belt they have been termed the Totnes Road formation, after the locality from which they were first described. The komatiitic rocks possess numerous unusual characteristics for ultramafic volcanic rocks including: fragmental textures, lack of spinifex texture, young eruption age (Paleoproterozoic), eruption through ancient continental crust, and enrichment in the HFSEs including the REEs. This places them in the uncommon and poorly understood sub-type of komatiites termed Karasjok-type komatiites. Given the ultramafic nature of the rocks and their within-plate geochemical signatures, a mantle plume is the most likely source of these rocks, with the komatiites being sourced from the hot plume axis and the tholeiites from the cooler plume head. Incorporation and melting of mantle enriched by the addition of subduction zone recycled, garnet-bearing eclogitic material, beneath thick lithosphere could cause the rocks geochemical enrichment.

Stratigraphically overlying the Totnes Road formation is a variety of chemical sedimentary rocks including chert, sulphide and silicate facies iron formation, and sulphide-rich boulders. Given their consistent stratigraphic position and parallel REE patterns, these rocks have been interpreted as a co-genetic suite and are grouped under the Clephane Bay formation, after a locality that exposes a spectacular section of the chemical rocks. The variety of lithologies is believed to be due to mixing of hydrothermal and detrital inputs during deposition within an anoxic basin.

Regional correlations in the area are tentative due to the lack of available geochronological and geochemical data. Mafic-ultramafic volcanic occurrences to both the north and the south of the Cumberland Peninsula show remarkably similar geochemical characteristics to the Totnes Road formation. Thus it is possible that one plume was the source for numerous volcanic occurrences within in the region but more detailed study is required to prove or disprove this possibility.

ACKNOWLEDGEMENTS

First of all I could like to thank my family and friends for their support throughout this project. Being able to go to my parents' house for a home cooked meal after long days in front of the computer was lovely. A special thank-you must go out to Matthew White for putting up with numerous rants and for helping me prepare many of my figures in Matlab.

To my two amazing CPIG bosses, Mary Sanborn-Barrie and Mike Young, I would like to extend a huge thank-you. I learned an incredible amount under your tutelage and gained the most valuable experience I can imagine. Many of the things you have taught me will stay with me my entire career and for that I am eternally in your debt. Your comments and suggestions with regards to my thesis have helped to shape it and mold it into something I can be proud of.

My supervisor, Kevin Ansell, also deserves a big thank-you. Being able to walk into your office at any time, with any question or concern was truly appreciated. Your patience, guidance, and support were a huge part of keeping me calm and working towards an end goal. Your many, many edits of my thesis, posters, papers (past and future) are greatly valued.

For all of their support and discussions, both in and out of the field, I would like to thank Joe Whalen, Dave Lentz, John Percival, Marc St-Onge, Don James, Nicole Rayner, Natasha Wodicka, Brett Hamilton, and Carl Nagy. Greg Dobbelsteyn, Norm Kopalie, and the entirety of the CPIG crew were an astounding crew to work with and provided necessary and valuable assistance in the field.

My other committee members, Drs. Yuanming Pan, and Kyle Larson, were always willing to discuss metamorphism, alteration, and structure with me. Thank-you very much for your time and for sharing your knowledge.

Funding for this project was provided through Natural Resources Canada's Geo-mapping for Energy and Minerals (GEM) program, a NSERC Discovery Grant to K. Ansdell, and a University of Saskatchewan Graduate Scholarship and NSERC PGS-M to R. Keim. Blaine Novakovski, Tom Bonli, and Tim Prokopiuk in the Department of Geological Sciences at the University of Saskatchewan are thanked for thin section preparation, microprobe analysis, and for geological discussions, respectively.

TABLE OF CONTENTS

Chapter 4

Tectonic setting, petrogenesis, and regional correlations of the Totnes Road formation and Clephane Bay formation, Cumberland Peninsula, Baffin Island

Chapter 5

Refining the classification of komatiitic rocks using constraints from the Totnes Road formation, Cumberland Peninsula, eastern Baffin Island

Chapter 6

Conclusions

LIST OF TABLES

LIST OF FIGURES

CHAPTER 1

INTRODUCTION AND BACKGROUND

1.1 Purpose and Objectives

Baffin Island's eastern Cumberland Peninsula represents 30,000 km^2 of rugged frontier Arctic territory (Figure 1-1a and 1-1b). The Cumberland Peninsula Integrated Geoscience project (CPIG) was launched in 2008 under the federal government's Geo-mapping for Energy and Minerals (GEM) initiative in order to address the significant geoscience knowledge gap that existed due to limited and out-dated mapping (Jackson and Taylor 1972) for this extensive region of Baffin Island. The ultimate goals of this multidisciplinary geoscience project are to produce updated and detailed geological maps of the region, to assess the region's potential for gold and base metals, and to gain an understanding of its geologic history. The first goal was accomplished through acquisition of high-resolution aeromagnetic data (Coyle, 2009) and systematic surficial (Dyke 3 maps published, 3 should be out this month; Gammon et al., 2011) and bedrock (Sanborn-Barrie, 2010; Sanborn-Barrie et al. 2011a,b,c; Sanborn-Barrie and Young 2012a, b,c; Sanborn-Barrie et al., 2012a,b) mapping across the peninsula during the summers of 2009 and 2010 (Figure 1-2). Research at the Geological Survey of Canada, University of Saskatchewan (this M. Sc. Thesis and a B.Sc. project by Cam Mackay), Dalhousie University, and the University of Calgary will contribute to refining geological relationships and provide insight into the peninsula's metallogenic potential and geological history.

The geology of eastern Baffin Island, particularly the Cumberland Peninsula, is relatively poorly understood when compared to southwestern and central Baffin Island, which were the focus of recent mapping projects (St. Onge et al., 2009; Sanborn-Barrie et al., 2008, Scott et al., 2002). Prior to this GEM initiative, the bedrock geology of Cumberland Peninsula had been mapped at a reconnaissance (1:1 million) scale (Jackson 1971) and only a regional compilation of that mapping was published (St-Onge et al., 2006a). Jackson and Taylor (1972) described much of Cumberland Peninsula as a "thick succession of intensely deformed, layered sedimentary rocks and intermediate to basic metavolcanic rock", possibly of Proterozoic (Aphebian) age, and designated these rocks the Hoare Bay group (Jackson, 1971). With only this

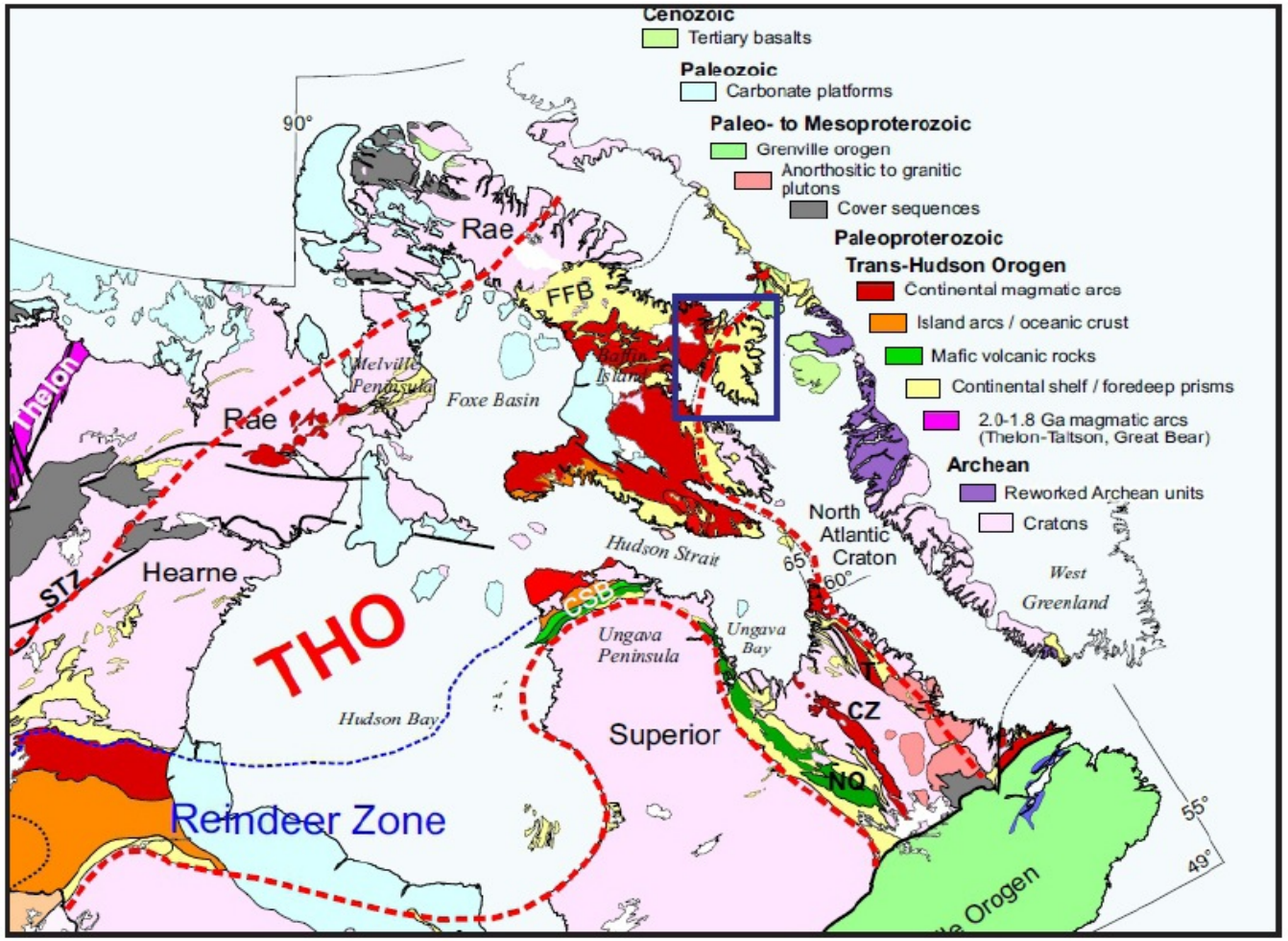

Figure 1-1a. Geological map of the northern part of Laurentia in Canada highlighting the extent of the Trans-Hudson Orogen (THO) (map from Corrigan et al., 2009). In this compilation map, which predates the initiation of the CPIG project, the Cumberland Peninsula is underlain by Paleoproterozoic continental shelf and foredeep rocks and continental magmatic arc rocks. Important abbreviations: FFB – Foxe Fold Belt, CSB – Cape Smith Belt, STZ – Snowbird Tectonic Zone, SK – Sask Craton, CZ – Core Zone, NQ – New Quebec Orogen.

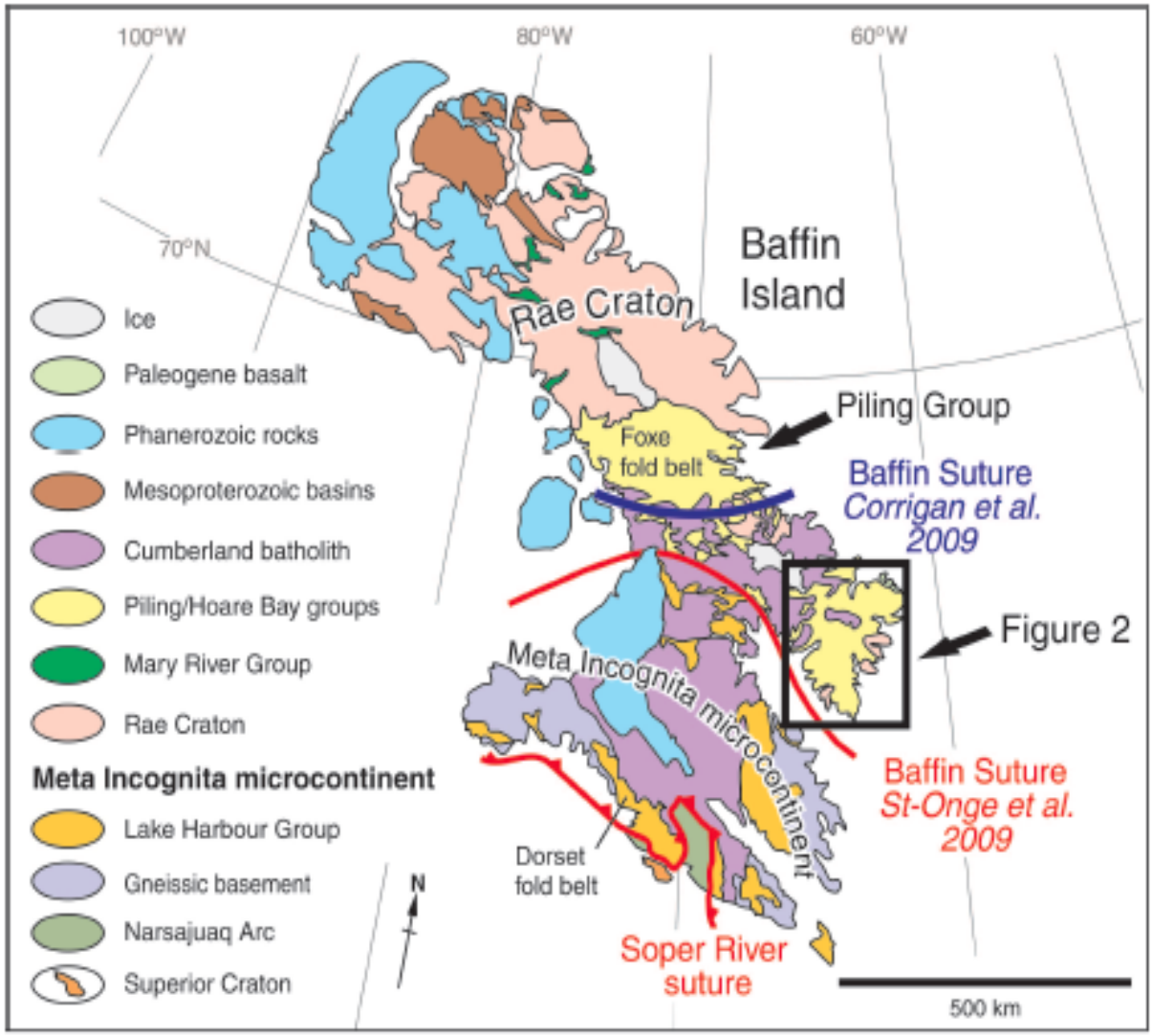

Figure 1-1b. Geological map of Baffin Island showing location of Piling, Hoare Bay, and Lake Harbour Groups. The possible locations of the Baffin Suture according to Corrigan et al., (2009) and St-Onge et al., (2009) are shown. The black box outlines the area shown in Figure 2, which is the location of the Cumberland Peninsula Integrated Geoscience (CPIG) project. Map modified from St-Onge et al., (2009).

reconnaissance-scale data available, the regional geologic context of Cumberland Peninsula has remained elusive. As a result of this description, the peninsula was considered correlative with the Paleoproterozoic Piling Group of central Baffin Island (St-Onge et al. 2006). Mapping in 2009 and 2010 along with supporting isotopic and geochronologic data revealed that, in fact, the Cumberland Peninsula exposes Archean plutonic basement with strands of Archean supracrustal rocks, and that the character, extent and relationships of the peninsula's cover sequence, the Hoare Bay group, needed to be established. The large knowledge gap regarding the Hoare Bay group needed to be filled before the Cumberland Peninsula region could be placed in an appropriate regional context with regards to the other tectonic elements of the Trans-Hudson Orogen and adjacent Archean cratons.

In 2009, an isolated exposure of fragmental, green-weathering volcanic rocks, located on a peninsula on the shore of Totnes Road Fiord was the focus of B.Sc. research by the author (Keim 2011; Keim et al., 2011), which established:

1. an association of volcanic and chemical sedimentary rocks at the Totnes Road Fiord locality.
2. that the green-weathering volcanic rocks consisted of komatiites and komatiitic basalts with unusual enrichment in Ti and other high-field-strength elements (HFSE), not commonly found in other komatiite occurrences.
3. that a mantle plume was a contributing factor to the development of the Hoare Bay group.

In 2010, mapping established a belt of volcanic and chemical sedimentary rocks, discontinuously exposed for some 150km from north of Touak Fiord, though Totnes Road Fiord, to Cape Dyer (Figure 1-2). This volcano-chemical sedimentary sequence defines what is referred to herein as the North Touak-Cape Dyer volcanic belt. This important and diagnostic component of the dominantly clastic Hoare Bay group is the focus of this research, which aims to determine the architecture, geochemical affinity and tectonic setting of this part of the Cumberland Peninsula.

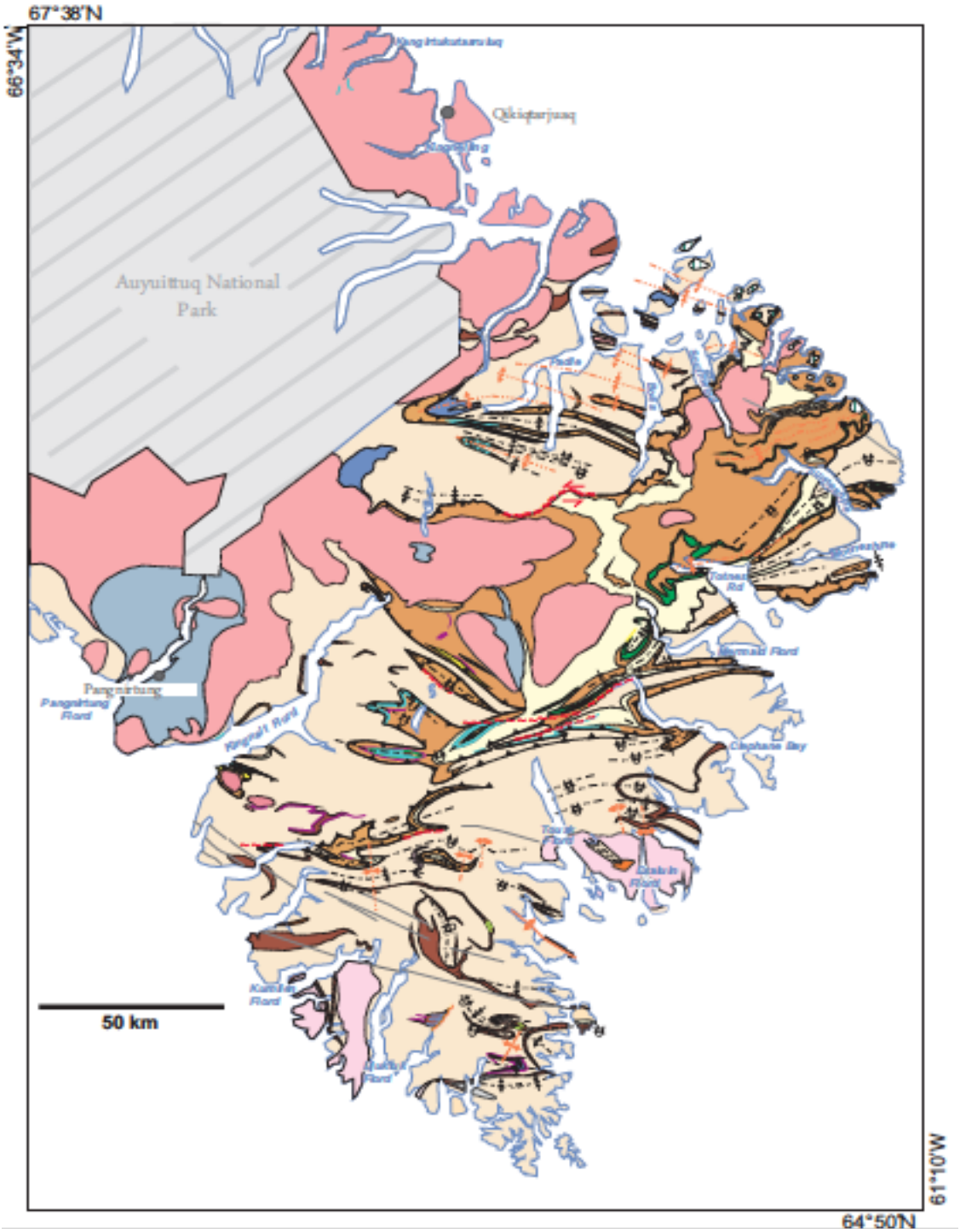

Figure 1-2 a). Map of the Cumberland Peninsula after bedrock mapping in the summers of 2009 and 2010. Note the occurrence of mafic-ultramafic volcanic rocks (green) in the central portion of the mapping area and small marble occurrences (light blue) to the west. Large black rectangle outlines the volcanic belt found on Cumberland Peninsula; small rectangles outline the areas covered during relevant foot traverses for the purpose of M.Sc.. research. Map annotated from Sanborn-Barrie et al., (personal communication).

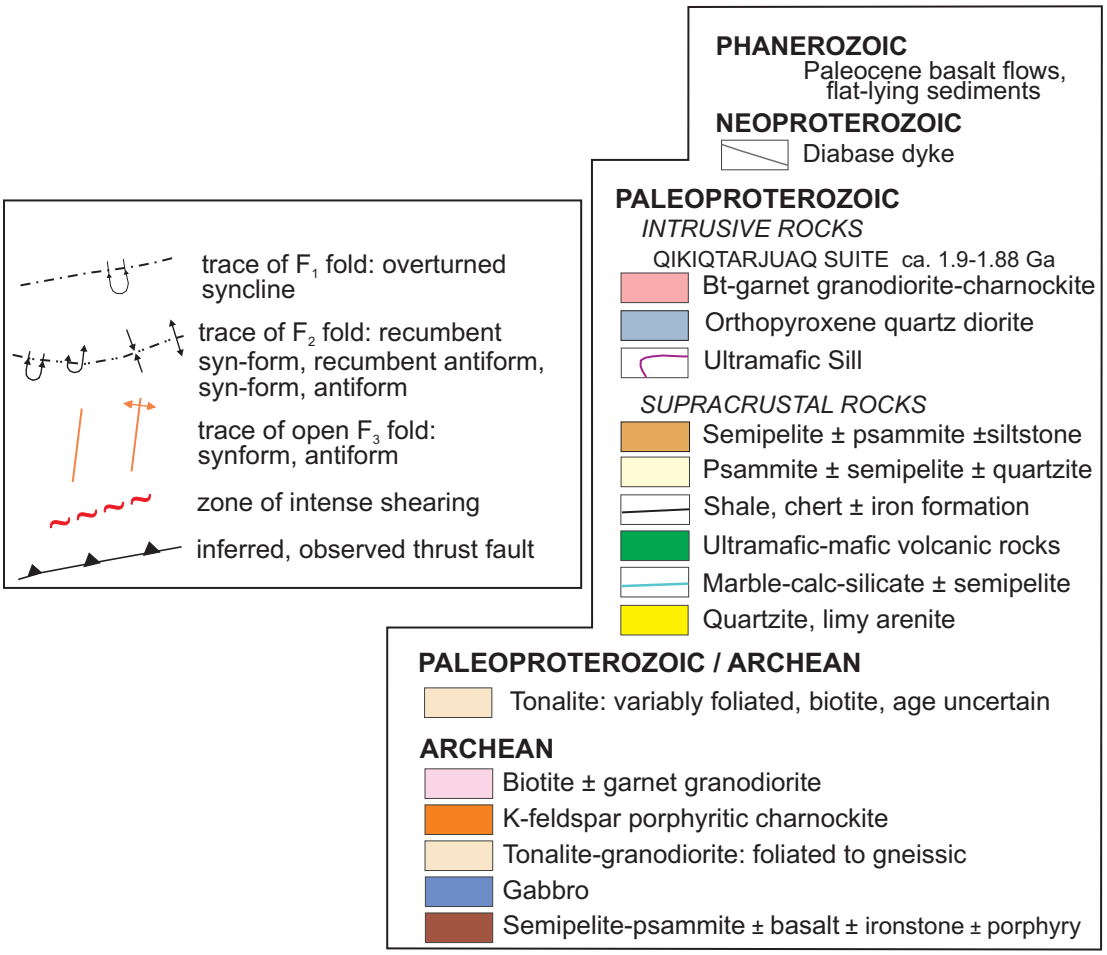

Figure 1-2 b). Lithologic and structural legend for above regional map of the Cumberland Peninsula (Figure 1-2a).

The principal objective of this research is to provide a description and initial interpretation of the North Touak-Cape Dyer volcanic belt in order to better define and understand the Hoare Bay group, an integral component to the overall CPIG project. Specific goals of this MSc research are as follows:

1. To further advance B.Sc. work done at the Totnes Road Fiord locality, and to broaden the scope of research to include other volcanic occurrences within the Hoare Bay group, in order to assess the continuity of the volcanic rocks found on the Cumberland Peninsula.

2. To expand research to include the chemical sedimentary rocks found associated with the volcanic rocks, to gain a better understanding of the architecture and development of the North Touak-Cape Dyer volcanic belt, and to assess the metallogenic potential of the belt.

3. To determine if formations can be designated for the above-mentioned lithologies to further advance the definition of the Hoare Bay group.

4. To determine the tectonic setting of the volcanic and chemical sedimentary rocks and use this new data in assessing the geologic history of the Cumberland Peninsula, in order to start filling in the significant geoscience knowledge gap for the area.

5. To utilize the increased geologic knowledge for the volcanic rocks of the North Touak-Cape Dyer volcanic belt to further regional correlations, which will help contribute to the understanding of the evolution of the eastern Trans-Hudson Orogen.

1.2 Methodology

The entirety of this project was based on fieldwork conducted in the summers of 2009 and 2010 when the author was employed by the Geological Survey of Canada as a junior and senior mapper, respectively. Detailed mapping and sampling specifically for this M.Sc. thesis was conducted at six localities throughout the volcanic belt. This was supplemented by grab

samples obtained during heli-traverses within the volcanic belt by other members of the CPIG mapping team. All information gathered in the field, including sample and photo locations, descriptions, stratigraphic relationships, and structural measurements were recorded on an air photo, in a notebook, and in a handheld electronic digital database. Entry of information in digital format in the field allowed data to be easily uploaded into a master ArcGIS database, to provide valuable spatial relationships. Field data was incorporated into a detailed geologic map and cross section of the Totnes Road Fiord locality, where the lithologies of the volcanic belt are best exposed, and also used to formulate stratigraphic columns for the six localities where detailed traverses were conducted. Thin sections were prepared for all lithologies in order to provide information on mineralogy and aid in classification. Geochemical analyses for major and trace elements were obtained for a suite of volcanic rocks (n=43), of which 12 analyses contributed to BSc research and are previously published (Keim et al., 2011), and chemical sedimentary rocks (n=15).

Collectively, the above-mentioned data allowed detailed descriptions and classifications for all lithologies, and guided interpretations regarding petrogenesis, tectonic setting, and regional correlations. These results are presented and discussed in the following chapters.

Chapter 2 is a detailed account of the petrology and proposed stratigraphy of the volcanic and chemical sedimentary rocks found throughout the North Touak-Cape Dyer volcanic belt. Special emphasis is placed on the Totnes Road Fiord locality, as this locality has received the most amount of mapping and has the greatest portion of samples taken. The Totnes Road Fiord information on the volcanic rocks has been published (Keim et al., 2011) but much of the data is also presented here for the sake of completeness and continuity.

Chapter 3 presents an in-depth analysis of the geochemical aspects of the volcanic and chemical sedimentary rocks throughout the length of the volcanic belt. Collectively, the data reveal that the unusual geochemical features of the Totnes Road Fiord locality volcanic rocks (Keim et al., 2011) are continuous throughout the North Touak-Cape Dyer volcanic belt. The ultimate goal of this chapter will be to determine if the available stratigraphic, petrologic, and

geochemical data allows for the designation of formation names for the two rock varieties discussed.

Chapter 4 presents a discussion on the petrogenesis and tectonic setting of the volcanic and chemical sedimentary rocks and how this new data relates back to the formation of the Hoare Bay group and the geologic history of the Cumberland Peninsula as a whole. This will lead into a discussion on possible regional correlations for the Hoare Bay group with a specific focus on the rocks of the North Touak-Cape Dyer volcanic belt.

Chapter 5 presents a discussion on the current classification system in place for Karasjok-type komatiites, an unusual subset of the komatiite family, given new data available from the Cumberland Peninsula. This chapter is written as a stand-alone chapter with the aim of its possible publication in a peer-reviewed journal. Therefore there is some overlap in the discussion of geochemical analyses occurs between Chapter 4 and Chapter 3.

Chapter 6 provides a succinct summary and the conclusions of this thesis.

CHAPTER 2

THE NORTH TOUAK-CAPE DYER VOLCANIC BELT OF THE CUMBERLAND PENINSULA, BAFFIN ISLAND: FIELD OBSERVATIONS, STRATIGRAPHY, AND PETROLOGY.

2.1 Introduction

The North Touak-Cape Dyer volcanic belt comprises green and black-weathering volcanic rocks, as well as a variety of chemical sedimentary rocks. The aim of this chapter and Chapter 3 is a regional analysis of the North Touak-Cape Dyer volcanic belt through field and petrologic descriptions of the rocks, assessment of the relationships between exposures of the volcanic and chemical sedimentary rocks (Chapter 2), and by geochemical classification and characterization (Chapter 3). The results will greatly enhance the understanding of the Hoare Bay Group and will help to place this supracrustal package in a regional tectonic context.

The initial analyses will focus on the Totnes Road Fiord locality, centrally located in the North Touak-Cape Dyer volcanic belt. The exposure and preservation at Totnes Road Fiord is superior to any other location on Cumberland Peninsula. Mapping at Totnes Road Fiord has revealed a spectacular section of fragmental ultramafic volcanic (Keim, 2010) and associated chemical sedimentary rocks. Descriptions of other occurrences of volcanic rocks and chemical sedimentary rocks within the North Touak-Cape Dyer volcanic belt will follow with the aim of determining if the unusual textural and chemical characteristics of the volcanic rocks at Totnes Road Fiord are continuous throughout the volcanic belt, and to determine if the association of chemical sedimentary rocks and volcanic rocks is a diagnostic stratigraphic horizon throughout the belt.

2.2 Regional Geology

The Cumberland Peninsula is situated between the Archean Rae Craton to the northwest and the Meta-Incognita micro-continent to the south (Figure 1-1b). It is thought that these two terranes collided during the Foxe Orogen, one of several collisional events that collectively

define the Trans-Hudson Orogen (St-Onge et al., 2006b). This collision is purported to occur between 1.88-1.865 Ga (St-Onge et al., 2006b) and to be demarcated by the Baffin Suture (Figure 1-1b). St. Onge et al. (2009) correlated the Hoare Bay group to central Baffin Island's Piling Group, a Paleoproterozoic supracrustal sequence deposited on the margin of the Rae craton, and thus placed the Baffin Suture to the south of Cumberland Peninsula. In contrast, Corrigan et al. (2009) suggested that the Hoare Bay group may not have been deposited on the Rae craton and tentatively placed the Baffin Suture to the north of the Cumberland Peninsula. One of the goals of the Cumberland Peninsula project is to assess regional stratigraphic correlations and provide insight into the tectonic significance of the Hoare Bay group.

In stark contrast to earlier reconnaissance mapping (Jackson 1971), systematic, 1:200,000-scale mapping during the present study revealed vast expanses of plutonic and lesser supracrustal rocks (Sanborn-Barrie et al., 2010; 2011*a,b,c*) determined to be of Archean age (Rayner et al., 2012; N. Wodicka 2010 unpublished data). Recent mapping also revealed that the Paleoproterozoic cover rocks of the Hoare Bay group are much more restricted than previously interpreted (Jackson and Taylor, 1972; St-Onge et al., 2006) and mainly occur in central and northeastern Cumberland Peninsula. The exact nature of the contact between the Archean basement rocks and the Paleoproterozoic cover sequence is debatable as it not known whether the Hoare Bay group is autochthonous or allochthonous with regards to the Archean basement. Surrounding the area of the contact both the cover and basement rocks are strongly deformed with abundant shear zones and mylonites and the basement-cover contact is tectonically transposed into parallelism. The presence of minor marble and quartzite near the basement-cover contact (central portion of Cumberland Peninsula), and thick successions of clastic rocks with associated volcanic rocks and chemical sedimentary rocks (NE portion of Cumberland Peninsula), in the interpreted central to upper portion of the package, presents a distribution suggestive of a shallow-shelf depositional environment transitioning to a deeper basinal environment through time (Figure 1-2).

The North Touak – Cape Dyer volcanic belt is a deformed, discontinuous entity trending NE-SW for ~150km and rarely reaching thickness' greater than 2.5km. Complex map patterns,

especially to the west of Totnes Road Fiord, are a product of topography combined with regional folding.

The Cumberland Peninsula has experienced at least two penetrative deformation events. Throughout the Cumberland Peninsula, rocks display strong $S_1 \pm S_0$ fabrics, which are closely to isoclinally folded (F_2) and a strong, west-plunging $L_2 \pm L_1$ lineation. F2 folds are primarily recumbent which has resulted in a regionally extensive, strongly developed, flat-lying tectonic fabric. Open F_3 folds result in variability in the trend of the L_2 as well as warping of the limbs of the F_2 folds. Tight to isoclinal parasitic folds commonly occur on the limbs of the F_2 folds. The regional metamorphic grade consistently reaches amphibolite facies with some rocks adjacent to younger intrusions recording granulite-facies conditions.

2.3 Geology of the Totnes Road Fiord Locality

The Totnes Road Fiord locality affords one of the best opportunities to understand the nature of the volcanic rocks, and provides critical insight into the stratigraphy of the North Touak-Cape Dyer volcanic belt as a whole. Mapping at Totnes Road identified three main lithologic units (Figure 2-1a). From east to west, these are: 1) fine-grained, grey biotite-muscovite psammite (Figure 2-8a) and biotite-muscovite ± staurolite ±garnet semi-pelite both with local calc-silicate concretions (Figure 2-2a); 2) fragmental, pillowed and massive green-weathering volcanic rocks; and 3) chemical sedimentary rocks including pyritic-graphitic schist (Figure 2-2b&c), a variety of iron formations (Figure 2-2d&e), and gossanous boulders (Figure 2-2ef). A thin, <2m thick, discontinuous quartzite is found in contact with the volcanic rocks at certain locations on the Totnes Road peninsula but is absent at other locations, either due to depositional or preservation differences. Detrital zircons from this quartzite yielded a dominant population with a mean age of ca. 2 Ga (N. Wodicka 2011, unpublished data) providing a maximum depositional age of ca. 2.0 Ga for the sedimentary sequence and associated volcanic rocks. A minimal depositional age of ca. 1.89 Ga for the Hoare Bay group is established by dating of the Qikiqtarjuaq plutonic suite (pink and dark blue units on Figure1-2), a charnokitic plutonic suite that is intrusive into the Hoare Bay group psammite-semi-pelite package (Rayner et al., 2012).

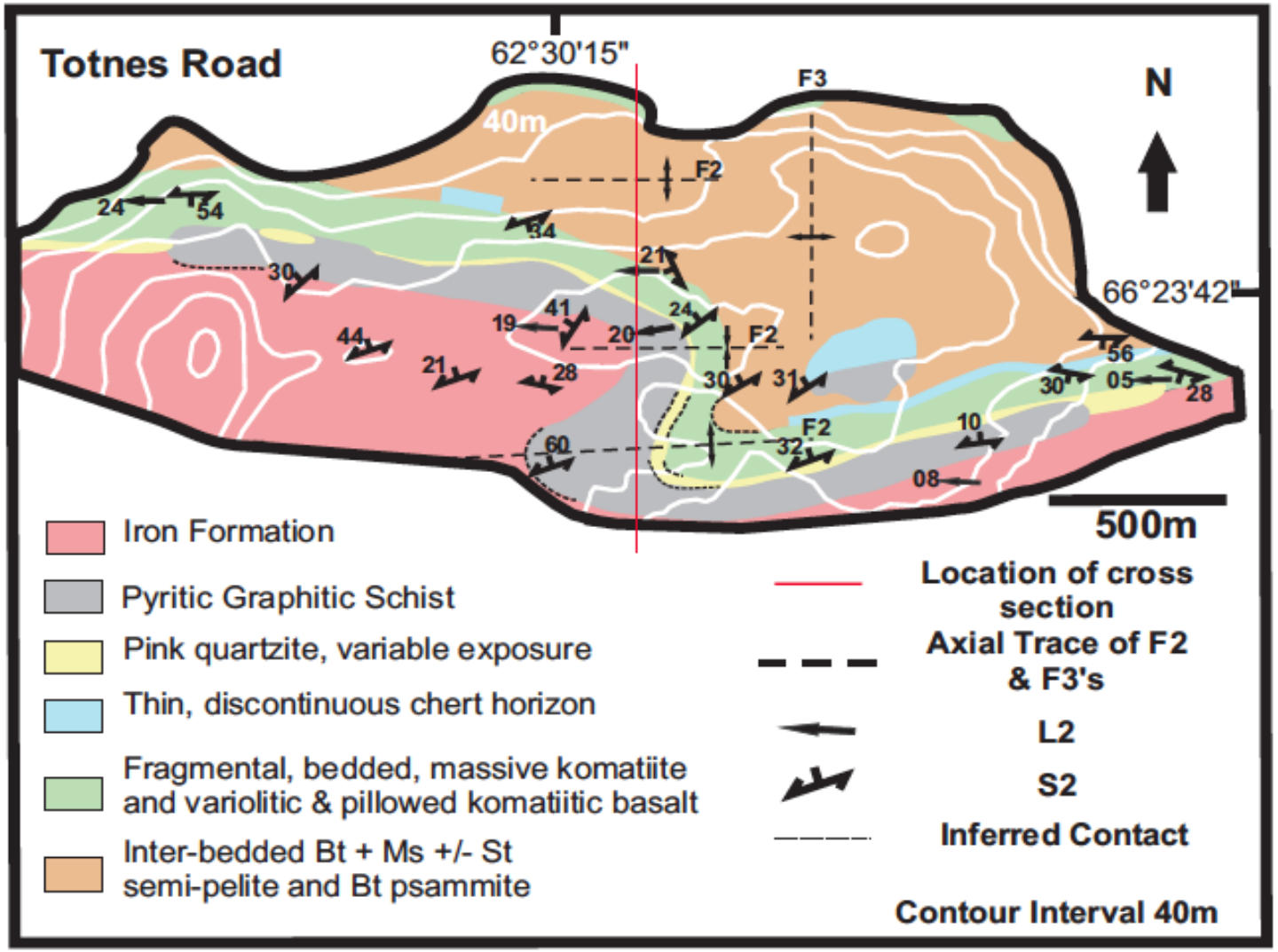

Figure 2-1. a) Geologic map of the peninsula on the south shore of Totnes Road Fiord. Abbreviations: Grt – garnet, Amp – amphiboles, Bt – biotite, Ms – muscovite, St – staurolite.

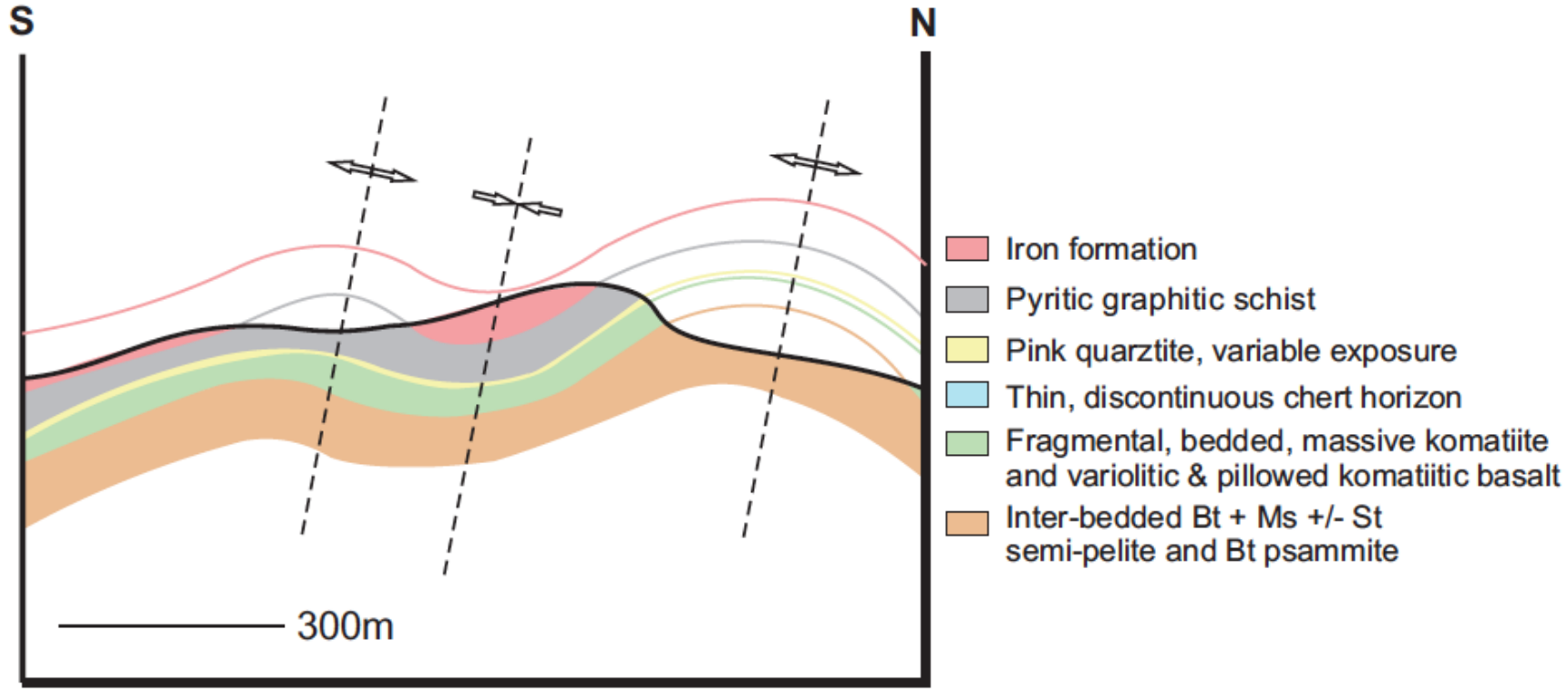

Figure 2-1b) North-south cross-section constructed perpendicular to F2 fold axes and showing the open and slightly inclined geometry of F2 folds. See Figure 2-1a for location.

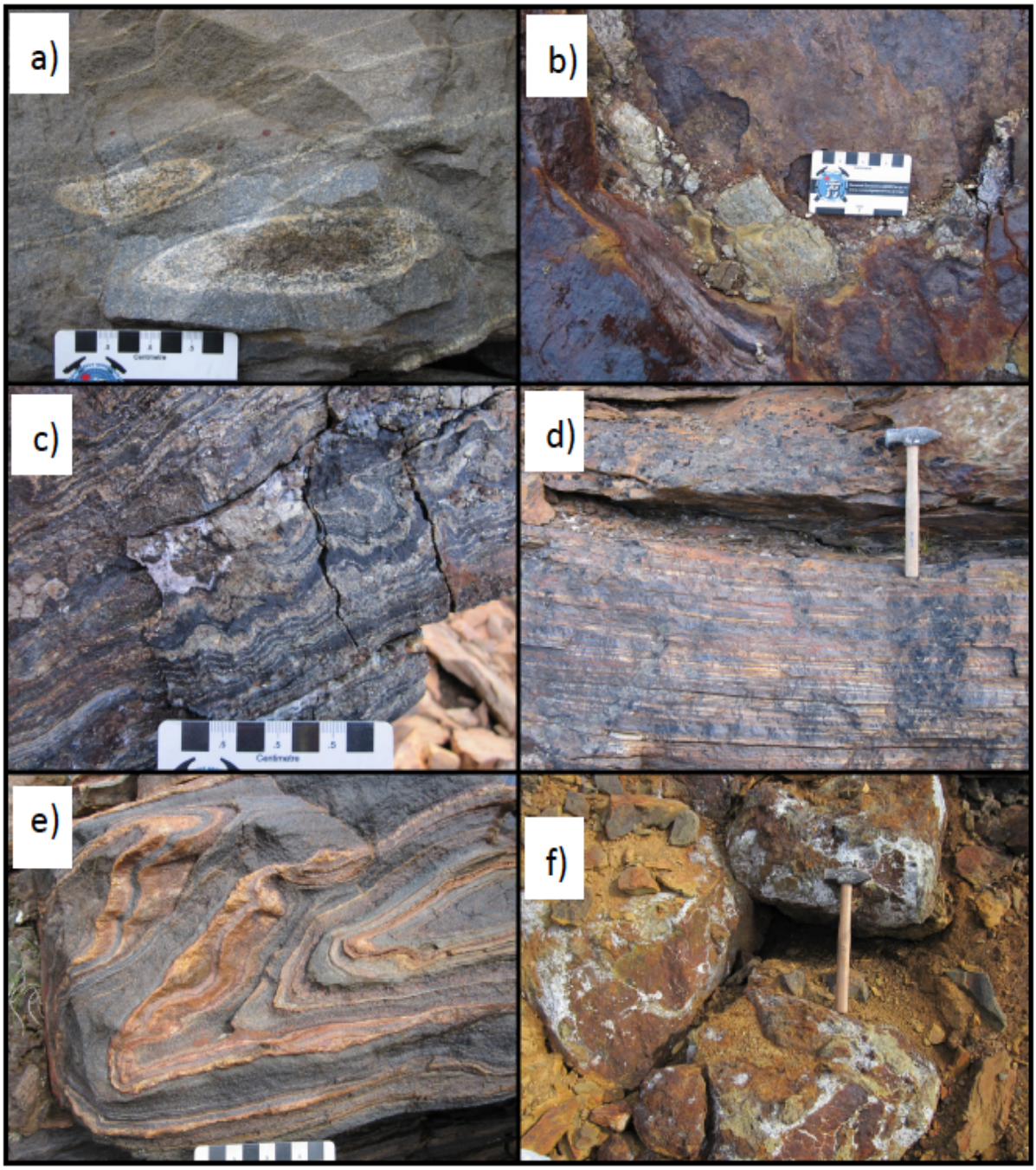

Figure 2-2. Examples of the variety of lithologies exposed at the Totnes Road locality. a) Calc-silicate concretions located within biotite-psammite. b) Pyrite layer in graphitic schist. c) Well-developed F_2 folds folding S_0+S_1 fabric in pyritic-graphitic schist. d) Layered Fe-rich exhalites. e) Layered, folded Fe-rich exhalites. f) Distinctive, round, gossanous boulders with white weathering (caliche?), from northwest Totnes Road valley traverse.

2.3.1 Totnes Road Fiord volcanic rocks

The volcanic suite at Totnes Road Fiord weathers a distinctive bright green colour, with a colour index of ~98, and can be subdivided into eight separate subunits based primarily on textural differences observed in the field (Figure 2-3). Deformation has resulted in the development of a strong stretching lineation and weak to moderate planar fabric with domains of intense shearing. Primary textures are generally well-preserved perpendicular to the lineation and moderately to poorly-preserved in other planes. These textures are used to define the eight subunits which, from east to west, are: 1) schistose, 2) bedded, 3) fragmental, 4) schistose, 5) pillowed and variolitic, 6) fragmental, 7) schistose and 8) fragmental. Two contradictory indicators of younging direction were found within the volcanic succession. The first seemingly indicates younging in a westerly direction due to the presence of variolitic accessory fragments in unit 6, which is exposed west of variolitic unit 5 (Figure 2-4a). This indicator was noted first in the field and therefore the numbering of the different units within the volcanic package was based on this, with unit 1 being the most easterly and unit 8 the most westerly. The second indicator seemingly designates east as the direction of younging, whereby at one location it appears as if the volcanic material extruded through the quartzite (Figure 2-4b) that forms the western boundary of the volcanic package. However pervasive folding is present at the Totnes Road locality and therefore this apparent relationship may actually be a result of later folding. The presence of accessory fragments is currently the clearest indicator, such that the stratigraphic 'way up' is interpreted to be westward at the Totnes Road locality.

The most easterly unit of the Totnes Road Fiord volcanic suite (unit 1) is 2m thick, medium grained and gossanous. Unit 2 is bright green and characterized by layering, 5-8 cm thick, (Figure 2-5a) interpreted to represent bedding. Layering is defined by subtle changes in grain size and colouration. Unit 3 displays distinct fragments (Figure 2-5b) evident by grain size and mineralogical variations, as well as alteration differences. Throughout unit 3, fragments range from 5 mm to approximately 10 cm and vary from angular to well-rounded, consistent with a volcanic breccia. Tectonic alignment of fragments and stretching parallel to regional L_2 defines a strong L>S fabric in this unit. Unit 4 is a green, fine-grained schist with no visible bedding or fragments. Pillowed and variolitic unit 5 (Figure 2-5c, 2-5d) occurs in the central portion of the volcanic package. This unit weathers black-green, with a colour index of 75-80,

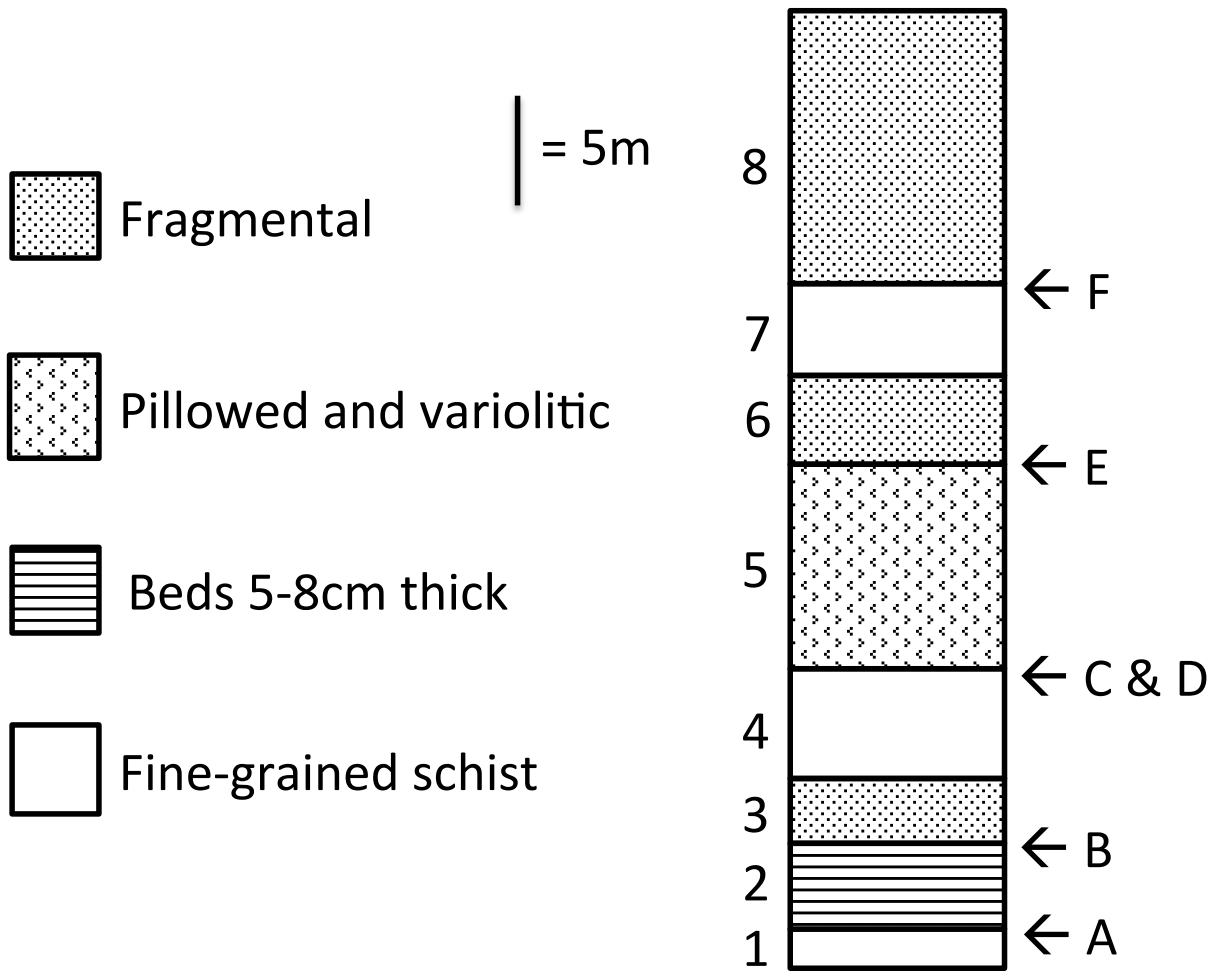

Figure 2-3. Proposed stratigraphy for the volcanic sequence exposed on Totnes Road Fiord (from Keim 2010). Arrows with letters correspond to location where field pictures in Figure 2-3 were taken. The unit numbers 1 to 8 are located at the base of the unit to which they correspond. See text for discussion of stratigraphic younging direction.

rather than the more typical bright green, a reflection that that this central package is more basaltic in composition (Keim, 2010). Varioles, or ocelli, 1 cm long, occur as elliptical patches that are plagioclase-rich and hence more leucocratic than the host rock (Gélinas et al, 1977; Fowler et al., 1986; Fowler et al., 2002). The origin of varioles is still enigmatic with interpretations including alteration, metamorphism, liquid immiscibility, processes during chilling (Arndt and Nesbit, 1982), and mingling between basalt and rhyolite (Fowler et al., 2002), however, the most likely explanation is that they are the result of spherulitic crystallization due to undercooling of the liquid (Gélinas et al, 1977). In unit 5, varioles are most concentrated in the core of each pillow, where they coalesce such that the weathered colour of the rocks changes from dark black-green to light grey (Figure 2-5d). Unit 6, a volcanic breccia, is similar to unit 3, except that unit 6 contains variolitic fragments (Figure 2-5e), suspected to be derived from unit 5. This is the main criterion in support of westward younging of the Totnes Road sequence. Unit 7 is a fine-grained schist, similar to unit 4. Uppermost unit 8 is a clast-supported volcanic breccia (Figure 2-5f) with the largest (up to 20 cm) and most rounded fragments of the entire sequence.

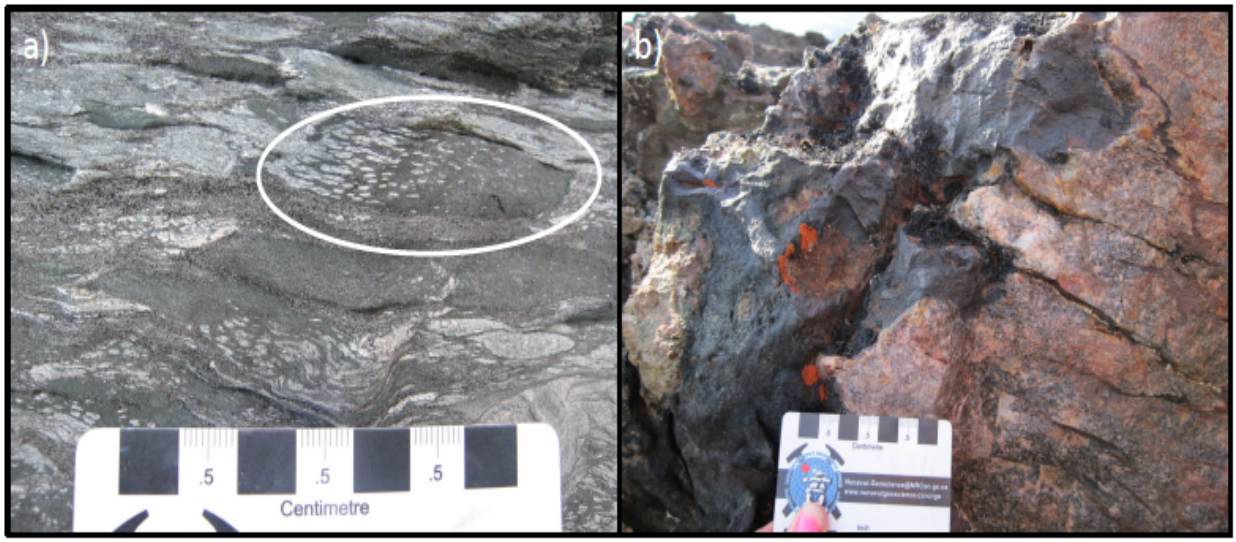

Figure 2-4. Photographs depicting two contradictory way-up indicators found at Totnes Road Fiord. a) volcanic breccia unit 6 with fragments containing varioles from unit 5. White ellipse highlights one of these fragments. b) interesting relationship between volcanic rocks on the left and quartzite on the right, possibly an extrusive relationship or possibly related to folding.

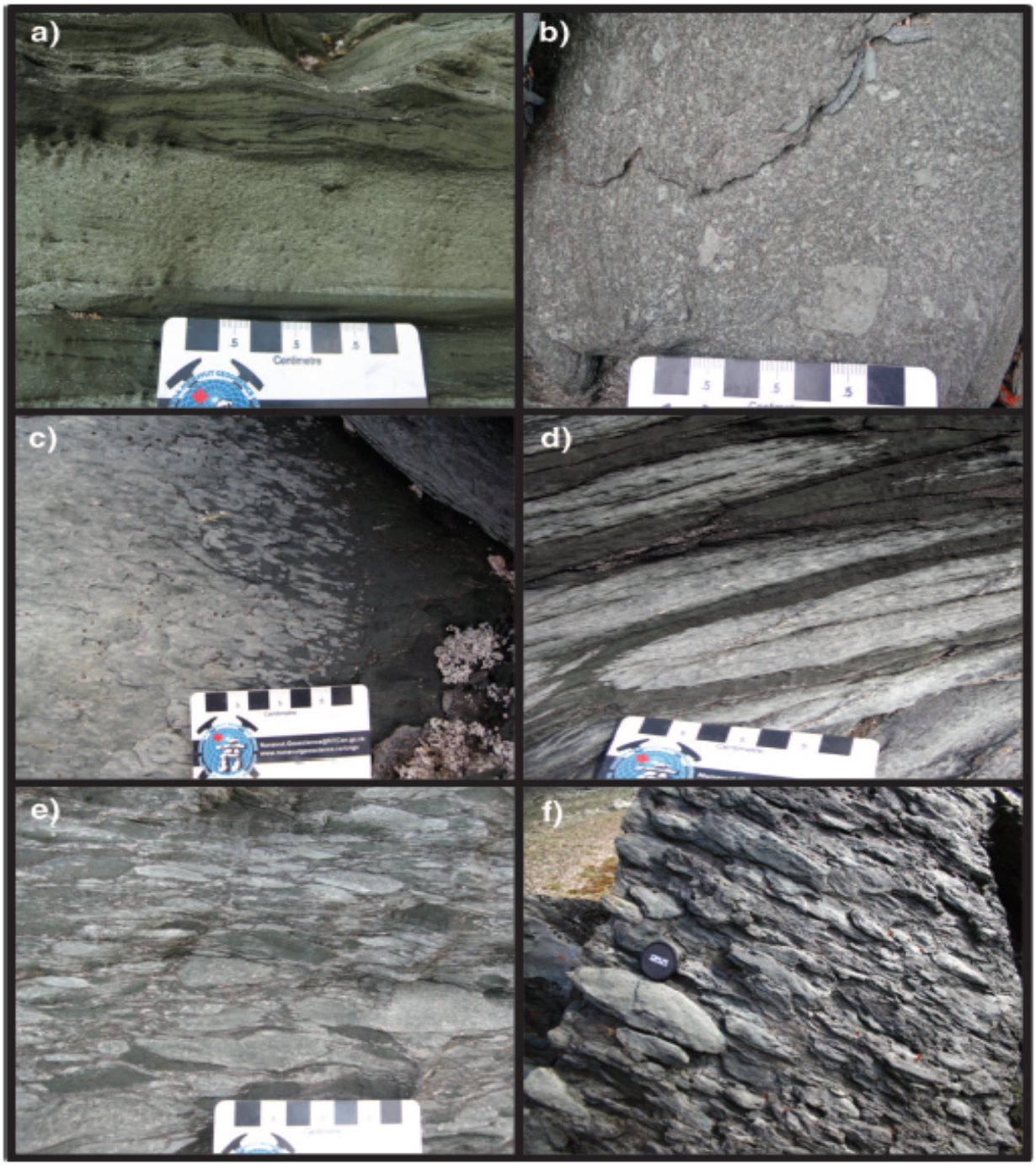

Figure 2-5. Primary textures preserved in volcanic rocks at Totnes Road Fiord. a) Bedded tuff. b) Volcanic breccia showing fragmental nature on smaller scale. Photograph taken down plunge of L_2. c) Varioles coalescing to cover entire outcrop surface. d) Pillow selvages with varioles concentrated in centers of individual pillows. e) Volcanic breccia with some variolitic fragments. f) Volcanic breccia (possible volcaniclastic) highlighting highly fragmental nature of the komatiites, lens cap for scale. See Figure 2-2 for locations of photographs.

Mineralogical differences between the units are minimal, with all units dominated by amphibole, primarily strongly pleochroic green magnesiohornblende, with lesser amounts of pale, weakly pleochroic amphibole, possibly ferrohornblende or actinolite (Figure 2-6). Titanite grains on the scale of 10-80μm are pervasive throughout the volcanic rocks. Minor mineral phases include chlorite, ilmenite with exsolved magnetite, and secondary carbonate. Plagioclase is the dominant mineral in the varioles. This mineral assemblage suggests that the rocks currently preserve amphibolite facies, having undergone complete recrystallization of the original magmatic pyroxenes and olivine.

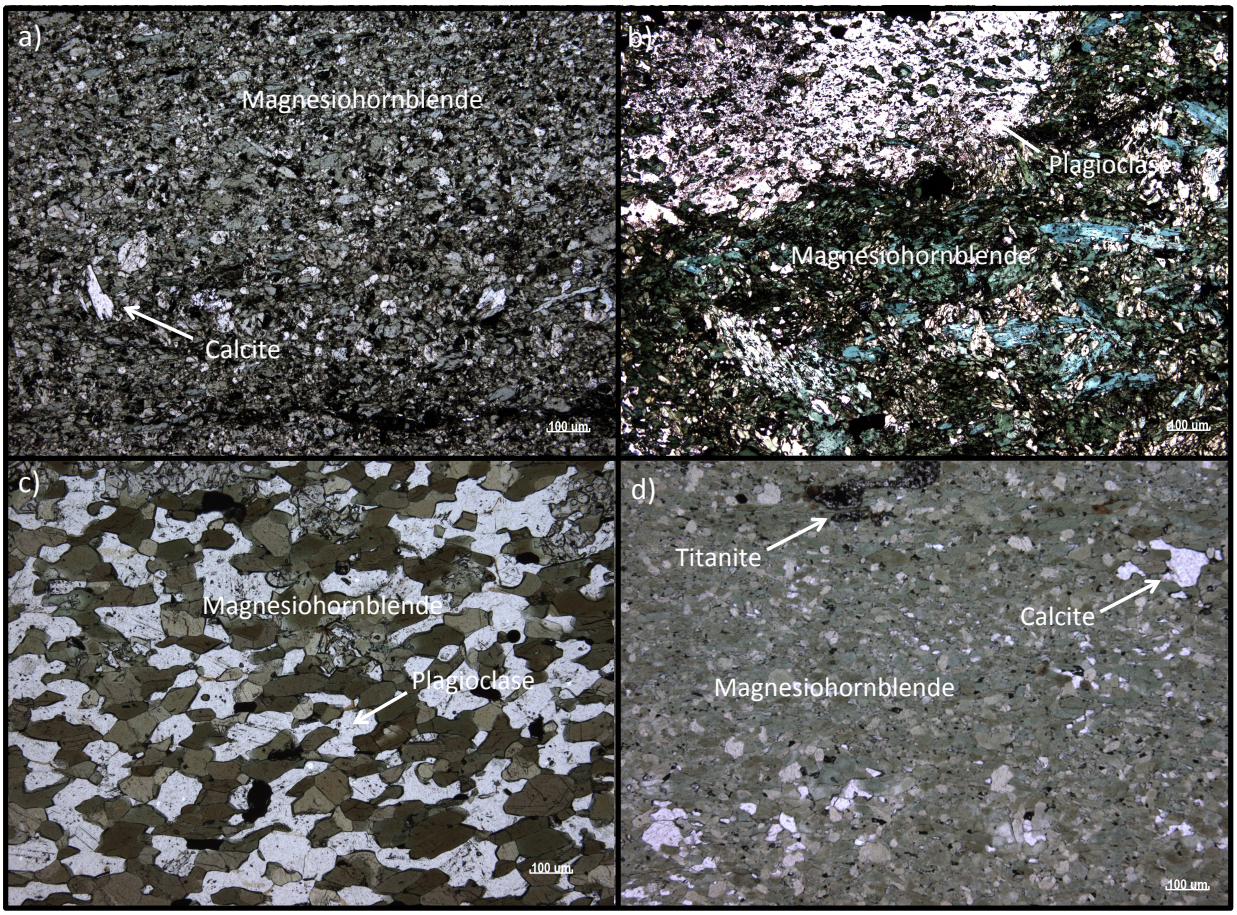

Figure 2-6. Thin section photomicrographs of Totnes Road Fiord volcanic rocks. a) green-weathering, massive volcanic rock, dominated by magnesiohornblende with minor calcite, b) green-weathering, variolitic volcanic rock, plagioclase in upper left is a variole, c) polygonal granoblastic magnesiohornblende and plagioclase in a black-weathering volcanic rock, d) green-weathering massive volcanic rock, with large titanite grain visible at the top.

2.3.2 Totnes Road Fiord chemical sedimentary rocks

In addition to the spectacular exposure of green-weathering volcanic rocks, the Totnes Road Fiord locality also possesses expansive gossanous outcrops of chemical sedimentary rocks. The chemical sedimentary rocks occur immediately to the west of the volcanic rocks, which if the way-up indicators within the volcanic suite are correct, indicates that the chemical sedimentary rocks are younger than the volcanic rocks. A number of lithologies are present within the chemical sedimentary package exposed at Totnes Road Fiord. The four main categories, designated by virtue of field observations and petrologic work are as follows:

Chert: Chert typically occurs as massive, thin (1-5m thick) gossanous outcrops (Figure 2-7). It is the one chemical sedimentary unit that outcropped structurally beneath the volcanic rocks to the east and is thus, some chert beds are likely older than the volcanic rocks. Chert horizons were variably mapped throughout the supracrustal package (Figure 1-2) giving the impression that the chert is not genetically tied to the main package of chemical sedimentary rocks. The unit is dominated by recrystallized quartz with variable amounts of magnetite, pyrite, garnet, graphite, and minor amounts of other sulphides.

Iron Formations: The dominant lithology within the chemical sedimentary package at Totnes Road Fiord is iron formation. The iron formations are lithologically quite variable and occur as bedded units up to 5m thick, comprised of <1-5cm thick beds. This unit can be split into three distinct groups based on mineralogy and general appearance.

Group I consists of green biotite + garnet + quartz ± magnetite ± grunerite. The outcrops are generally green, variably magnetic, and quite coarse grained with garnets up to 3mm across (Figure 2-9a). Varying grain size and garnet abundance define individual beds. Group II is dominated by grunerite with minor amounts of biotite and/or garnet ± magnetite (Figure 2-8b). In outcrop this group manifests itself by being variably magnetic and thinly bedded (10mm – 5cm thick beds), with mineralogical differences defining individual beds. Grunerite dominated beds are beige in colour, biotite or garnet dominanted beds are green or red, respectively, and magnetite dominanted beds are black (Figure 2-9b). The third and final group consists of an assemblage of only grunerite and magnetite. Outcrops exhibit alternating beige (grunerite) and

Figure 2-7. Photograph of typical chert outcrop from Totnes Road Fiord (top). Close up of chert outcrop, note recrystallized appearance and gossanous weathering from northwest of Mermaid Fiord (bottom).

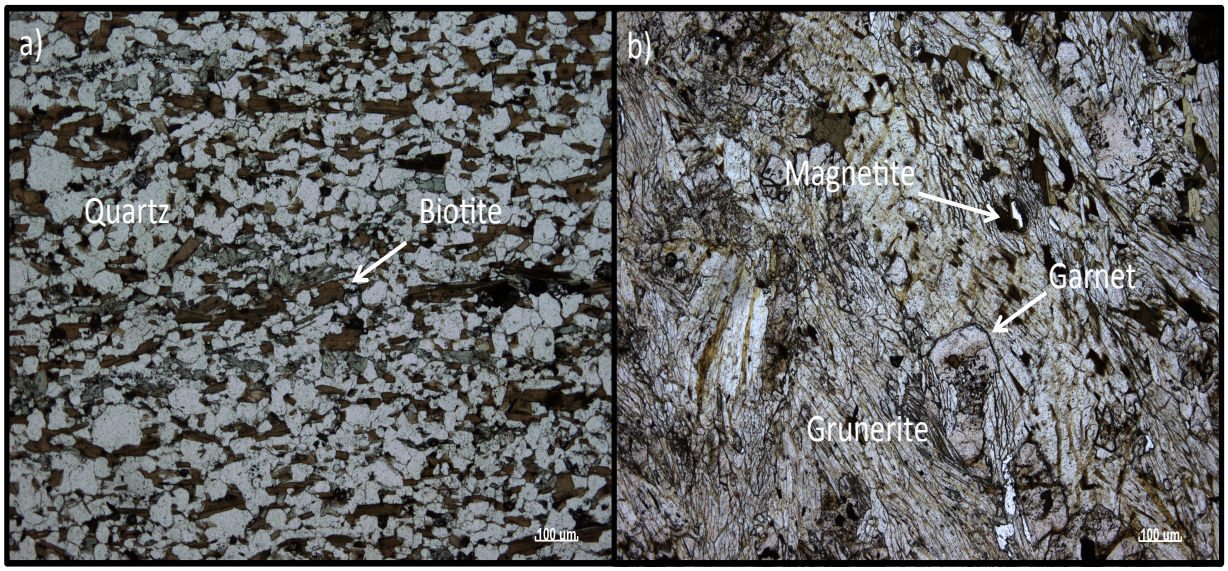

Figure 2-8. a) Thin section photomicrograph of biotite psammite found structurally beneath green-weathering volcanic rocks at Totnes Road Fiord locality. b) Thin section photograph of group II silicate facies iron formation from Totnes Road Fiord locality.

black (magnetite) beds on a 0.5 - < 5cm thick basis, and thus group III strongly resemble oxide facies iron formation (Figure 2-9c). All three groups belong to the silicate-facies iron formation family because even though magnetite is present, it generally makes up only 30-40% of the unit and is interbedded with Fe-silicates not chert, quartz, or carbonate as would be expected for oxide facies iron formations.

Graphitic-Pyritic Schist: This unit is quite friable and therefore crops out poorly. It occurs immediately above the pink quartzite in a recessive ~3m thick layer as well as in a few isolated 3-5m thick layers structurally below the silicate facies iron formation. The unit is composed of roughly equal amounts of graphite, quartz, and pyrite. The pyrite occurs in thin bands, 1-2mm thick, within a schistose, graphite and quartz matrix (Figure 2-2c&d). At the contact with the pink quartzite, pyrite layers define bedding-cleavage relationships. Pyrite-rich graphitic schists are not uncommon and are known from numerous locations worldwide. They have generally been referred to as sulphide-facies iron formation, although they are *sensu stricto* not iron formations, and can generally be said to represent the distal portions of VMS deposits (Bekker et al., 2010).

Gossanous boulders: Present within the overall chemical sedimentary package was a zone of gossanous rubble ~25m wide, which contained scattered gossanous boulders <1m across with patches of powdery white-weathering material (caliche?) (Figure 2-2f). Although there was no outcrop present, it is believed that this unit is in situ due to its concordant nature with the surrounding silicate facies iron formation. The boulders were incredibly dense and thus it was impossible to obtain a fresh surface.

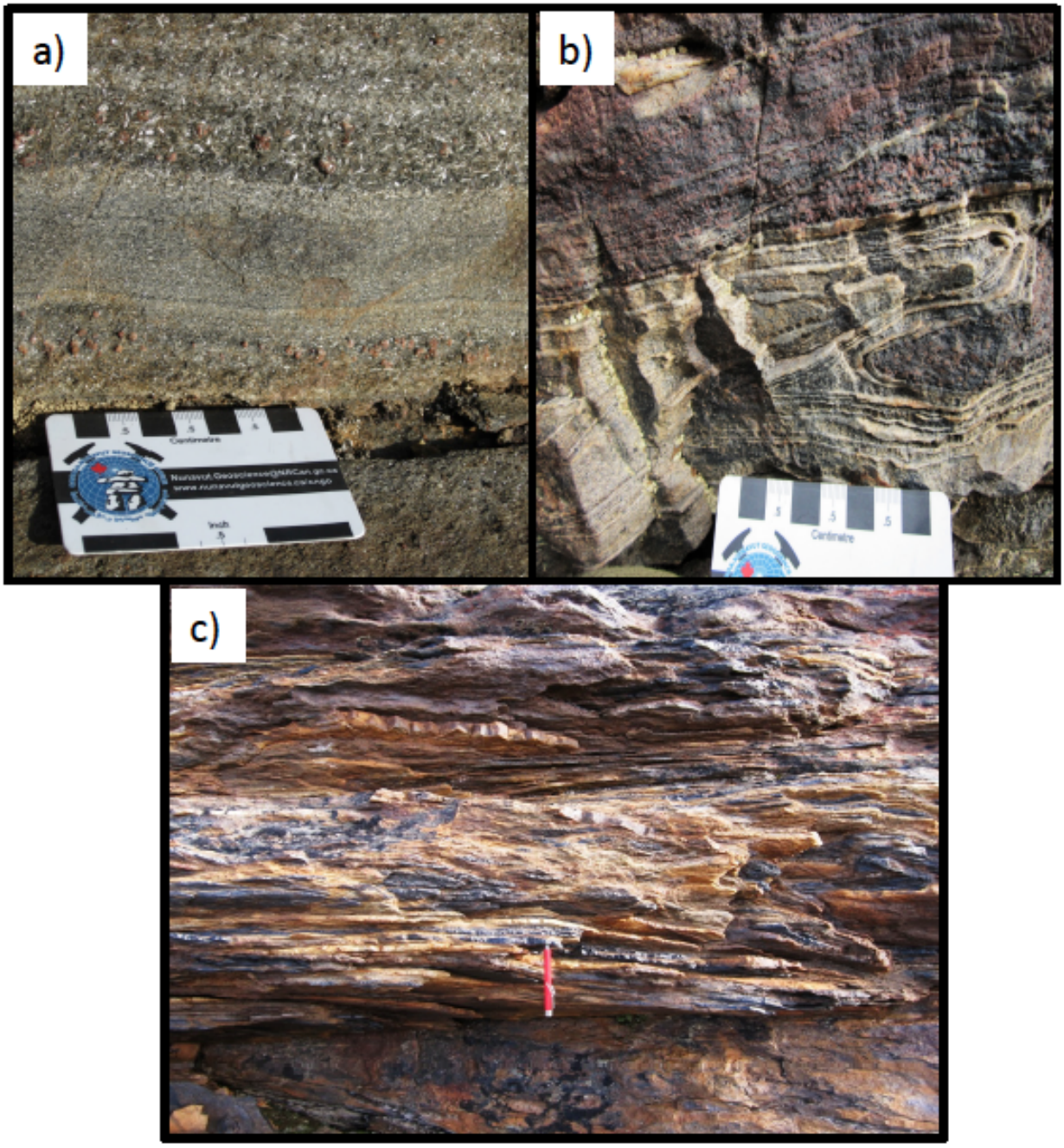

Figure 2-9. Iron formations found at Totnes Road Fiord. a) group I iron formation showing bedding defined by compositional and grain size variations. Note green colour from green biotite, large red garnets, and bedded nature. b) group II iron formation with green biotite rich layers, pink garnet rich layers, and beige grunerite layers. c) group III iron formation with 7 cm magnet hanging from black magnetite layer for scale, with interlayered beige-weathering grunerite.

2.3.3 Structural geology of Totnes Road Fiord locality

The Totnes Road area records evidence of two penetrative deformation events, which are similar in timing, geometry and finite strain to those observed in other parts of the Cumberland Peninsula. At the Totnes Road locality, F_2 folding has resulted in 200-500m scale, close folds of a strong bedding-parallel fabric (Figure 2-1a and 2-1b). Close to isoclinal parasitic folds occur on the limbs of the F_2 folds. A strong, moderately west-plunging L_2 lineation is developed throughout the area consistent with regional trends. A broad, open north-trending F_3 fold changes the plunge and warps the limbs of F_2 folds, as well as slightly reorienting the L_2 lineation.

2.4 Geology of other volcano-chemical sedimentary occurrences

During the summers of 2009 and 2010, numerous other occurrences of volcanic and chemical sedimentary rocks were identified, during the course of regional integrated bedrock mapping, which collectively define the North Touak-Cape Dyer volcanic belt. Individual volcanic units are a maximum of a few hundred meters thick and associated chemical sedimentary rocks generally <100m thick. Outside of the North Touak-Cape Dyer belt, volcanic and chemical sedimentary rocks are rare.

Detailed mapping at six localities along the length of the North Touak-Cape Dyer volcanic belt (Figure 2-10) revealed that the association of volcanic and chemical sedimentary rocks was a diagnostic feature throughout its strike length. Green-weathering volcanic rocks and gossanous chemical sedimentary rocks, similar to those exposed at the Totnes Road Fiord locality, were mapped. In addition, black-weathering volcanic rocks were also identified.

The six localities mapped occur throughout the 150km length of the North Touak-Cape Dyer volcanic belt, with exposures separated by distances of up to 40km. From southwest to northeast these localities are: North Touak Fiord (off to the southwest on Figure 2-10), Mermaid Fiord, Totnes Road Fiord, northwest valley of Totnes Road Fiord, Mooneshine Fiord, and Sunneshine Fiord.

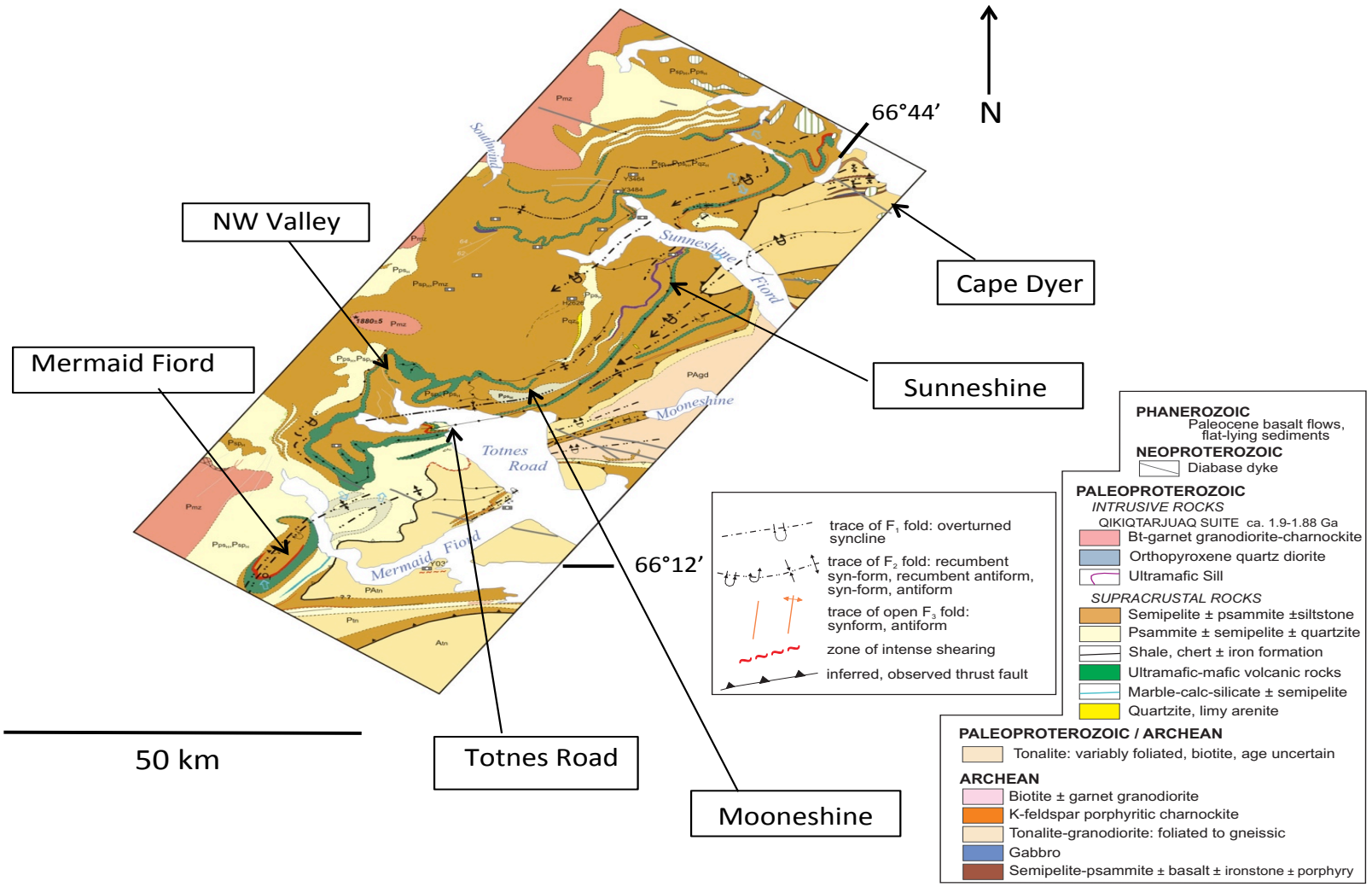

Figure 2-10. Map of the northeastern portion of the North Touak-Cape Dyer volcanic belt. The map pattern is related to the intersection of folds, regional scale boudinage, and significant topographic relief. Locations of detailed traverses are marked by arrows: 1- Mermaid Fiord, 2- Northwest Valley, 3- Totnes Road Fiord, 4- Mooneshine Fiord, 5- Sunneshine Fiord, 6- Cape Dyer. Map modified from Sanborn-Barrie et al. (2011c).

North Touak Fiord: A north-dipping ~75m thick package of green, dominantly fragmental volcanic rocks (Figure 2-11a) is exposed to the northeast of North Touak Fiord. The volcanic unit is a clast-supported volcanic breccia with sub-angular to well-rounded fragments up to 50cm in length. To the north, and structurally overlying the volcanic rocks, is a biotite-muscovite psammite, whereas exposed to the south and structurally underlying the volcanic rocks is a biotite ± garnet psammite. A ~5m horizon of chemical sedimentary rocks occurs ~50m to the south of the volcanic rocks. The chemical sedimentary rocks are composed of gossanous, dense, rounded boulders and grunerite + magnetite silicate facies iron formation, similar to the lithologies described from the Totnes Road Fiord locality. The stratigraphy here is inverted compared to other localities, possibly due to recumbent F_2 folding inverting the stratigraphy on the overturned limb. The North Touak area is located near the contact with the Archean basement rocks, and the overlying Paleoproterozoic Hoare Bay group, a contact which appears to be the focus of shear zones and folding. The North Touak area described above is the more northern exposure of two volcanic-bearing packages in the region. The southern package is thinner, with much less of the stratigraphy represented, and is contained within an overturned antiform. The folding present in the southern package, combined with the presence of clastic sedimentary enclaves within the northern volcanic package (along strike from traverse), hint at the possibility of folding being present within the northern exposure as well, which could account for the repetition of rock units and the apparent reversal in the stratigraphy.

Interestingly, dating of an intermediate clast contained within the fragmental green-weathering volcanic rocks from the North Touak Fiord locality, gave a crystallization age of 2.77 Ga (Wodicka, unpublished data, 2011), indicating that the volcanic rocks erupted through Archean basement of similar age to that exposed on Cumberland Peninsula.

Mermaid Fiord: Consists of a northwest-dipping, thick (~500-750m), package of plagioclase-porphyritic, black-weathering volcanic rocks with some zones containing euhedral 1cm sized garnets (Figure 2-11b). Thin (<1m) beds of tuffaceous material displaying bedding on a 1-2cm scale were found in the central portions of the package (Figure 2-11c). Exposed immediately to the northwest of the volcanic rocks, is ~25m of gossanous, highly weathered material with scattered, dense, gossanous boulders. Visible on some surfaces of the boulders are rounded chert

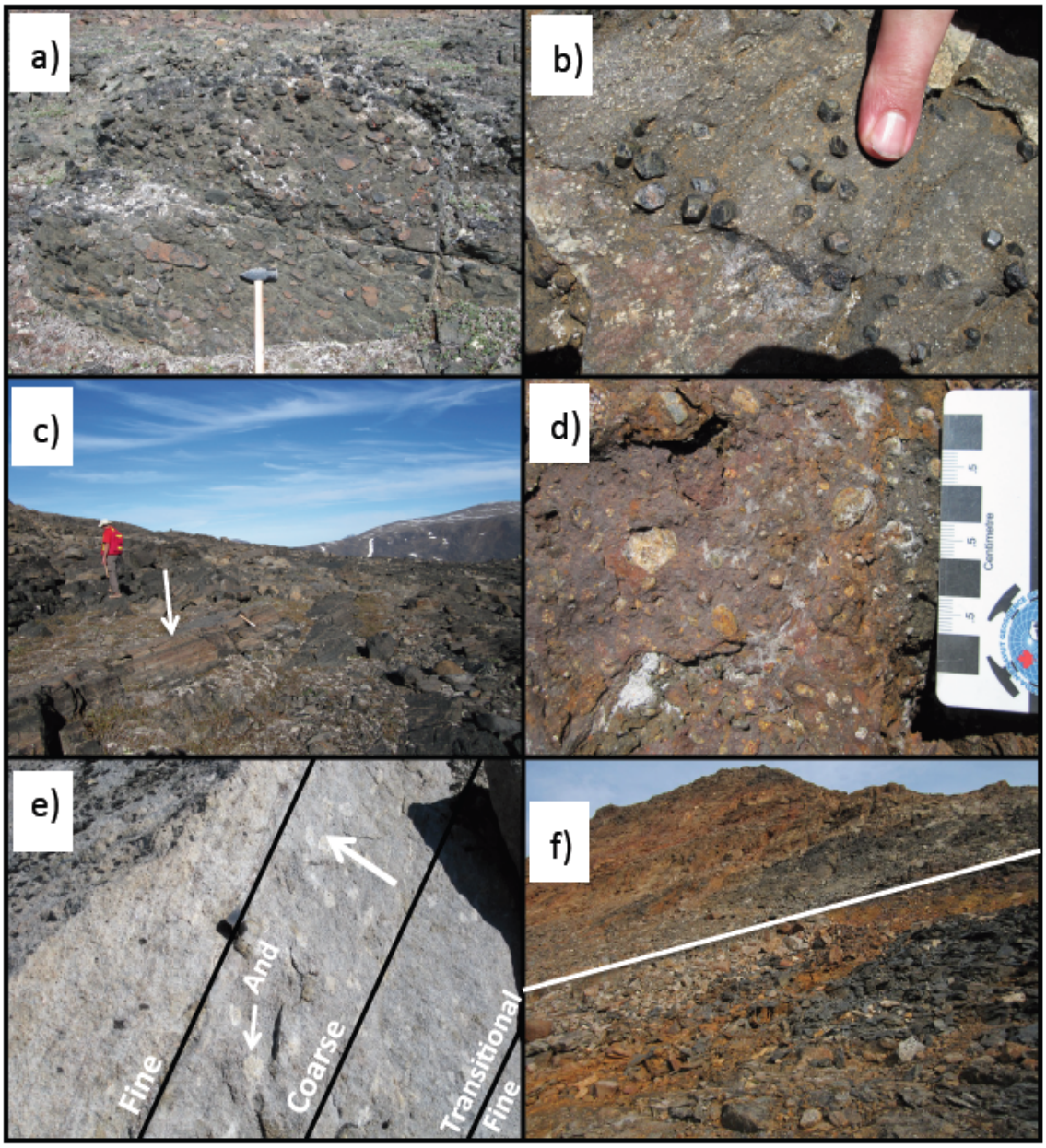

Figure 2-11. Photographs of different lithologies from supracrustal package; localities highlighted by black boxes on Figure 1-2. a) Fragmental komatiite from North Touak Fiord locality, a tuff breccia, hyaloclastite, or re-worked volcanic material. b) Euhedral, cm-scale, garnets within black-weathering volcanic rocks from Mermaid Fiord locality. c) Bedded tuffaceous unit, marked by arrow, approximately 1m thick within black-weathering volcanic package at Mermaid Fiord locality. d) Rounded quartz rich (chert?) fragments within deformed sulphide boulder at Mermaid Fiord locality (discussed more fully in Ch. 5). e) Way-up indicator: coarsening Andalusite crystals in semi-pelite (abbreviated to And in the photograph) recording fining upwards sequence, arrow indicates way up, Mermaid Fiord. f) North-west valley locality where volcanic-chemical sediment portion of stratigraphy was repeated due to folding. White line marks approximate location of repetition.

and pyrite fragments (Figure 2-11d). On a cut surface (Figure 2-12a), the boulders can be seen to be composed of a massive pyrrhotite and graphite matrix containing rounded grains and fragments of: individual pyrite grains (1-5mm), quartz-rich muscovite and phlogopite-bearing fragments (1-5cm long) interpreted to be chert, and fragments of pyritic-graphitic schist up to 8cm in length (Figure 2-12a).

This distinctive texture has been observed in massive sulphide deposits, including the Sullivan ore deposit (Figure 2-12b; Lydon et al., 2000), and has been termed "*durchbewegung texture*" (Marshall and Gilligan, 1989), a German term that has no English equivalent but directly translated means '*by motion*'. This texture is believed to be the result of post-consolidation deformation rather than a primary texture. According to Marshall and Gilligan (1989) pyrrhotite is a weak mineral and deforms easily, therefore during deformation it will behave in a ductile, plastic manner. Pyrite and other minerals such as quartz, are much more resistant to deformation and will behave in a brittle manner under the same conditions. Field observations indicate that the chert, the deformed boulders, and the pyritic-graphitic schist are in close association. During deformation the pyrrhotite behaved plastically and formed a layer of sulphide slush, whereas the surrounding lithologies and pyrite behaved in a brittle manner, broke up, and were incorporated into this pyrrhotite slush, where they were milled against each other resulting in their rounded shape (Marshall and Gilligan, 1989). Accordingly, the sulphide-rich boulders present at Totnes and Mermaid fiords may represent an initial massive sulphide deposit containing pyrite, pyrrhotite, and minor chalcopyrite that was deformed during intense regional deformational events.

The gossanous zone at Mermaid Fiord is overlain by ~25m of grunerite + magnetite ± garnet silicate facies iron formation. Farther to the northwest, and structurally overlying the chemical sedimentary rocks, is a package of andalusite-biotite ± garnet-muscovite semi-pelite. Graded bedding manifests itself within the semi-pelite as numerous sequences displaying a gradual increase toward the northwest in both the size and abundance of andalusite crystals (Figure 2-11e). Assuming that the current presence of andalusite points to an Al-rich parental material, layers with more andalusite represent muddier Al-rich beds. Accordingly, at Mermaid Fiord younging is interpreted to be toward the northwest, based on metamorphic grading

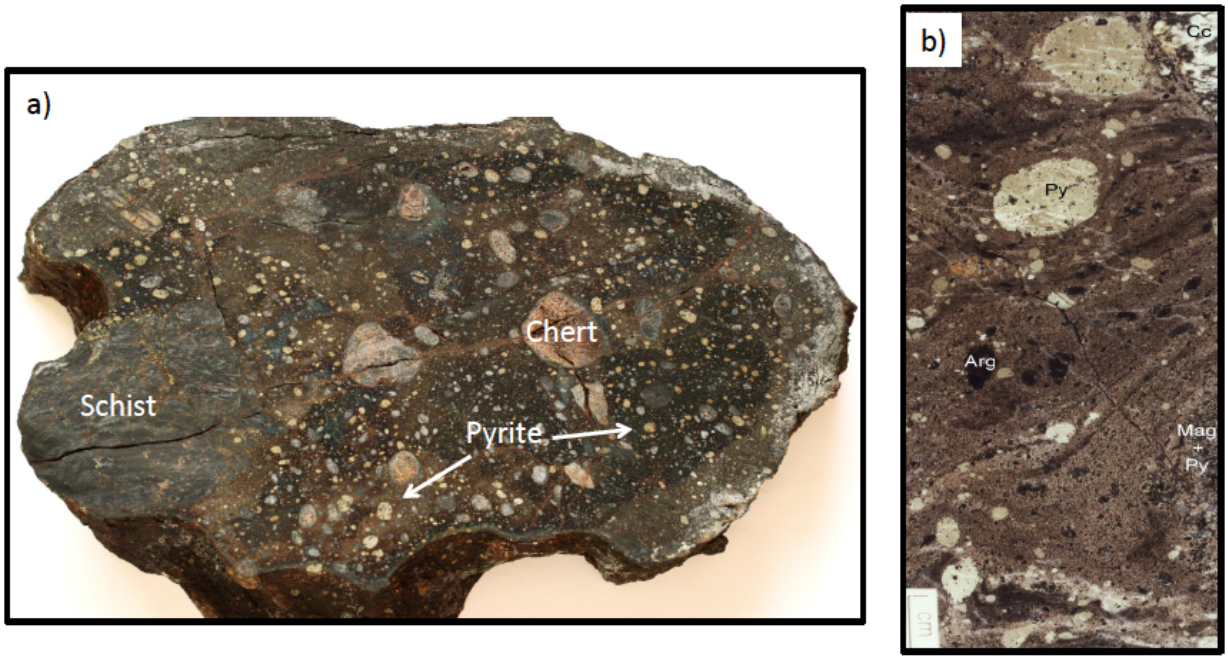

Figure 2-12. a) Photograph of interpreted durchbewegung texture from North Touak-Cape Dyer volcanic belt. Note metallic matrix composed of pyrrhotite with some pyrite and rounded fragments of pyritic-graphitic schist, chert, and pyrite. b) Durchbewegung texture from the Sullivan Deposit (Lydon et al., 2000) showing metallic pyrrhotite dominant matrix, rounded pyrite grains (Py), pyrite and magnetite (Mag+Py) grains, and rounded exotic argillite (Arg) and calcite (Cc) fragments.

delineated by variations in the size and abundance of andalusite crystals. The southeastern, and thus stratigraphically lowest, volcanic rocks are in contact with biotite psammite, which locally contains calc-silicate nodules.

Northwest Totnes Road Fiord Valley: A northwest-trending valley from the head of Totnes Road fiord exposes dominantly northwest-dipping strata. The structural top of the sequence (in the NW) consists of interbedded beige to light brown biotite-sillimanite-garnet semi-pelite and biotite psammite, which are structurally underlain by chemical sedimentary rocks. A younger hornblende gabbro dyke occurs along this contact. The chemical sedimentary sequence, from north to south, consists of ~10m of quartz + magnetite ± grunerite ± garnet ± biotite silicate facies iron formation, ~2-3m of sulphidic boulders and gossanous weathered material, and a thin (<2m) chert bed.

Structurally underlying the chemical sedimentary rocks is a <25 m thick package of black volcanic rocks with 25-30% plagioclase phenocrysts, 1-3 mm long, stretched parallel to the fabric of the rock. Immediately to the south, the stratigraphy described above is repeated and the dip direction changes from NW to E (Figure 2-11f). The exact cause of the repetition and dip change is uncertain; possibly the repetition was caused by faulting and the dip differences are related to regional folding, rotational faulting or fault propagation folding are also possibilities, however more detailed mapping would be required to say for certain. Structurally beneath the repeated stratigraphy is a thick (~750m) package of biotite psammite, which is clearly distinct, due to its grey colouring, from the structurally higher biotite psammite. South of the biotite psammite is a ~25m thick outcrop of green-weathering volcanic rocks, structurally underlain by biotite-garnet-sillimanite pelite. An approximately ~30m wide horizon of green-black volcanic rocks occurs within the pelite package at the southern end of the valley. In summary, a total of four exposures of volcanic rocks were mapped at this locality, however, the upper two exposures are interpreted as the same unit, repeated due to regional deformation. Thus, three volcanic packages were mapped within a distance of 3.5km and only the upper, folded sequence was associated with chemical sedimentary rocks.

Moonshine Fiord: At this locality, north-dipping quartzite and andalusite-biotite-muscovite-garnet pelite in the northwest are structurally underlain by chemical sedimentary and volcanic rocks to the south. Outcrops are sporadic in the south and consist of 1-4m thick horizons of silicate facies iron formation structurally underlain by a package of fragmental green volcanic rocks (~25m), black volcanic rocks (<25m), sulphidic boulders with rounded chert fragments and gossanous weathered material. Lowermost is a <10 m thick iron formation of 5-10cm thick beds of magnetite.

Sunneshine Fiord: The stratigraphy and structure at Sunneshine Fiord is poorly constrained due to the lack of outcrop and dominance of vertically orientated felsenmeer. A clastic package of interbedded biotite psammite and biotite-garnet-sillimanite semi-pelite with green hornblende-rich gabbro intrusions occurs to the northwest. This is interpreted to be the lower clastic package, since elsewhere within the North Touak-Cape Dyer volcanic belt, mafic-ultramafic intrusions were only found to occur within the lower sedimentary package, that is, the clastic package not in contact with chemical sedimentary rocks. To the southeast, are <10m thick horizons of green fragmental volcanic rocks with local varioles, intermediate (dioritic) rocks, iron formation, and gossanous biotite psammite. Farther to the southeast, is a monotonous sequence of biotite-sillimanite psammite and biotite-garnet semi-pelite, inferred to be the upper clastic package. Exposures at this locality show a similar stratigraphy to elsewhere in the volcanic belt. Based on the interpretation that the chemical sedimentary rocks are younger than the volcanic rocks and that the mafic sills only occur within the lower clastic package the direction of younging appears to be to the south. Accordingly, the stratigraphy appears to be inverted at Sunneshine Fiord, possibly due to regional folding, however, lack of detailed mapping and scarcity of way-up indicators in the area preclude a definitive interpretation.

Mapping at six localities along the North Touak-Cape Dyer volcanic belt have confirmed the presence of two major, cogenetic, volcanic units with associated chemical and clastic rocks; this association forms a volumetrically lesser but important and diagnostic part of the Hoare Bay group. The most abundant and widespread volcanic rocks are aphanitic rocks that weather a distinctive medium to bright green, and appear similar to the volcanic rocks exposed at the Totnes Road Fiord locality. Despite having experienced regional amphibolite-facies

metamorphism, these volcanic rocks locally preserve primary textures including fragmental and hyaloclastite deposits, varioles, as well as inferred bedding. A second volcanic type was identified at five localities in the central portion of the belt and consists of foliated to schistose black-weathering rocks that generally lack primary features, except local plagioclase phenocrysts at Mermaid Fiord and fragmental textures observed directly across the fiord from the Totnes Road locality. Two varieties of mafic-ultramafic sills occur within the clastic sedimentary package, as well as within the Archean basement rocks, and are believed to represent a feeder system to the volcanic belt (Mackay, 2011) (Figure 2-13). The first group are thin, <5m, fine-grained ilmenite-bearing amphibolite layers and the second are bright-green-weathering spotted sills, up to 200 m thick, which display a blastoporphyritic texture characterized by cm-size, brown-weathering olivine crystals (Figure 2-13b).

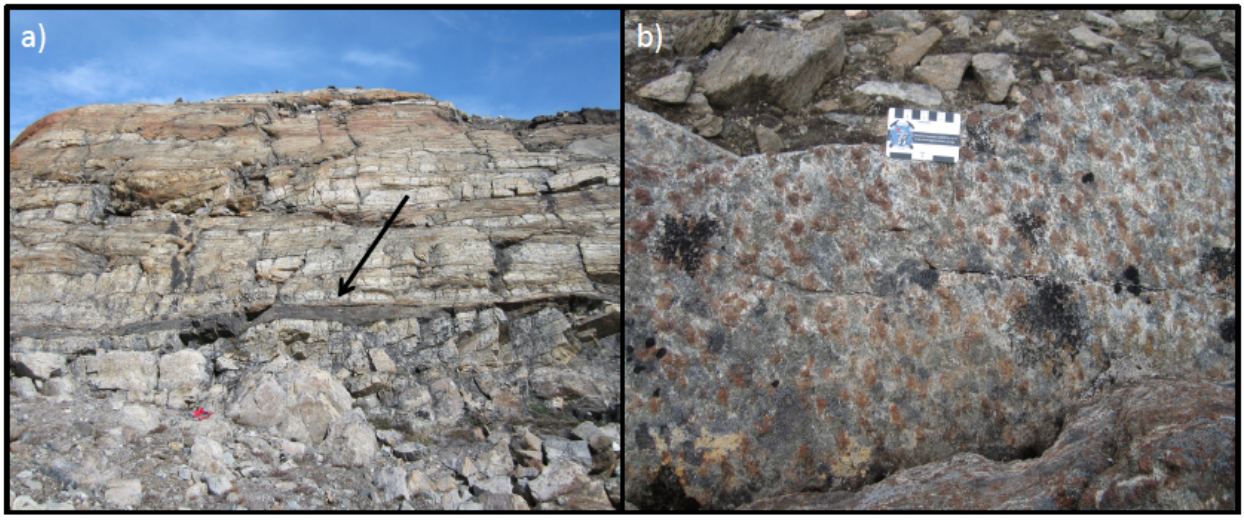

Figure 2-13. Field photographs of presumed feeder sills and dykes to volcanic rocks. a) Thin, fine-grained, homogeneous black amphibolite. b) Olivine-porphyroblastic sill characterized by 1 cm size olivine crystals within a green amphibolite matrix.

Petrographic work further confirmed the consistency of the two groups of volcanic rocks identified in the field. The 'green-weathering' volcanic rocks have a colour index of ~98 and are dominated by randomly orientated, bright-green, strongly-pleochroic magnesiohornblende with lesser amounts of other amphiboles including actinolite and anthophyllite as well as chlorite. Trace amounts of biotite, titanite, ilmenite, magnetite, pyrite, and chalcopyrite are

also present. Fragments are well-rounded to sub-angular and consist of very fine-grained material assumed to be similar in composition to the coarser-grained amphibole matrix. A small number of samples have rounded aggregations of carbonate interpreted as microscopic amygdules. Given the similarities in colour index, textures, and mineralogy it is established that the volcanic suite exposed at Totnes Road Fiord occurs throughout the North Touak-Cape Dyer volcanic belt. The black-weathering volcanic rocks have a colour index of 50-60 and consist of roughly equal amounts of polygonal-granoblastic hornblende and plagioclase (Figure 2-6) with minor quartz and trace amounts of titanite, ilmenite, magnetite, pyrite, and chalcopyrite. The olivine-blastoporphyritic sills have a similar mineral assemblage to the 'green rocks' and are dominated by amphibole with the addition of large cm-sized poikilitic (amphibole inclusions) olivine phenocrysts that have experienced varying degrees of serpentinization.

At all 6 localities, most occurrences of volcanic rocks are associated with chemical sedimentary rocks, but it is also clear that the stratigraphy of the volcanic belt is varied and therefore correlations must be made cautiously. Apart from the NW valley locality, all of the examined sections show a similar stratigraphy, whereby volcanic rocks underlie chemical sedimentary rocks and these collectively are bound both above and below by thick clastic packages (Figure 2-14). The North Touak Fiord and Sunneshine Fiord localities exhibit the same association but the stratigraphy appears to be inverted, likely due to regional folding.

During detailed mapping in the summer of 2011 it was recognized that the mafic-ultramafic feeder sills occurred in the clastic sedimentary rocks in contact with the volcanic rocks, as well as the Archean basement rocks, but are absent in the clastic sedimentary rocks in contact with the chemical sedimentary rocks (Brett Hamilton, personal communication). This evidence supports the interpretation made at the Totnes Road and Mermaid Fiord localities that the volcanic rocks underlie the chemical sedimentary rocks. If one assumes that there was one main period of volcanism and hydrothermal activity, then all of the described localities can be considered to preserve rocks of equivalent age.

In addition to the sections described above, isolated exposures of both green- and black-weathering volcanic rocks were mapped and sampled by other members of the CPIG mapping

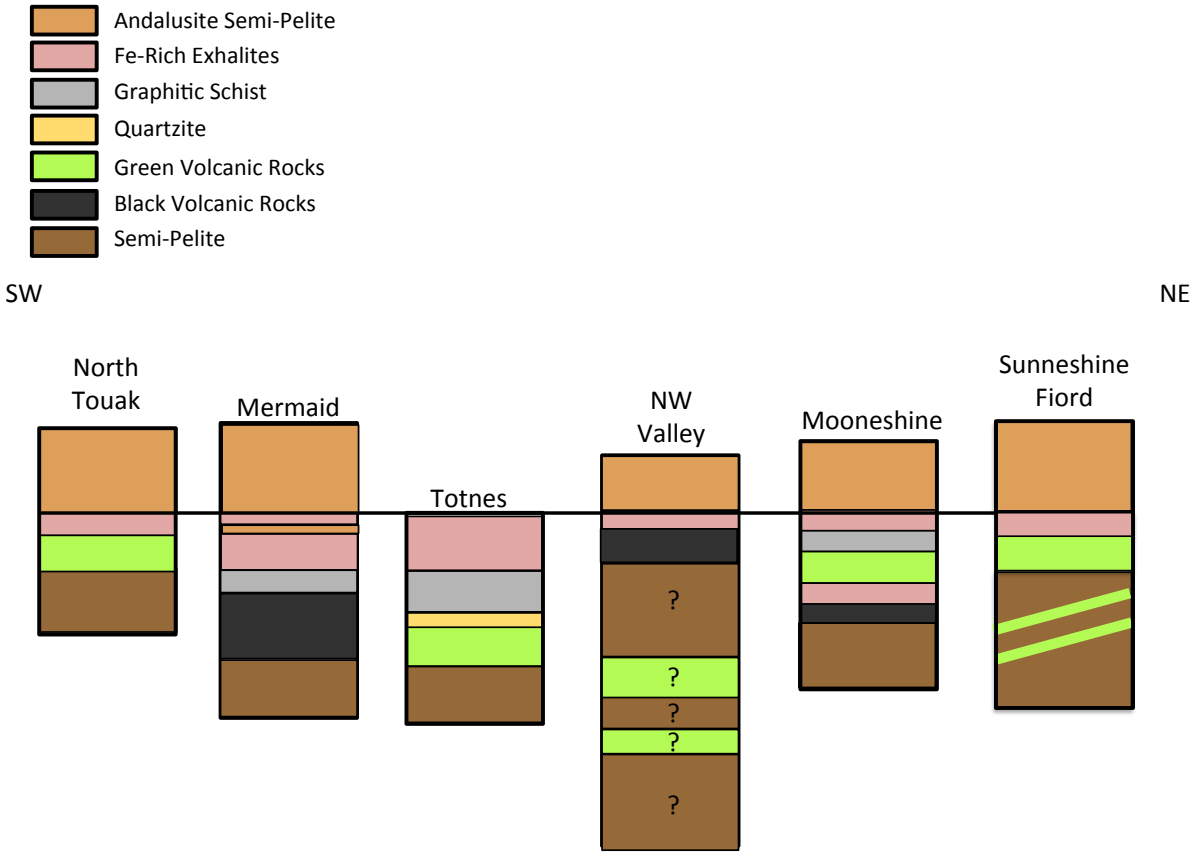

Figure 2-14. Schematic stratigraphic columns from southwest to northeast of all localities that received detailed work. The diagram is not to scale as the exact thickness of the clastic sedimentary is not known, however the relative structural thicknesses especially for the volcanic and chemical sedimentary rocks is accurate. Question marks over clastic sedimentary rock intervals indicate uncertainty regarding what clastic package (upper or lower) the rocks belong to. Columns are hung from the top of the chemical sedimentary packages and are shown with the interpreted stratigraphic bottom at the bottom. For the NW Valley traverse the column was hung from the structurally lower chemical sedimentary package that was a repeat of the upper package due to regional scale folding.

team. These isolated occurrences, together with the southern-end of the NW-valley traverse, appear to lack the association with chemical sedimentary rocks that typifies the majority of the volcanic occurrences. It is possible that these isolated units are actually thick sills and may represent additional feeders to the volcanic rocks. The other possibility is that there are two or more distinct volcanic packages and that all the volcanic rocks in the belt are not cogenetic.

However, if an exposure of volcanic chemical sedimentary rocks is followed along strike the thickness of the exposure generally decreases, and in numerous instances the stratigraphy pinches out. In a few localities, a stacked sequence consisting of a single occurrence of volcanic and associated chemical sedimentary rocks and one, or more, without associated chemical sedimentary rocks occurs intercalated with clastic sedimentary rocks. The volcanic belt has thus potentially been boudinaged and in localities of intense deformation, tectonically interleaved with clastic sedimentary rocks (Brett Hamilton, personal communication). Lithologic variations, reflected by the green versus black volcanic rocks, could be caused by chemical heterogeneities within the source region. Therefore, lithologic variation within the volcanic belt does not negate the validity of the interpretation that the belt is the result of one main period of volcanism and associated hydrothermal activity.

More detailed mapping and geochronological work will be necessary to determine which of the above scenarios (feeder system, distinct volcanic events, tectonic intercalating of units, basin scale heterogeneities) is correct. Given the similar appearance and mineralogy of the volcanic and chemical sedimentary rocks throughout the belt, and the overall similar stratigraphy observed of chemical sedimentary rocks overlying volcanic rocks, it seems reasonable to interpret the volcanic and chemical sedimentary rocks as being related to the same volcanic and hydrothermal event. Thus, this volcano-chemical package is a distinctive stratigraphic horizon within the Cumberland Peninsula's Paleoproterozoic cover sequence.

2.5 Discussion

Detailed mapping conducted at six localities throughout the North Touak-Cape Dyer volcanic belt established that the stratigraphy first observed at Totnes Road Fiord occurs along

the belt. Although the exact age of the upper and lower boundaries of the Hoare Bay group have yet to be defined, field-work has confirmed that the North Touak-Cape Dyer volcanic belt is contained within the sequence, and is bound on both sides by clastic rocks. Way-up indicators found at both the Mermaid and Totnes Road Fiord localities, as well as the occurrence of presumed feeder sills in the clastic package not in contact with the chemical sedimentary rocks, indicate that the volcanic rocks were erupted before the chemical sedimentary rocks were deposited. Both green and black volcanic rocks were mapped within the volcanic belt, and although there are mineralogical variations between the two volcanic rock types, their similar stratigraphic position suggests one main period of volcanic activity and associated hydrothermal activity. Geochemical analyses in Chapter 3 will help shed light on the accuracy of this interpretation.

CHAPTER 3

GEOCHEMICAL ANALYSIS OF VOLCANIC ROCKS AND ASSOCIATED CHEMICAL SEDIMENTARY ROCKS OF THE HOARE BAY GROUP, CUMBERLAND PENINSULA, BAFFIN ISLAND

3.1 Introduction

As established in Chapter 2, two different varieties of volcanic rocks occur throughout the North Touak-Cape Dyer volcanic belt. They consist of green-weathering volcanic rocks, presumed to be ultramafic given their overall similarity to the komatiitic suite at Totnes Road Fiord (Keim, 2010), and black-weathering, presumed, mafic volcanic rocks. Both varieties are found at a similar stratigraphic position, namely, beneath associated chemical sedimentary rocks. Green-weathering, olivine-blastoporphyritic sills were mapped within the Archean basement rocks, as well as within the clastic sedimentary package in contact with the volcanic rocks. Geochemical characterization of the two groups of volcanic rocks and the ultramafic sills will shed further insight into the field-based interpretations that there was one main period of volcanism within the North Touak-Cape Dyer volcanic belt, and that the sills are cogenetic with the volcanic rocks.

Geochemical trends of both the volcanic rocks and chemical sedimentary rocks will be investigated in Chapter 3 and used in Chapter 4 to interpret petrogenesis and tectonic setting. Geochemical analysis of the volcanic and chemical sedimentary rocks will allow for detailed comparison between the different occurrences of the above-mentioned lithologies throughout the North Touak-Cape Dyer volcanic belt. The ultimate goal of this work will be to determine if all the volcanic and chemical sedimentary rocks can be considered correlative throughout the belt. Once the geochemical characteristics are understood they can be combined with field observations and used in correlating the Hoare Bay group with other Paleoproterozoic cover sequences in the region (Chapter 4).

3.2 Sampling and Analytical Methods

3.2.1 Sampling

All the rocks on Cumberland Peninsula have experienced numerous deformation events. In the field, care was taken to sample fresh rocks with minimal weathered surfaces and carbonate to avoid the effects of weathering and metasomatic alteration. Faults, highly fractured areas, and shear zones were avoided, as these could be areas where later fluid movement was concentrated. When sampling near the fragmental units, care was taken to insure no fragments of older rock (crystalline basement or clastic sedimentary rocks) were contained within the samples. Through the use of optical microscopy, samples that contained carbonate in the form of filled vesicles were flagged for further geochemical screening. A total of 42 volcanic rock samples were taken for geochemical analysis as well as thin section preparation, 16 were prepared for thin section only, and 12 were used as hand samples only (Appendix 1 & 2). The 13 geochemical samples that were included in Keim (2010) and Keim et al., (2011) will be included with the new samples taken specifically for this MSc. project, to ensure that all available data is considered and presented herein. A total of 13 chemical and 2 clastic sedimentary rock samples were taken for geochemical analysis and thin section preparation, 15 chemical and 6 clastic samples were prepared for thins section only, and 13 chemical and 7 clastic were used as hand samples only (Appendix 1 & 2).

3.2.2 Analytical Methods

Whole rock major and trace element data for select samples (n=13) from Totnes Road, one regional sample (H68A3), and appropriate duplicates (n=2) were obtained at the Ontario Geological Survey (OGS) Geoscience Laboratories. Samples with minimal to no visible alteration were pulverized using an agate mill in order to significantly reduce the amount of contamination. Major elements were determined by analysis of a borate-fused glass bead by X-ray fluorescence spectroscopy (XRF) on an Axios wavelength dispersive spectrometer. The lower detection limit for all major elements was 0.01 wt% and final totals are all 100±1.6%. FeO was determined by dichromate titration with a lower detection limit of 0.06 wt%. All trace element data was obtained using a closed-system digest, followed by inductively coupled plasma mass spectrometry (ICP-MS) carried out on a Perkin Elmer Elan 9000. Samples were calibrated

using a combination of synthetic multi-element solutions and certified reference solutions. Lower detection limits for select elements are as follows: Zr-6ppm, Nb-0.028ppm, Th-0.018ppm, La-0.04ppm, Yb-0.009ppm, Nd-0.06ppm, and Sm-0.012ppm.

Whole-rock major-element data for the remaining regional volcanic samples (n=32), chemical sedimentary rock samples (n=13), and clastic sedimentary rock samples (n=2) were obtained by borate-fused glass disc XRF analysis at SGS Mineral Services following pulverization in agate to reduce contamination. The lower reporting limit for all major elements was 0.01% and final totals are all 100±1.58%. Trace element data including duplicates (n=3) were obtained in the Department of Geological Sciences at the University of Saskatchewan. Samples were digested using HF-HNO_3 in a closed system for 3 days followed by an open system to evaporate the acid. Inductively coupled plasma mass spectrometry was carried out on a PerkinElmer 5000 system. Lower detection limits for select elements are as follows: Zr-0.09ppm, Nb-16.67ppm, Th-0.02ppm, La-0.01ppm, Yb-0.04ppm, Nd-0.08ppm, and Sm-0.05ppm.

The complete data set is shown in Table 3-1, and locations of important transects are indicated on Figure 2-6.

Table 3-1. Whole rock analyses for volcanic rocks of the North Touak-Cape Dyer volcanic belt

Sample Name	R097C	R097C-1	R097-C2	R097E-1	R097F-4	R097F1-0	R097F1-1	M105A-1	M105A-2	R098B-2	R098B-3	R098B-4	R098B-5
Unit	2	2	2	4	5	5	5	6	6	7	8	8	8
Location	Totnes Road	Totnes Road	Totnes Road	Totnes Road	Totnes Road	Totnes Road	Totnes Road	Totnes Road	Totnes Road	Totnes Road	Totnes Road	Totnes Road	Totnes Road
(wt%)													
SiO_2	44.79	44.17	45.99	44.53	53.03	48.57	51.20	43.12	43.14	47.20	43.44	49.03	45.29
TiO_2	1.24	1.35	0.97	1.63	1.36	1.80	1.44	1.01	0.95	0.83	0.89	1.05	0.84
Al_2O_3	8.71	9.26	11.28	8.36	10.55	9.86	11.38	11.06	9.39	8.10	8.66	5.41	8.60
Fe_2O_3	2.19	2.21	2.26	5.48	8.05	7.01	7.11	3.73	2.05	1.90	1.77	1.59	2.36
FeO	10.18	10.66	9.28	8.87	7.73	9.75	7.92	10.29	9.51	8.37	9.34	8.40	8.73
MnO	0.15	0.15	0.20	0.17	0.12	0.17	0.14	0.29	0.17	0.21	0.18	0.20	0.19
MgO	17.94	17.47	14.43	16.14	5.99	9.10	7.26	15.66	20.27	15.16	20.03	18.03	20.25
CaO	9.27	9.15	11.90	11.45	7.23	7.80	7.48	10.33	7.87	13.76	9.13	12.14	8.56
Na_2O	0.61	0.69	1.42	0.97	5.06	3.42	4.62	1.57	0.49	1.33	0.52	0.85	0.55
K_2O	0.53	0.57	0.15	0.15	0.09	0.68	0.28	0.13	0.04	0.09	0.07	0.10	0.06
P_2O_5	0.12	0.14	0.08	0.13	0.17	0.13	0.17	0.06	0.07	0.04	0.06	0.04	0.06
LOI	3.45	3.18	0.77	1.25	0.09	0.13	-0.04	2.08	4.97	2.03	5.20	2.84	4.11
Total	99.18	99.00	98.73	99.13	99.47	98.42	98.96	99.33	98.92	99.02	99.29	99.68	99.60
(ppm)													
Cr	1903	1464	2009	1533	1354	1639	1323	1869	2206	1697	2144	1061	2192
Ni	909	597	640	1046	426	861	458	690	1141	757	1139	703	1122
Co	86.4	83.1	75.1	98.3	55.8	117	85.5	85.0	95.0	83.7	95.8	77.3	92.5
Sc	44.4	30.5	37.0	32.0	26.6	36.3	27.6	39.7	33.4	33.6	36.7	32.5	33.6
V	318	291	287	311	326	365	319	294	262	298	283	269	281
Cu	849	229	63.7	73.5	68.9	159	81.8	70.3	110	9.60	89	46.2	177
Pb	1.10	1.30	0.80	0.60	1.80	1.80	2.60	0.80	0.90	1.30	1.10	1.30	0.70
Zn	95	98	79	104	84	124	95.0	87.0	81.0	85.0	79.0	74.0	79.0
Cd	0.11	0.08	0.08	0.12	0.09	0.11	0.08	0.14	0.12	0.12	0.09	0.39	0.12
In	0.05	0.06	0.06	0.06	0.06	0.08	0.06	0.06	0.04	0.06	0.04	0.05	0.04
Sn	1.00	1.34	0.74	1.07	1.03	1.15	1.15	0.66	0.60	0.82	0.70	0.71	0.54
W	0.12	0.15	0.11	0.12	0.12	0.11	0.12	0.25	0.14	0.12	0.09	0.12	0.08
Mo	1.29	0.98	0.31	0.19	0.12	ud	0.13	0.63	0.12	0.18	0.10	0.24	
Sb	0.24	0.23	0.36	0.22	0.36	0.16	0.20	0.21	0.44	0.20	0.31	0.52	0.25
Rb	14.9	16.8	1.76	0.54	0.30	13.68	4.00	0.36	0.31	0.52	1.20	1.53	0.66
Cs	3.59	3.97	0.24	0.03	0.00	0.30	0.08	0.12	0.13	0.04	0.47	0.38	0.24
Ba	465	462	17.0	37.2	47.0	228	156	9.40	2.10	18.9	13.20	17.50	7.10
Sr	119	116	130	143	239	262	420	68.6	80.0	202	129	202	88.6
Ga	12.3	13.2	14.1	15.2	15.9	18.3	18.3	15.6	13.4	10.3	12.2	7.91	12.0
Li	32.5	33.2	14.6	13.5	5.30	22.2	10.8	32.4	23.5	9.40	34.1	9.00	24.9
Be	0.74	0.77	0.31	0.81	0.66	1.01	1.02	0.48	0.39	0.34	0.62	0.40	0.48
Ta	0.49	0.67	0.26	0.66	0.56	0.70	0.58	0.20	0.27	0.23	0.23	0.45	0.25
Nb	8.32	10.48	3.87	10.6	9.37	11.3	9.69	3.49	4.10	3.78	3.46	6.18	3.93
Hf	1.91	2.00	1.41	2.64	2.26	2.79	2.28	1.38	1.30	1.31	1.14	1.82	1.10
Zr	74.0	77.0	51.0	105	88.0	111	90.0	50.0	48.0	48.0	39.0	69.0	39.0
Y	9.79	14.7	14.7	16.6	17.1	18.5	18.4	14.0	12.8	12.7	11.8	16.3	11.8
Th	0.72	1.23	0.37	0.88	0.79	0.94	0.81	0.28	0.26	0.32	0.27	0.54	0.31
U	0.31	0.39	0.10	0.29	0.21	0.18	0.21	0.10	0.11	0.30	0.09	0.16	0.10
La	6.0	10.2	4.43	6.53	12.7	10.1	10.9	4.05	3.27	3.38	2.36	3.60	3.49
Ce	15.7	24.7	9.65	18.1	28.2	25.6	27.8	10.1	8.93	8.85	6.90	9.60	9.15
Pr	2.12	3.17	1.43	2.87	3.80	3.78	4.05	1.53	1.38	1.38	1.13	1.54	1.40
Nd	9.23	13.8	6.87	14.0	16.8	17.8	18.7	7.37	6.87	7.00	6.01	8.06	6.75
Sm	2.19	3.48	2.17	3.88	4.09	4.65	4.56	2.22	2.10	2.14	1.98	2.60	1.98
Eu	1.05	1.46	0.92	1.19	1.28	1.39	1.43	0.95	0.60	0.91	0.92	0.78	0.77
Gd	2.27	3.59	2.60	4.03	4.10	4.87	4.66	2.64	2.49	2.40	2.31	3.10	2.24
Tb	0.35	0.57	0.41	0.60	0.61	0.70	0.67	0.43	0.41	0.40	0.39	0.51	0.37
Dy	2.09	3.36	2.69	3.52	3.55	4.06	3.92	2.73	2.59	2.44	2.40	3.14	2.27
Ho	0.39	0.62	0.54	0.64	0.65	0.73	0.71	0.54	0.51	0.48	0.48	0.62	0.45
Er	1.05	1.61	1.56	1.65	1.71	1.85	1.82	1.46	1.40	1.36	1.29	1.71	1.27
Tm	0.15	0.21	0.22	0.22	0.22	0.24	0.23	0.21	0.19	0.19	0.18	0.23	0.17
Yb	0.93	1.21	1.45	1.25	1.27	1.45	1.33	1.30	1.16	1.17	1.06	1.40	1.08
Lu	0.13	0.17	0.23	0.17	0.17	0.20	0.19	0.19	0.16	0.17	0.15	0.19	0.15

LOI, loss on ignition. ud, undetected.

Table 3-1 cont. Whole rock analyses for volcanic rocks of the North Touak-Cape Dyer volcanic belt

Sample Name	H68A3	G52B	G52A	M273C-1	C119A	T75D1	C118A	Y218B	Y218A	Y218C	G101A-1	R303G-1	Y222
Location	North Touak	North Touak	North Touak	Mermaid	Mermaid	Mermaid	Mermaid	West of Totnes	West of Totnes	West of Totnes	NW Valley	NW Valley	NW Valley Area
Classification	Kom Bas	Komatiite	Komatiite	Tholeiite	Tholeiite	Tholeiite	Tholeiite	Kom Bas	Spotted Dyke	Tholeiite	Kom Bas	Tholeiite	Kom Bas
(wt%)		44.30											
SiO2	40.30	44.30	43.50	49.00	47.70	47.50	47.90	43.70	42.90	48.50	43.10	49.40	49.00
TiO2	1.72	1.61	1.77	1.67	1.74	2.16	1.68	3.07	0.95	1.00	0.91	1.58	1.37
Al2O3	7.75	5.65	5.89	14.20	14.00	13.80	13.70	7.88	9.85	13.90	9.52	14.10	11.20
FeO*	14.40	14.10	13.60	14.60	14.40	16.40	15.30	15.60	12.70	13.20	12.40	13.90	15.00
MnO	0.19	0.17	0.19	0.22	0.22	0.28	0.22	0.20	0.20	0.22	0.17	0.23	0.26
MgO	14.40	20.90	18.60	6.91	6.98	5.58	6.54	15.00	22.20	7.90	18.70	6.85	10.20
CaO	12.50	7.67	9.58	9.24	12.00	10.10	11.20	11.10	5.56	11.50	9.07	11.30	8.84
Na2O	1.46	0.33	0.39	3.80	1.77	3.23	2.30	1.12	0.84	3.34	0.64	2.76	3.29
K2O	1.23	0.06	0.05	0.12	0.49	0.21	0.15	0.83	3.04	0.13	0.08	0.42	0.19
P2O5	0.12	0.14	0.10	0.14	0.13	0.20	0.15	0.31	0.07	0.08	0.06	0.15	0.13
Cr2O3	0.27	0.19	0.17	0.02	0.02	0.01	0.01	0.19	0.32	0.04	0.28	0.03	0.23
V2O5	0.05	0.04	0.04	0.06	0.06	0.06	0.08	0.05	0.04	0.05	0.04	0.06	0.03
LOI	4.32	4.16	5.61	0.27	0.67	0.33	0.91	<0.01	0.57	<0.01	3.90	0.52	0.27
Total	94.39	95.16	93.88	99.98	99.51	99.53	99.23	99.05	98.67	99.86	94.97	100.78	99.74
(ppm)													
Cr	2274	1637	1427	171	179	73.2	73.0	1661.13	2575.92	309.48	2471.43	229.67	1856.72
Ni	1722	1227	1068	86.7	106	80.4	79.7	902.58	955.72	123.99	1080.48	82.57	521.15
Co	90.5	90.0	83.3	47.0	54.1	51.5	51.8	89.37	79.94	50.40	82.80	42.27	62.42
Sc	17.0	20.9	24.0	44.0	23.8	29.6	38.1	31.00	30.50	48.90	27.80	42.86	31.61
V	277	219	233	406	349	397	410	279.49	227.65	329.68	257.27	370.98	235.60
Cu	1032	87.1	144	25.2	155	62.7	236	68.12	11.49	41.21	79.95	61.93	6.18
Pb	4.82	1.44	2.17	2.36	1.46	3.42	2.69	1.94	2.43	0.68	1.44	1.20	0.37
Bi	1.20	0.15	0.15	0.07	0.04	0.08	0.19	0.06	0.06	ud	0.17	0.03	0.03
Zn	133	131	124	123	128	150	146	137.04	98.05	101.62	99.35	117.38	94.79
Cd	ud	ud	ud	ud	ud	ud	ud	0.25	ud	ud	0.41	ud	ud
Sn	2.18	1.59	1.80	1.18	5.21	2.03	2.40	8.70	1.66	1.07	1.40	2.72	3.30
W	0.25	0.84	0.95	1.34	0.35	0.38	0.43	0.46	0.18	0.07	0.41	0.53	0.32
Mo	0.24	0.26	0.50	0.74	0.38	0.75	1.55	1.69	0.41	0.17	0.13	0.94	0.12
Ag	0.92	0.15	ud	ud	ud	0.07	ud	ud	ud	0.07	ud	ud	ud
Sb	7.38	0.19	0.22	0.24	0.60	0.26	0.16	ud	ud	ud	0.17	ud	0.24
Rb	35.3	2.07	0.90	0.49	5.22	1.83	2.27	11.18	78.91	2.00	0.40	5.75	1.96
Cs	34.37	6.38	1.22	0.02	0.04	0.13	0.08	0.26	3.81	ud	0.27	ud	0.06
Ba	618	10.0	18.6	37.7	129	53.3	177	676.34	376.65	96.43	4.73	98.87	21.61
Sr	736	273	338	308	230	297	475	294.87	129.49	191.57	93.18	247.31	65.81
Li	54.1	6.86	5.31	28.1	7.83	8.68	13.1	11.98	54.94	18.33	8.45	8.98	14.22
Be	1.45	2.57	ud	ud	0.62	1.49	0.82	ud	ud	ud	0.75	1.29	2.08
Ge	1.63	1.74	1.97	1.94	1.65	1.62	1.92	1.63	1.30	1.99	1.94	2.07	2.26
As	623	4.63	8.61	ud	ud	ud	1.42	ud	1.06	ud	13.20	ud	ud
Ta	1.01	1.12	1.24	0.67	0.87	0.69	1.33	3.05	0.54	0.45	0.30	0.65	0.96
Nb	16.7	19.8	22.1	11.7	14.1	12.6	22.9	49.07	10.63	7.12	4.96	11.23	16.09
Hf	2.53	2.75	2.83	2.85	2.91	1.94	3.47	6.74	1.23	1.19	1.17	1.91	2.63
Zr	89.3	106	112	93.9	42.5	62.8	128	240.71	35.29	28.12	38.08	49.62	88.75
Y	17.6	13.5	12.3	28.1	25.7	27.6	30.3	21.43	11.05	20.21	12.25	27.15	17.35
Th	1.39	1.39	1.32	0.88	1.11	0.97	1.67	3.14	0.67	0.58	0.31	0.54	1.43
U	0.38	0.35	0.31	0.23	0.27	0.24	0.41	0.82	0.20	0.14	0.13	0.18	0.27
La	15.39	15.1	13.7	8.05	10.5	7.43	19.0	37.53	7.45	5.87	4.27	8.57	12.25
Ce	36.96	34.2	32.6	20.1	24.3	21.4	43.6	86.94	15.89	13.54	10.36	22.00	30.34
Pr	5.01	4.34	4.19	3.03	3.33	3.14	6.02	11.22	2.09	2.05	1.68	3.18	4.03
Nd	21.40	17.8	17.3	13.4	14.7	14.1	24.1	45.28	9.50	8.80	8.03	15.02	17.09
Sm	3.91	3.76	3.38	3.98	3.48	3.69	5.57	8.90	2.08	2.63	1.69	3.77	3.82
Eu	1.79	0.82	0.74	1.35	1.03	1.46	2.02	2.63	0.78	0.91	0.62	1.34	1.13
Gd	4.33	3.72	3.47	5.02	4.23	5.00	6.36	8.34	2.53	3.46	2.72	5.15	4.13
Tb	0.65	0.52	0.47	0.81	0.78	0.84	1.02	1.08	0.40	0.58	0.41	0.85	0.65
Dy	3.73	2.77	2.36	4.90	5.48	5.30	6.16	5.22	2.42	3.71	2.39	5.26	3.89
Ho	0.60	0.50	0.47	1.00	1.03	1.13	1.14	0.89	0.52	0.70	0.46	1.08	0.68
Er	1.58	1.37	1.11	3.06	3.36	3.31	3.26	2.02	1.32	1.83	1.47	2.96	1.91
Tm	0.25	0.18	0.16	0.40	0.43	0.47	0.48	0.25	0.15	0.32	0.19	0.43	0.26
Yb	1.27	1.02	1.10	2.69	2.44	2.79	3.06	1.62	1.19	2.15	1.10	2.95	1.61
Lu	0.16	0.13	0.14	0.38	0.32	0.34	0.38	0.18	0.15	0.25	0.15	0.37	0.23

LOI, loss on ignition. ud, undetected. Kom Bas, komatiitic basalt.

Table 3-1 cont. Whole rock analyses for volcanic rocks of the North Touak-Cape Dyer volcanic belt

Sample Name	R186C	Y188B	H270	H271	R275A	R275D	H272A	H242	R181E2	H320	R162	Y227B	Y227A	R284B	Y205
Location	Mooneshine	Near Mooneshine	Sunneshine	Sunneshine	Sunneshine	Sunneshine	Sunneshine	Sunneshine Area	Sunneshine Area	Cape Dyer	Cape Dyer	North Cape Dyer	North Cape Dyer	North of Belt	North of Belt
Classification	Kom Bas	Kom Bas	Kom Bas	Kom Bas	Kom Bas	Kom Bas	Komatiite	Kom Bas	Tholeiite	Kom Bas	Spotted Dyke	Komatiite	Spotted Dyke	Spotted Dyke	Kom Bas
(wt%)															
SiO2	45.20	47.60	44.90	43.50	48.80	43.20	43.10	43.30	44.80	45.70	44.80	43.60	43.80	44.30	47.30
TiO2	2.68	2.20	1.90	1.75	2.01	2.61	1.46	2.16	3.32	0.83	1.68	0.84	0.89	0.79	1.32
Al2O3	12.40	10.30	8.54	9.30	10.10	9.27	6.45	9.90	14.90	9.23	5.81	9.72	5.57	8.60	11.20
FeO*	15.70	13.80	13.40	14.10	13.00	14.70	13.20	14.50	17.10	12.00	14.80	12.30	13.00	12.00	14.90
MnO	0.25	0.22	0.25	0.21	0.18	0.20	0.17	0.22	0.21	0.19	0.18	0.18	0.16	0.18	0.27
MgO	9.88	12.70	15.10	16.60	12.00	11.90	19.90	16.00	6.56	15.60	20.80	22.20	23.70	20.50	11.20
CaO	12.00	8.86	13.20	9.85	10.00	13.00	8.51	9.57	9.66	11.60	8.66	5.52	6.80	8.59	9.48
Na2O	0.81	2.16	0.91	0.78	2.12	2.25	0.98	0.78	2.55	1.71	0.39	0.59	0.28	0.87	2.99
K2O	0.14	0.15	0.08	0.11	0.32	0.47	0.04	0.10	0.33	0.15	0.07	0.29	0.08	0.12	0.11
P2O5	0.27	0.04	0.16	0.16	0.20	0.24	0.19	0.21	0.34	0.10	0.18	0.06	0.03	0.06	0.09
Cr2O3	0.11	0.18	0.10	0.27	0.12	0.14	0.16	0.21	0.02	0.28	0.19	0.26	0.28	0.27	0.21
V2O5	0.06	0.05	0.05	0.05	0.06	0.05	0.04	0.05	0.08	0.04	0.04	0.04	0.03	0.04	0.06
LOI	0.07	0.74	0.32	2.17	0.24	0.81	4.55	2.01	0.10	1.08	2.54	4.07	3.80	3.49	0.16
Total	99.50	98.26	98.59	96.68	98.91	98.03	94.20	97.00	99.87	97.43	97.60	95.60	94.62	96.32	99.13
(ppm)															
Cr	905	1477	827	2229	950	1159	1346	1828	136	2320	1620	2180	2407	2206	1740
Ni	315	531	367	500	347	511	1062	489	91.7	825	879	932	1795	1012	573
Co	66.1	65.5	64.3	63.8	57.8	70.7	79.8	70.6	56.1	70.3	78.3	80.3	105.3	80.8	71.0
Sc	39.4	36.6	44.1	34.2	27.6	32.2	20.1	32.7	32.4	27.5	25.1	30.6	21.3	30.3	33.4
V	349	316	284	262	300	283	212	286	441	232	232	240	195	209	280
Cu	61.6	62.5	179	40.3	51.2	161	72.6	40.1	14.4	17.8	69.2	20.9	144	36.4	19.4
Pb	5.22	4.75	11.9	1.37	7.15	2.32	1.82	1.64	4.76	1.49	1.06	1.23	0.79	1.06	2.65
Bi	0.08	0.14	0.33	0.27	0.03	ud	0.10	0.46	0.10	0.13	0.03	0.13	0.58	0.16	0.37
Zn	146	115	219	122	108	125	113	125	165	99.1	121	103	104	79.7	108
Cd	ud	ud	ud	ud	ud	ud	ud	ud	ud	ud	0.31	ud	ud	ud	ud
Sn	3.46	7.20	1.78	6.71	2.38	2.25	1.99	2.22	11.8	1.84	1.93	1.45	2.29	0.91	9.53
W	0.08	0.12	0.96	1.28	ud	0.14	0.32	0.97	0.07	ud	0.22	ud	0.66	0.29	0.06
Mo	0.75	0.35	0.61	1.07	0.57	0.58	ud	0.50	1.32	ud	ud	ud	0.20	ud	0.29
Ag	ud	ud	0.57	ud	ud	ud	ud	ud	ud	ud	ud	ud	ud	ud	ud
Sb	ud	0.38	ud	0.18	ud	ud	ud	ud	0.57	ud	ud	0.33	0.26	ud	ud
Rb	5.04	4.49	0.65	0.98	14.1	8.45	0.46	1.10	3.41	0.82	0.75	11.18	3.60	1.20	0.40
Cs	1.26	0.15	0.06	0.34	0.46	0.75	0.18	0.15	0.03	0.28	ud	4.79	0.82	0.22	ud
Ba	29.5	126	3.83	29.4	185	200	9.87	26.9	223	38.2	12.2	53.1	5.19	32.4	57.1
Sr	535	846	148	49.65	752	416	157	163	544	115	130	56.4	131	124	266
Li	15.7	31.3	6.80	20.2	21.2	23.5	7.40	20.9	13.9	23.7	2.61	24.3	4.18	13.6	38.3
Be	ud	0.73	0.80	2.25	1.17	ud	ud	0.49	2.15	0.95	ud	ud	ud	0.96	ud
Ge	2.91	2.30	2.63	2.52	2.37	1.40	2.00	2.51	2.31	2.65	2.22	1.27	1.95	1.46	3.56
As	1.16	0.91	ud	38.3	0.78	0.77	3.20	1.31	2.36	ud	ud	23.9	7.89	ud	0.99
Ta	3.01	1.90	1.32	1.62	2.15	2.82	0.92	2.16	3.05	0.24	1.23	0.21	0.36	0.25	0.53
Nb	50.4	30.7	22.7	27.9	34.2	49.0	14.7	36.5	49.4	4.28	21.3	3.72	7.01	3.89	10.1
Hf	5.17	4.28	2.27	2.38	3.68	3.67	2.09	3.21	5.09	1.21	1.64	1.11	1.16	1.36	2.68
Zr	196	156	ud	89.0	138	131	78.8	96.1	194	43.8	43.3	25.3	32.0	42.1	79.3
Y	24.9	22.6	13.4	17.4	19.4	20.2	12.8	19.4	26.1	11.5	13.4	12.5	7.7	11.2	18.1
Th	3.95	2.35	1.51	1.77	2.45	3.30	0.93	2.38	3.12	0.25	1.49	0.26	0.40	0.32	0.99
U	0.91	0.45	0.34	0.44	0.64	0.79	0.31	0.53	0.71	0.15	0.34	0.08	0.10	0.07	0.31
La	33.61	9.43	13.91	17.71	15.27	26.92	14.6	22.59	32.0	3.44	16.3	2.75	3.8	3.19	8.56
Ce	76.04	38.66	32.79	43.27	45.76	63.56	33.5	53.23	77.0	8.79	35.8	7.83	10.0	8.06	21.99
Pr	10.01	4.58	4.33	5.60	5.49	8.25	4.63	6.88	9.98	1.34	4.70	1.22	1.47	1.25	2.88
Nd	37.41	21.02	18.78	24.30	22.75	32.20	19.7	28.43	41.7	6.93	20.1	6.23	7.15	6.51	12.95
Sm	7.79	5.31	3.97	4.91	5.40	6.87	4.69	5.71	8.03	1.68	3.79	1.80	1.62	1.57	3.29
Eu	2.21	1.79	1.01	1.46	1.55	1.96	0.82	1.80	2.31	0.92	1.04	0.59	0.45	0.55	1.14
Gd	6.82	5.64	4.69	5.21	5.30	6.90	3.89	5.56	8.09	2.41	4.25	2.13	1.92	2.37	3.54
Tb	0.96	0.79	0.60	0.71	0.73	0.91	0.52	0.82	1.14	0.38	0.57	0.36	0.29	0.37	0.59
Dy	5.12	4.14	2.89	3.67	3.73	4.52	2.66	4.50	6.04	2.27	2.84	2.28	1.68	2.20	3.65
Ho	0.85	0.78	0.51	0.67	0.64	0.85	0.56	0.78	0.98	0.43	0.50	0.53	0.31	0.39	0.71
Er	2.46	2.03	1.40	1.84	2.08	2.00	1.37	1.94	2.63	1.14	1.36	1.46	0.91	1.23	1.77
Tm	0.27	0.28	0.18	0.24	0.24	0.28	0.15	0.26	0.32	0.19	0.18	0.19	0.10	0.19	0.27
Yb	1.90	1.50	1.21	1.53	1.53	1.84	0.89	1.69	1.93	1.08	0.99	1.35	0.68	1.17	1.52
Lu	0.21	0.17	0.14	0.17	0.19	0.19	0.10	0.19	0.25	0.12	0.14	0.13	0.07	0.13	0.22

LOI, loss on ignition. ud, undetected. Kom Bas, komatiitic basalt.

3.3 Volcanic Rocks Geochemistry

3.3.1 Classification

The two groups of volcanic rocks identified in the field (green versus black-weathering) and petrographically also correspond to two chemical groups (Figure 3-1). The green-weathering volcanic rocks, including the olivine-blastoporphyritic sills, have the highest Mg values and are therefore komatiitic in nature (Figure 3-1). The black-weathering volcanic rocks have a narrow geochemical range, with higher concentrations of Al and lower concentrations of Mg, placing them dominantly within the Fe-rich tholeiitic field (Figure 3-1). Most localities expose samples with a range in composition. For instance, the Totnes Road and Sunneshine localities include komatiites, komatiitic basalts, and tholeiites. The North Touak and Cape Dyer (Figure 2-6) localities expose both komatiites and komatiitic basalts, and the NW valley locality has both komatiitic basalts and tholeiites. Less compositional diversity was documented at the Mermaid Fiord (tholeiitic basalt) and Mooneshine (komatiitic basalt) localities (Figure 2-6). Given the lithologic variability present at any one locality, the samples in this chapter will be divided based upon their classification as komatiites, komatiitic basalts, and tholeiites, with the exception of the Totnes Road Fiord locality samples, as they have been the focus of a previous publication (Keim et al., 2011).

3.3.2 Geochemistry of the komatiitic volcanic rocks

The definition of a komatiite states that they have >18wt% MgO, <52wt% SiO_2 with values generally between 40-45%, high Cr (>800ppm) and high Ni (>400ppm) (Arndt, 2008). In accordance with this definition, the komatiitic volcanic rocks and the olivine-blastoporphyritic sills have the highest MgO, Cr, and Ni values ranging from 18.03-23.70 wt%, 1061-2575 ppm, and 703-1795 ppm, respectively, and low SiO_2 values of 43.48-50.63 wt%. The komatiitic basalts have intermediate MgO, Cr, and Ni values ranging from 9.10-20.03 wt%, 826-2471 ppm, and 298-1721 ppm, respectively, with low SiO_2 values of 42.70-49.34 wt%.

Subdivision of komatiites on the basis of alumina was proposed by Nesbit et al. (1979) given the observation that alumina values varied among komatiites worldwide and the understanding that alumina content is controlled by the depth of the melt source. Alumina-

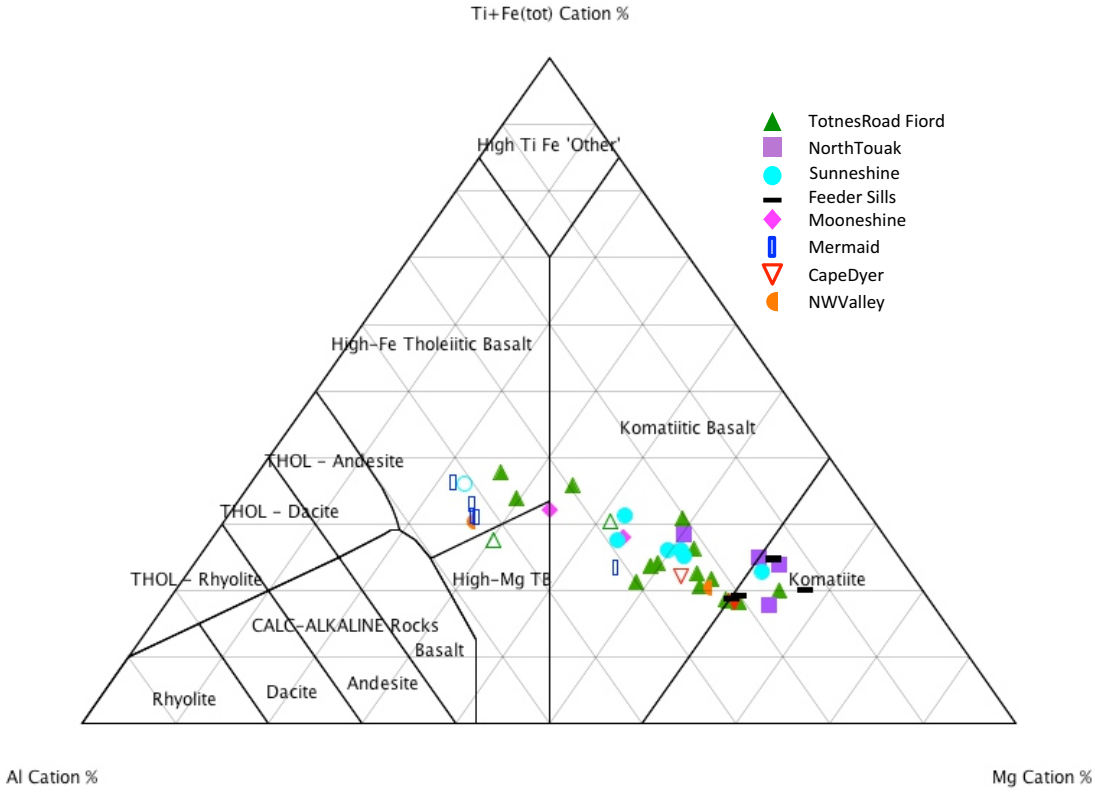

Figure 3-1. Jensen (1979) classification diagram for volcanic rocks showing the spread of the North Touak-Cape Dyer volcanic rocks from komatiites to komatiitic basalts and into the high-Fe tholeiitic basalt field.

depleted komatiites (ADK), first described from the Barberton Greenstone Belt in South Africa (Viljoen & Viljoen, 1969), are characterized by CaO/Al_2O_3 around 1.5, low Al_2O_3 / TiO_2 of approximately 11, and HREE depletion relative to the LREE (Nesbit, 1979). Depletion in alumina and the HREEs is consistent with majorite garnet being present in the residue during melting (Herzberg, 1995). Alumina-undepleted komatiites (AUK), first described in the Munro Township in the Abitibi Greenstone Belt of Canada (Pyke et al., 1973), are characterized by chondritic ratios of CaO/Al_2O_3 (~ 1) and Al_2O_3 / TiO_2 (~20), with flat REE patterns (Nesbit et al., 1979). Majorite garnet is only stable in the mantle at depths of >250km, therefore ADK reflect deep-mantle melting, whereas AUK reflect relatively shallow (i.e., <250km) melting. The komatiites of the North Touak-Cape Dyer volcanic belt have an average CaO/Al_2O_3 of 1.2 and an average Al_2O_3 / TiO_2 of 7.19. The komatiitic basalts have average CaO/Al_2O_3 and Al_2O_3 / TiO_2 ratios of 1.15 and 6.61, respectively, comparable to those of the komatiites. As such, the komatiitic and komatiitic basaltic volcanic rocks of the North Touak-Cape Dyer volcanic belt appear to show affinity for the alumina-depleted group (Nesbit, 1979), however, enrichment in other trace elements highlights that further examination of this characteristic is warranted.

A distinctive geochemical aspect of the North Touak-Cape Dyer volcanic rocks is their unusually high concentrations of TiO_2 (Figure 3-2a), which range between 0.79-1.77 wt% for the komatiites and 0.83-3.03wt% for the komatiitic basalts (Table 3-1). In contrast, AUK and ADK typically contain 0.3-0.4wt% TiO_2 (Viljoen et al., 1983 and Xie & Kerrich, 1993). Although there is no strict definition of Ti enrichment in komatiites, an examination of available literature suggests that komatiites with >0.5wt% TiO_2 are considered enriched. Given that the komatiites and komatiitic basalts appear to be enriched in TiO_2, it may not be appropriate to use Nesbit's classification scheme, given that TiO_2 is used as a proxy to determine Al depletion. Closer examination of the Al_2O_3 values (komatiites = 5.41-9.85 wt%; komatiitic basalts = 6.29-12.40wt%) compared to Al-undepleted komatiites from the Munro Township (4.3-9.6wt%) suggests that these rocks are not, in fact, alumina-depleted (Figure 3-2b). This is also reflected in Nesbit's classification scheme by the fact that the CaO/Al_2O_3 ratios of 1.15 and 1.2 for the komatiitic basalts and komatiites, respectively, are closer to ~1 (AUK) than to 1.5 (ADK).

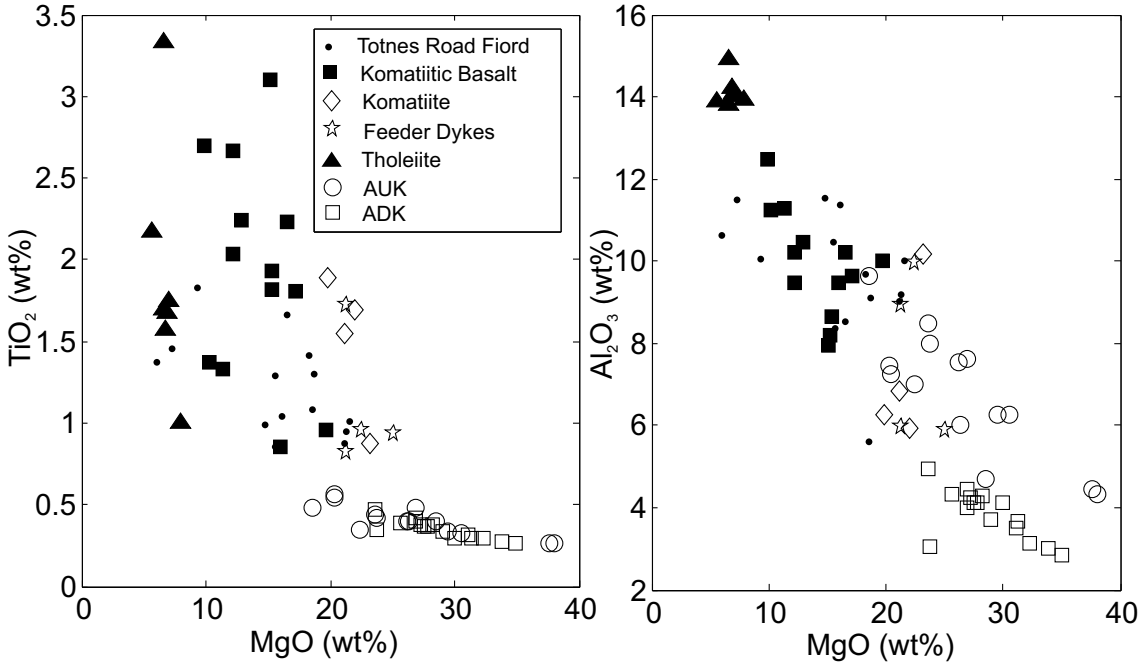

Figure 3-2. a) Plot of TiO_2 (wt%) versus MgO (wt%) for all volcanic samples from the North Touak-Cape Dyer volcanic belt, AUK, and ADK highlighting the apparent enrichment of Ti throughout the Totnes Road formation compared to 'classic' komatiites. b) Plot of Al_2O_3 (wt%) versus MgO (wt%) highlighting the fact that the volcanic rocks are not depleted in alumina. Data for AUK from Munro Township (Fan and Kerrich, 1997) and for ADK from the Barberton area (Viljoen et al., 1983).

Another unusual feature of the komatiites and komatiitic basalts, is that, in addition to being enriched in Ti, the rocks are also enriched in other high-field strength elements (HFSE) including Zr, Nb, Th, and the rare-earth elements (REE). On MORB-normalized diagrams Al-undepleted (Fan & Kerrich, 1997; Xie et al., 1993) and Al-depleted komatiites (Viljoen et al., 1983 and Chavagnac, 2004) have the conjunction of flat unfractionated patterns and depletion of all the HFSE relative to MORB (Figure 3-3). A key feature of the Al-depleted komatiites is a negative Nb anomaly related to magma-crust interaction (Pearce 2007), which is absent in all komatiitic samples from the North Touak-Cape Dyer volcanic belt. The komatiites have strongly fractionated patterns with enrichment of all HFSE except the HREE, which are depleted relative to MORB (Figure 3-3). The komatiitic basalts display the greatest enrichment with average $Th/Yb_{MORB} = 25.12$ compared to the komatiites value of 17.62. Negative anomalies of Zr-Hf, as well as Y, characterize the komatiitic basalts (average $Sm/Zr_{MORB} = 1.22$) and komatiites (average $Sm/Zr_{MORB} = 1.40$).

Both the komatiites and komatiitic basalts are characterized by LREE enrichment with average La/Yb_{cn} values between 1.41 and 11.45 for the komatiites and between 1.55 and 16.07 for the komatiitic basalts. Both lithologies also display distinct HREE depletion with average Gd/Yb_{cn} values between 1.30 and 3.61 for the komatiites, and between 1.49 and 4.26 for the komatiitic basalts. On chondrite normalized diagrams, all komatiitic samples show smooth, fractionated REE profiles (Figure 3-4). Some of the samples from the volcanic belt exhibit positive and negative Eu anomalies; this is likely due to the documented mobility of Eu during alteration and metamorphism compared to the other REE (Sun & Nesbitt, 1978 and Barley et al., 2000), rather than representing a primary magmatic feature.

3.3.3 Geochemistry of the tholeiitic volcanic rocks

The black-weathering volcanic rocks from the North Touak-Cape Dyer volcanic belt have lower MgO, Ni, and Cr values and higher SiO_2 values than the komatiitic rocks, with their high values of $FeO+TiO_2$ establishing them as tholeiites. The rocks MgO values vary from 5.58-7.90 wt%, Cr from 73-310 ppm, Ni from 80-124 ppm, and $FeO+TiO_2$ from 14.22-20.45 wt% compared to 11.44-18.85 wt% for the komatiitic rocks. The tholeiites also show strongly fractioned, enriched patterns on MORB-normalized diagrams with average Th/Yb = 14.08

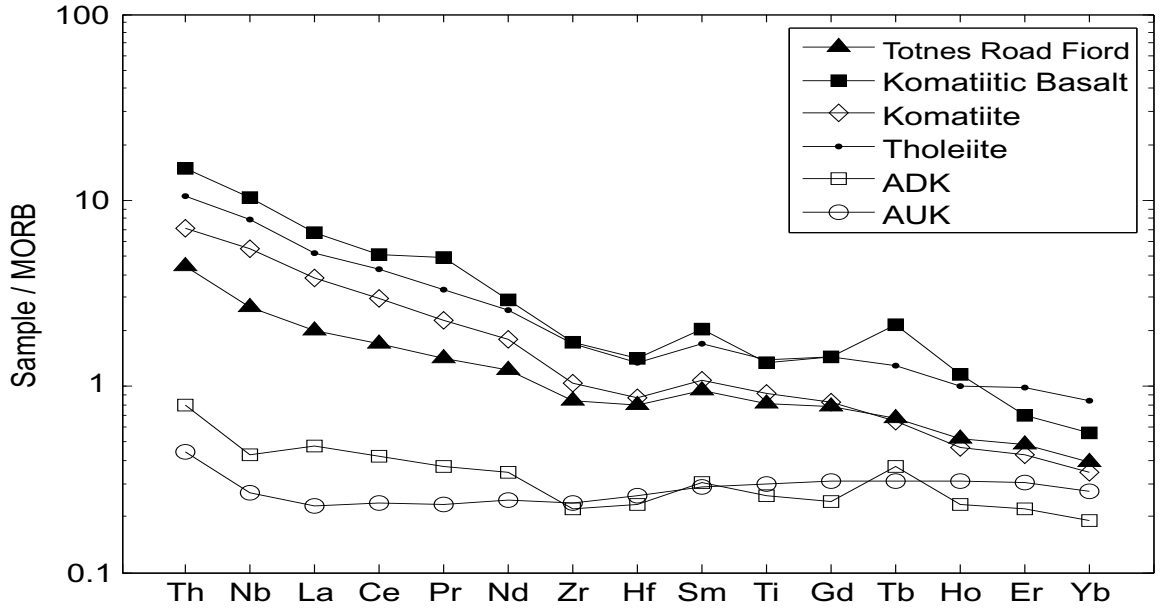

Figure 3-3. MORB normalized plot of select HFSE and REE for the volcanic samples from the North Touak-Cape Dyer volcanic belt, AUK, and ADK, which shows that all of the North Touak-Cape Dyer volcanic samples are strongly fractionated, with enrichment of HFSE compared to AUK and ADK. Note negative Zr-Hf anomaly for the volcanic belt samples and ADK. Data sources as in Figure 3-2. MORB value from Sun and McDonough, 1983.

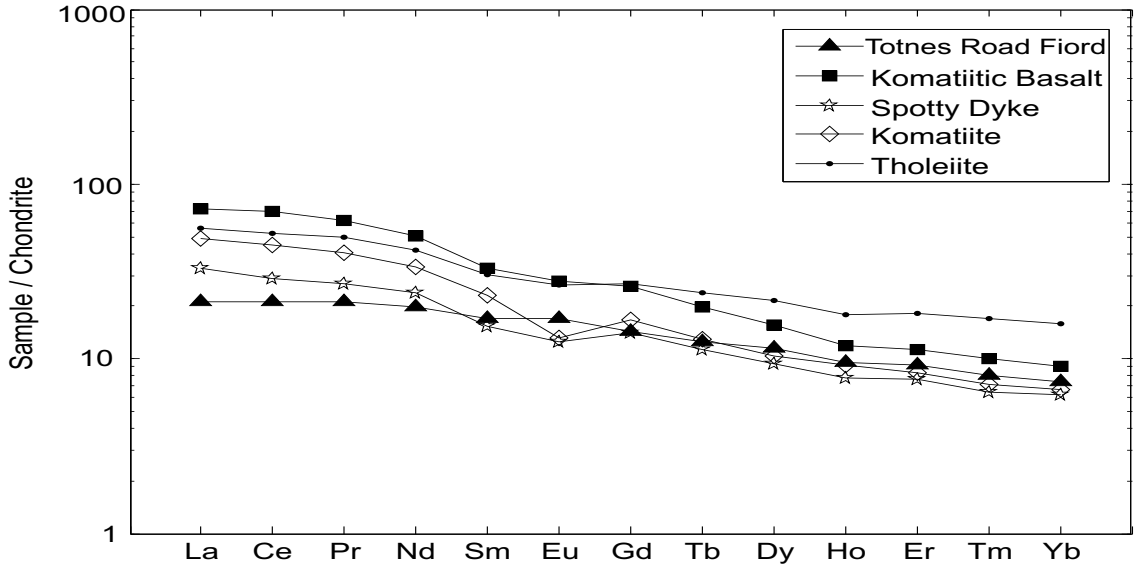

Figure 3-4. Chondrite normalized (Anders and Grevesse, 1989) plot for the volcanic samples from the North Touak-Cape Dyer volcanic belt showing that the samples exhibit LREE enrichment relative to HREE.

(Figure 3-3). Zr-Hf and Y anomalies are present with average Sm/Zr = 1.44. The tholeiites exhibit LREE enrichment with La/Yb_{cn} values between 1.8 and 11.51 and distinct HREE depletion with Gd/Yb_{cn} values between 1.34 and 3.47 (Figure 3-4). The majority of the tholeiitic samples are from Mermaid Fiord (4/10) and Totnes Road Fiord (3/10) with one from the NW Valley locality, one from the Sunneshine area, and one from just west of the Totnes Road Fiord locality. Thus, although they represent a small proportion of the geochemical dataset, the tholeiites are found throughout the length of the North Touak-Cape Dyer volcanic belt, and with the exception of the Mermaid Fiord locality, are always found in association with komatiitic volcanic rocks.

3.3.4 Geochemical effects of Alteration and Metamorphism

All of the volcanic rocks within the North Touak-Cape Dyer volcanic belt likely experienced some degree of seawater alteration given their extrusive ultramafic nature and subsequently were subjected to amphibolite-facies metamorphism. Therefore, care must be taken when selecting elements to use for petrogenetic and tectonic interpretations, as some elements may have been mobilized during alteration and/or metamorphism possibly resulting in modification of their primary concentrations.

Although primary textures are preserved in the volcanic rocks, primary minerals are not. All of the rocks studied are composed of a secondary mineral assemblage dominated by amphiboles and chlorite. The presence of this secondary mineral assemblage, combined with the large geographic spread of the samples, and lack of locations with multiple samples, makes determining the amount of major and trace element mobility within the volcanic rocks difficult. Comparing elements from individual grab samples located tens to hundreds of kilometers apart leads to inherent variability.

Based on a large number of studies of mafic and ultramafic rocks it is generally accepted that most major elements, the high field-strength elements (HFSE), the rare-earth elements (REE), transition metals, and Y are generally immobile during alteration and metamorphism; whereas, the large ion lithophile (LILE) elements such as Cs, Na, K, Rb, Ba, Ca, Pb, and Sr are

generally mobile (Cann, 1970; Winchester and Floyd, 1975; Sun and Nesbitt, 1978; Arndt and Nesbitt, 1982; Barnes and Often, 1990; Fan and Kerrich, 1997; Barley et al., 2000; Hanski et al., 2001; Arndt, 2008; Said and Kerrich, 2009). However, under certain conditions immobile elements may become mobile. Lahaye et al., (1995) found that the HFSE and REE had been mobilized in carbonitized komatiites from the Texmont region in the Abitibi belt, likely by CO_2-rich fluids. Gruau et al., (1992) documented REE mobility in komatiites from eastern Finland, a feature also attributed to CO_2-rich fluids.

Detailed studies of alteration and element mobility usually consist of analysis of primary minerals and/or comparing element concentrations from multiple samples from a single flow. Given the baseline nature and large geographic area to sample, this type of detailed work is beyond the scope of this research. However, a variety of methods were used to try and determine which elements were mobile and which were immobile for the volcanic rocks including: comparison of normative mineralogy with known komatiites (Table 3-2), correlation matrices (Table 3-3), Pearce-element ratios (PER) (Figure 3-5), and incompatible element patterns (Figure 3-3 and 3-4).

The CIPW normative mineralogy was determined for the volcanic rocks in order to compare with classic komatiites. The volcanic rocks were first split up into five distinct groups: komatiites, komatiitic basalts, tholeiites, olivine-blastoporphyritic sills, and samples from the Totnes Road Fiord locality. Average normative mineralogies for the volcanic rocks as well as for classic komatiites (AUK and ADK) are presented in Table 3-2. The komatiitic samples including those from Totnes Road Fiord and the potential feeder sill samples have comparable olivine and clinopyroxene to AUK and ADK, with less orthopyroxene but more plagioclase. Predictably, the Totnes Road Fiord basalt (variolitic unit 5, Chapter 2) and regional tholeiite samples have less olivine and orthopyroxene, with greater concentrations of plagioclase. Overall, the normative mineralogy of the North Touak-Cape Dyer volcanic rocks is comparable to 'classic' komatiites. This suggests that the major elements were not mobilized enough to make an obvious discrepancy in the normative mineralogy of the volcanic rocks. Although variations exist between the different lithologies, overall patterns exist that make sense given the mafic and ultramafic nature of these rocks. The tholeiite and Totnes Road Fiord basalt samples contain the

least amount of olivine and most amount of plagioclase, consistent with their mafic, versus ultramafic, nature. The komatiites and feeder sills have the highest concentrations of olivine and lowest of plagioclase, consistent with them being the most ultramafic samples. The remaining Totnes Road Fiord samples and komatiitic basalt samples have near identical concentrations of all of the minerals and represent a middle ground between mafic and ultramafic.

Locality	Clinopyroxene	Orthopyroxene	Olivine	Plag
Totnes	25.0	9.9	28.2	32.0
Totnes Basalts	21.5	0.9	19.8	52.0
Komatiitc Basalts	26.1	6.2	25.0	35.0
Komatiites	18.6	20.1	31.6	26.0
Feeder Sills	17.2	14.2	37.4	20.0
Tholeiites	20.7	3.0	16.2	54.0
AUK	15.3	25.1	35.8	23.0
ADK	23.3	30.5	28.7	17.0

Table 3-2. Normative mineralogy calculations for volcanic samples from the North Touak-Cape Dyer volcanic belt as well as 'classic' komatiites. Data sources as in Figure 3-3.

Titanite has been known to be enriched in the LREE as well as elements such as Zr and Nb (Henderson, 1980 and Vuorinen and Hålenius 2005). Lahaye et al. (1995) reported that in samples from the Alexo flow, found within the Abitibi greenstone belt, glass was altered to an assemblage of titanite and/or epidote. They found that Ti, the REE, and the HFSE were not mobilized in this flow because they were retained by titanite, a relatively resistant mineral. Flows in which the REE and HFSE were mobilized did not contain minerals such as titanite or abundant amphibole, which would have retained them in the rock (Lahaye et al., 1995). In their study on alteration of komatiites they found that elements generally considered to be immobile, were only mobilized by CO_2-rich fluids, with the related formation of carbonate alteration.

Volcanic samples from the North Touak-Cape Dyer belt contain only trace amounts of carbonate minerals, thus lacking pervasive carbonatization. In addition, they contain pervasive, small (micrometer scale) titanite grains and are dominated by a hydrous metamorphic mineral

assemblage. Therefore, the current mineralogy of the komatiitic and basaltic rocks strongly suggests that immobile elements were retained and preserved in titanite and/or amphibole.

With the aid of ioGAS geochemical software, a correlation matrix was created using Pearson's correlation coefficient for the five different groups of volcanic rocks from the North Touak-Cape Dyer volcanic belt (Tables 3-3a-e). For the purpose of this study, a R^2 value > 0.7 is taken as a strong correlation and sample pairs with R^2>0.7 are highlighted by bold font in the tables, those between 0.5-0.7 are considered moderately correlative, and < 0.5 weakly correlative. In these tables, it is clear that TiO_2, Fe_2O_3, the HFSE (represented by Th, Nb, and Zr), and the LREE (represented by La and Nd) correlate well with each other, MgO and the HREE (represented by Ho) show variable correlations, and Al_2O_3 correlates poorly. MgO may not always correlate well with other major elements but consistently shows the best correlations with the HREE. The komatiitic samples show strong correlations for all elements, however, this is likely related to the fact that most of the komatiite samples were of the olivine-blastoporphyritic sills or were from restricted geographic locations.

With the exception of the Totnes Road Fiord samples, the other groups represent samples taken from a broad geographic area, therefore much of the variability in their R^2 values could be related to a variety of factors including: different source region, interaction with different material during ascent, and/or eruption into a different environment. The most appropriate interpretation of this correlation matrix is that TiO_2, FeO*, the HFSE, and the LREE were immobile likely because they were retained in titanite and/or amphiboles, MgO and the HREE were variably mobile together, and Al_2O_3 was mobile.

Pearce element ratios (PER) (Pearce, 1968) were constructed to determine if the North Touak-Cape Dyer volcanic belt samples plot on a mineral control line. Mineral control lines are lines of constant slope on bivariate geochemical plots; if a single mineral species is controlling the rock suites geochemical characteristics then the samples will plot along its respective control line. Mg+Fe/Ti (cations) was used as the atomic ratio to determine if olivine or a pyroxene was the controlling mineral. Ti and Zr were chosen as denominators as they are usually considered

Table 3-3a. Select R values for Totnes Road Fiord

	TiO^2	Al^2O^3	Fe^2O^3	MgO	Nb	Zr	Th	La	Nd	Ho
TiO^2	**1**	0.21	**0.84**	-0.6	**0.93**	**0.98**	**0.85**	**0.79**	**0.89**	**0.74**
Al^2O^3	0.21	**1**	0.59	-0.54	0.13	0.11	0.079	0.45	0.36	0.22
Fe^2O^3	**0.84**	0.59	**1**	**-0.77**	**0.72**	**0.78**	0.61	**0.82**	**0.86**	0.68
MgO	-0.6	-0.54	**-0.77**	**1**	-0.54	-0.64	-0.45	**-0.8**	**-0.81**	**-0.72**
Nb	**0.93**	0.13	**0.72**	-0.54	**1**	**0.93**	**0.94**	**0.85**	**0.89**	0.66
Zr	**0.98**	0.11	**0.78**	-0.64	**0.93**	**1**	**0.84**	**0.79**	**0.9**	**0.76**
Th	**0.85**	0.079	0.61	-0.45	**0.94**	**0.84**	**1**	**0.83**	**0.82**	0.62
La	**0.79**	0.45	**0.82**	**-0.8**	**0.85**	**0.79**	**0.83**	**1**	**0.94**	**0.71**
Nd	**0.89**	0.36	**0.86**	**-0.81**	**0.89**	**0.9**	**0.82**	**0.94**	**1**	**0.82**
Ho	**0.74**	0.22	0.68	**-0.72**	0.66	**0.76**	0.62	**0.71**	**0.82**	**1**

Table 3-3b. Select R values for Spotted Sill

	TiO^2	Al^2O^3	Fe^2O^3	MgO	Nb	Zr	Th	La	Nd	Ho
TiO^2	**1**	-0.49	**0.97**	-0.35	**0.98**	0.53	**0.99**	**0.98**	**1**	0.56
Al^2O^3	-0.49	**1**	-0.64	-0.27	-0.38	0.021	-0.37	-0.33	-0.41	0.44
Fe^2O^3	**0.97**	-0.64	**1**	-0.12	**0.96**	0.32	**0.94**	**0.93**	**0.95**	0.41
MgO	-0.35	-0.27	-0.12	**1**	-0.26	**-0.97**	-0.37	-0.38	-0.4	-0.5
Nb	**0.98**	-0.38	**0.96**	-0.26	**1**	0.41	**0.99**	**0.99**	**0.98**	0.66
Zr	0.53	0.021	0.32	**-0.97**	0.41	**1**	0.52	0.52	0.56	0.45
Th	**0.99**	-0.37	**0.94**	-0.37	**0.99**	0.52	**1**	**1**	**1**	0.67
La	**0.98**	-0.33	**0.93**	-0.38	**0.99**	0.52	**1**	**1**	**0.99**	**0.7**
Nd	**1**	-0.41	**0.95**	-0.4	**0.98**	0.56	**1**	**0.99**	**1**	0.63
Ho	0.56	0.44	0.41	-0.5	0.66	0.45	0.67	**0.7**	0.63	**1**

Table 3-3c. Select R values for Komatiites

	TiO^2	Al^2O^3	Fe^2O^3	MgO	Nb	Zr	Th	La	Nd	Ho
TiO^2	**1**	**-0.97**	**0.9**	**-0.86**	**0.99**	**0.99**	**0.97**	**0.93**	**0.89**	-0.55
Al^2O^3	**-0.97**	**1**	**-0.94**	**0.75**	**-0.97**	**-0.97**	**-0.97**	**-0.98**	**-0.94**	0.4
Fe^2O^3	**0.9**	**-0.94**	**1**	-0.54	**0.92**	**0.94**	**0.98**	**0.89**	**0.8**	-0.51
MgO	**-0.86**	0.76	-0.54	**1**	**-0.82**	**-0.79**	**-0.7**	**-0.72**	**-0.75**	0.46
Nb	**0.99**	**-0.97**	**0.92**	**-0.82**	**1**	**1**	**0.98**	**0.9**	**0.85**	-0.61
Zr	**0.99**	**-0.97**	**0.94**	**-0.79**	**1**	**1**	**0.99**	**0.91**	**0.85**	-0.6
Th	**0.97**	**-0.97**	**0.98**	**-0.7**	**0.98**	**0.99**	**1**	**0.91**	**0.84**	-0.58
La	**0.93**	**-0.98**	**0.89**	**-0.72**	**0.9**	**0.91**	**0.91**	**1**	**0.99**	-0.22
Nd	**0.89**	**-0.94**	**0.8**	**-0.75**	**0.85**	**0.85**	**0.84**	**0.99**	**1**	-0.098
Ho	-0.55	0.4	-0.51	0.46	-0.61	-0.6	-0.58	-0.22	-0.098	**1**

Table 3-3d. Select R values for Komatiitic Basalts

	TiO^2	Al^2O^3	Fe^2O^3	MgO	Nb	Zr	Th	La	Nd	Ho
TiO^2	**1**	0.026	**0.89**	-0.48	**0.87**	**0.9**	**0.89**	**0.92**	**0.96**	**0.93**
Al^2O^3	0.026	**1**	-0.048	-0.56	0.31	0.3	0.34	0.0047	-0.02	0.2
Fe^2O^3	**0.89**	-0.048	**1**	-0.26	**0.8**	**0.79**	**0.83**	**0.93**	**0.94**	**0.85**
MgO	-0.48	-0.56	-0.26	**1**	-0.56	-0.66	-0.62	-0.34	-0.35	-0.49
Nb	**0.87**	0.31	**0.8**	-0.56	**1**	**0.86**	**0.99**	**0.81**	**0.83**	**0.86**
Zr	**0.9**	0.3	**0.79**	-0.66	**0.86**	**1**	**0.92**	**0.77**	**0.83**	**0.86**
Th	**0.89**	0.34	**0.83**	-0.62	**0.99**	**0.92**	**1**	**0.82**	**0.85**	**0.87**
La	**0.92**	0.0047	**0.93**	-0.34	**0.81**	**0.77**	**0.82**	**1**	**0.98**	**0.85**
Nd	**0.96**	-0.02	**0.94**	-0.35	**0.83**	**0.83**	**0.85**	**0.98**	**1**	**0.91**
Ho	**0.93**	0.2	**0.85**	-0.49	**0.86**	**0.86**	**0.87**	**0.85**	**0.91**	**1**

Table 3-3e. Select R values for Tholeiites

	TiO^2	Al^2O^3	Fe^2O^3	MgO	Nb	Zr	Th	La	Nd	Ho
TiO^2	**1**	**0.77**	**0.91**	-0.56	**0.98**	**0.94**	**0.97**	**0.96**	**0.98**	0.34
Al^2O^3	**0.77**	**1**	0.46	0.029	**0.8**	**0.71**	**0.74**	**0.75**	**0.78**	-0.15
Fe^2O^3	**0.91**	0.46	**1**	**-0.78**	**0.86**	**0.92**	**0.89**	**0.87**	**0.88**	0.51
MgO	-0.56	0.029	**-0.78**	**1**	-0.43	-0.59	-0.46	-0.5	-0.51	**-0.84**
Nb	**0.98**	**0.8**	**0.86**	-0.43	**1**	**0.93**	**0.99**	**0.99**	**0.99**	0.15
Zr	**0.94**	**0.71**	**0.92**	-0.59	**0.93**	**1**	**0.93**	**0.93**	**0.94**	0.27
Th	**0.97**	**0.74**	**0.89**	-0.46	**0.99**	**0.93**	**1**	**0.98**	**0.98**	0.15
La	**0.96**	**0.75**	**0.87**	-0.5	**0.99**	**0.93**	**0.98**	**1**	**0.99**	0.17
Nd	**0.98**	**0.78**	**0.88**	-0.51	**0.99**	**0.94**	**0.98**	**0.99**	**1**	0.23
Ho	0.34	-0.15	0.51	**-0.84**	0.15	0.27	0.15	0.17	0.23	**1**

immobile and showed good correlations with other elements. Major elements, such as Na and Al, were also plotted, even though those elements may be mobile, and the results were consistent with those obtained by using Ti and Zr. This indicates that the enrichment seen in Ti and Zr does not affect the outcome of the PER diagrams. The results of both graphs (Figure 3-5 a,b) give the same result. The komatiite and olivine-blastoporphyritic sill samples plot with a slope =1, tholeiites with a slope = 0.5, and the komatiitic basalts and Totnes Road samples with slopes between 1 and 0.5 (slopes of 0.765 and 0.896, respectively).

The well-defined slope of 1 for the komatiite and feeder sill samples, which reflects orthopyroxene control, is an unexpected result for komatiitic rocks, as one would expect the samples to plot on an olivine control line (Fan and Kerrich, 1997) if crystal fractionation was the dominant control. It is possible that the samples plot with a slope of 1 because of the 50:50 fractionation of clinopyroxene (slope 2) and olivine (slope 0.5). It is also possible that fractionation at the very onset of melting was the dominant control on the rocks' chemistry, in which case majorite garnet is a more likely key phase. Although the resultant slopes may be somewhat difficult to interpret, it is clear that the rocks fall on well-defined trends for both denominators, which indicates that element mobility was not significant.

MORB-normalized multi-element diagrams were used to examine the trace element (HFSE and REE) characteristics of the Cumberland samples. The exact concentrations of the trace elements vary throughout the belt yet the patterns exhibited by the trace elements are similar with LREE enrichment and negative Zr-Hf anomalies (Figure 3-3 and 3-4). This consistent variability among the trace elements would likely have been destroyed if the HFSE and REE were mobile during alteration and metamorphism, as the fluid composition and/or volume would likely have varied throughout the belt.

Combining literature research, mineralogy, correlation matrices, PER, and multi-element diagrams, it would appear that the elements TiO_2, FeO*, P_2O_5, the HFSE, and the LREE were likely immobile, possibly due to their retention in titanite; that MgO may have been slightly mobile in some samples; and that the HREE were either mobile or that decoupling between the LREE and HREE occurred at some point during the rocks' history. SiO_2, Al_2O_3, CaO, Na_2O, and

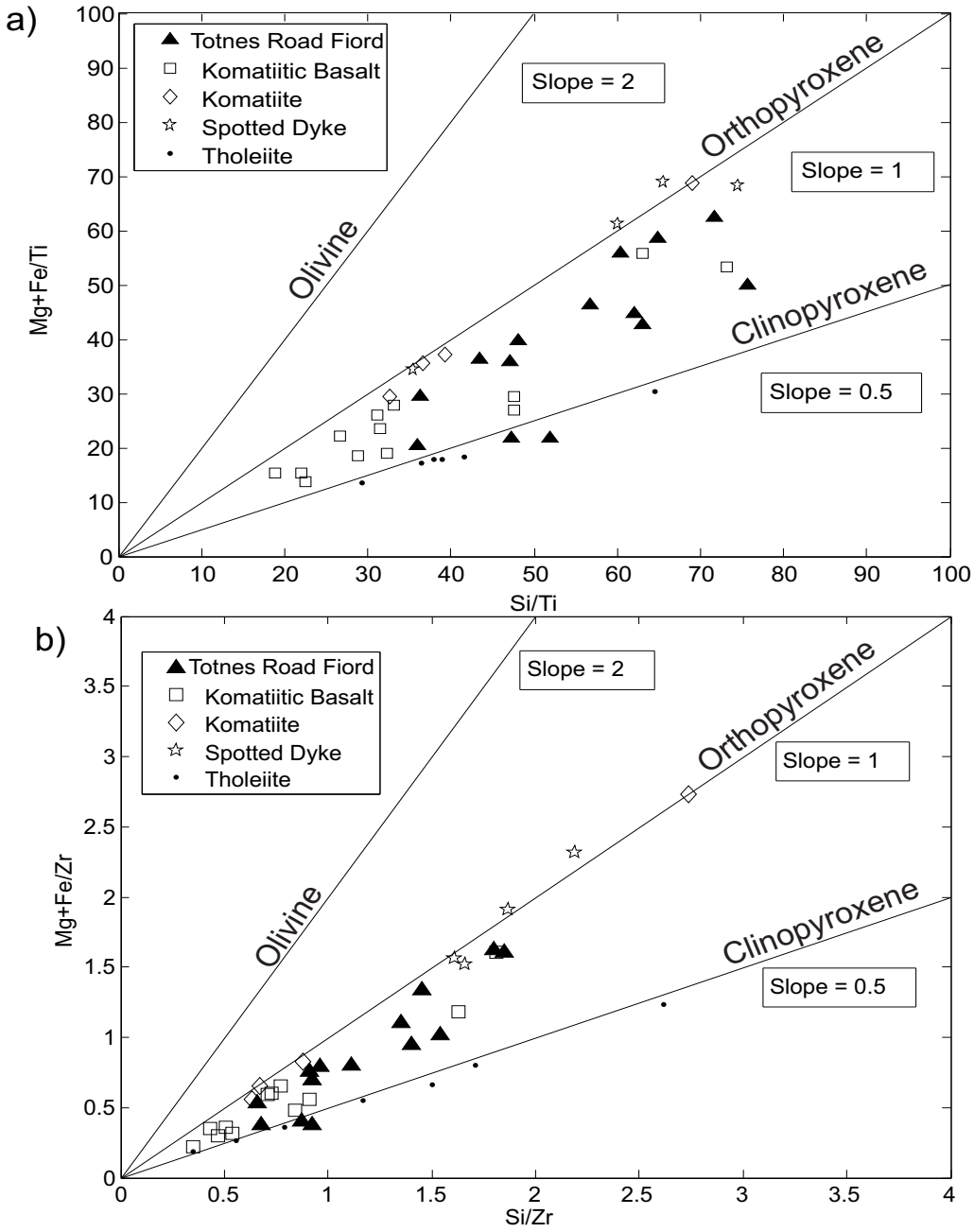

Figure 3-5 a) Plot of Mg+Fe/Ti vs. Si/Ti. b) Plot of Mg+Fe/Zr vs. Si/Zr to compare to plot a). Pearce element ratio plots after Pearce (1968) for the Totnes Road formation using two different denominators to show the consistency of the results. On both plots a slope = 2 represents an olivine control line, slope =1 represents an orthopyroxene control line, and slope =0.5 represents a clinopyroxene control line. The komatiite and spotted dyke samples plot with a slope =1, tholeiites with a slope = 0.5, and the komatiitic basalts and Totnes Road samples with slopes between 1 and 0.5. It appears that the chemistry of the Totnes Road formation was mainly controlled by pyroxene fractionation, slightly unusual for komatiites. (Note: spotted dyke is a field term used to refer to the olivine-blastoporphyritic sills)

K_2O were mostly mobile. For the purpose of this study, I will assume that the current concentrations of the immobile elements (TiO_2, FeO*, P_2O_5, the HFSE, and the LREE) are reasonable approximations of the primary magmatic concentrations and thus can be used as petrogenetic indicators. The enrichment of Ti, and the other HFSE, is a defining characteristic of the North Touak-Cape Dyer volcanic rocks, and given the above-mentioned data it is believed that these enrichments are not the result of secondary processes, but are caused by primary magmatic processes and therefore need to be explained petrogenetically (Chapter 4).

3.3.5 Geochemistry of the chemical sedimentary rocks

Representative geochemical samples were collected for the different varieties of silicate facies iron formation, the sulphide-rich boulders, and for associated clastic sedimentary rocks from the North Touak-Cape Dyer volcanic belt (Table 3-4). Geochemical analyses were performed to investigate constraints on the origin and depositional environment of the chemical sedimentary rocks from across the volcanic belt.

As mentioned in section 2.3.2, three varieties of iron formation were distinguished in the field. These three varieties can be seen to correspond to three distinct chemical groups based primarily on FeO and Al_2O_3 concentrations. Group I, which consists of green biotite + garnet + quartz ± magnetite ± grunerite has high FeO concentrations, average 30 wt%, indicative of a hydrothermal source, however, it also has moderate levels of Al_2O_3, average 10wt%, which is generally interpreted as representative of a detrital source (Boström, 1973; Peter, 2003). Group II, which consists of grunerite with minor amounts of biotite and/or garnet ± magnetite has higher FeO concentrations than group I, average 37.6 wt%, and lower but still appreciable Al_2O_3 values, average 4.7wt%. Group III which consists entirely of grunerite + magnetite has higher FeO concentrations than either group I or II, average 43 wt%, and negligible Al_2O_3 values, average 0.35 wt%. These chemical differences suggest that variable degrees of hydrothermal input may have resulted in the observed lithological variations.

Table 3-4. Whole-rock analyses for the North Touak-Cape Dyer volcanic belt chemical sedimentary rocks

Sample Name	R215B	R188	R216	R192A	Y76A	R201A-1	R236
Location	Totnes Road Fiord	Moonshine	Totnes Road Fiord	Moonshine	Totnes Road Fiord	North Touak	Totnes Road Fiord
Classification	clastic	SFIF	SFIF	SFIF	SFIF	SFIF	clastic
(wt%)							
SiO2	54.00	48.10	41.90	44.30	44.00	48.20	70.40
TiO2	0.66	0.38	0.57	0.27	0.02	0.02	0.60
Al2O3	16.50	7.98	12.70	3.93	0.37	0.24	11.40
FeO*	14.70	31.70	33.40	38.20	50.90	38.60	5.98
MnO	2.06	4.99	2.70	7.67	2.51	1.31	0.08
MgO	2.05	2.14	2.91	4.19	2.26	1.60	3.71
CaO	0.36	0.54	0.92	1.59	0.99	1.51	2.55
Na2O	5.03	3.53	0.03	0.03	<0.01	0.02	2.02
K2O	4.48	0.94	4.27	0.12	<0.01	0.02	2.25
P2O5	0.12	0.18	0.35	0.62	0.55	0.85	0.10
Cr2O3	0.02	<0.01	0.02	<0.01	<0.01	<0.01	0.04
V2O5	0.02	<0.01	0.02	<0.01	<0.01	0.01	<0.01
LOI	0.38	0.24	0.24	-0.85	-1.65	-1.59	1.06
Total	100.4	100.7	100.0	100.1	100.0	90.8	100.2
(ppm)							
Cr	114	88.2	187	48.4	20.9	23.2	314
Ni	57.9	42.3	52.4	41.7	16.4	10.3	66.2
Co	49.2	63.9	51.8	57.6	23.6	11.0	19.3
Sc	25.0	16.2	19.8	8.95	1.30	1.11	15.8
V	80.6	70.4	117	60.9	29.0	28.9	115
Cu	18.4	7.13	32.4	170	27.2	3.10	45.9
Pb	49.3	48.8	10.1	28.7	2.20	1.55	22.6
Bi	0.10	0.21	0.12	0.16	0.04	0.06	0.11
Zn	160	214	174	150	32.7	21.8	100
Cd	0.09	0.06	0.03	0.06	0.08	0.03	0.13
Sn	4.43	1.95	2.96	2.20	0.60	0.45	1.24
W	2.30	1.89	3.25	0.73	0.97	0.99	1.73
Mo	2.27	1.66	1.51	6.40	1.62	2.68	0.27
Ag	0.02	0.08	0.07	0.11	0.02	0.01	0.11
Sb	0.21	1.39	0.10	0.28	1.38	0.16	0.02
Rb	184	28.4	209	3.98	0.34	0.75	90.7
Cs	14.0	0.73	10.1	1.27	0.07	0.06	5.37
Ba	3437	499	902	926	23.7	26.6	491
Sr	60.0	14.1	5.38	59.5	11.2	36.7	164
Li	83.8	28.7	46.8	6.43	2.50	0.92	48.4
Be	0.87	1.48	0.75	2.74	0.96	0.29	0.76
Ge	3.71	9.28	8.00	9.98	9.98	7.56	1.67
As	2.79	4.76	1.52	1.81	3.67	2.23	1.41
Ta	1.94	0.83	1.30	0.64	0.04	0.04	0.68
Nb	17.2	10.6	15.8	12.7	1.02	1.10	8.50
Hf	3.46	2.50	3.24	1.50	0.11	0.04	5.10
Zr	81.8	83.2	92.4	56.1	8.00	6.56	167.95
Y	21.1	7.60	15.9	3.93	0.26	0.16	6.47
Th	1.39	0.81	1.45	0.68	0.26	0.28	1.28
U	15.3	15.4	24.6	21.1	18.8	18.6	14.1
La	46.3	32.9	26.9	11.5	14.3	3.96	10.8
Ce	106	118	84.7	41.2	44.0	8.30	33.3
Pr	10.4	8.04	7.40	3.14	3.88	0.76	3.11
Nd	35.4	29.7	28.1	13.4	16.4	3.45	11.4
Sm	6.44	5.55	5.60	3.54	4.03	1.26	2.40
Eu	1.31	1.27	1.23	1.32	1.06	0.41	0.63
Gd	5.05	5.11	6.04	4.76	4.29	2.37	2.34
Tb	0.64	0.64	0.90	0.74	0.67	0.42	0.36
Dy	3.72	3.66	5.65	4.60	4.12	3.12	2.55
Ho	0.76	0.75	1.14	0.96	0.85	0.71	0.57
Er	2.06	2.03	3.36	2.84	2.63	2.13	1.81
Tm	0.32	0.28	0.47	0.42	0.38	0.30	0.26
Yb	2.26	1.80	3.11	2.86	2.49	2.14	1.76
Lu	0.33	0.28	0.44	0.44	0.35	0.32	0.24

LOI, loss on ignition. SFIF, silicate facies iron formation.

Table 3-4 cont. Whole-rock analyses for the North Touak-Cape Dyer volcanic belt chemical sedimentary rocks

Sample Name	R203	R202B-4	R206	R191	R303E	R249B	R250	R201A-2
Location	Totnes Road Fiord	Totnes Road Fiord	Totnes Road Fiord	Moonshine	NW Valley	Totnes Road Fiord	Totnes Road Fiord	North Touak
Classification	SFIF	SFIF	SFIF	Sulphide Boulder	Sulphide Boulder	Clastic	SFIF	SFIF
(wt%)								
SiO2	51.10	48.10	46.40	42.80	9.49	52.60	49.60	52.60
TiO2	0.41	0.21	0.30	1.03	0.11	0.64	0.02	0.51
Al2O3	8.65	5.10	5.14	10.60	1.12	14.20	0.45	11.00
FeO*	30.10	36.30	38.30	18.60	60.70	19.80	39.90	26.00
MnO	0.91	5.55	5.92	0.29	0.09	2.66	2.26	5.47
MgO	3.69	4.30	3.87	6.97	0.11	2.69	7.12	1.66
CaO	0.36	1.42	1.15	8.12	0.03	0.70	0.61	1.98
Na2O	1.13	0.13	0.02	0.32	<0.01	0.28	0.11	0.05
K2O	3.31	0.19	0.15	0.90	0.11	3.54	<0.01	1.37
P2O5	0.12	0.21	0.14	0.18	0.11	0.19	0.01	0.17
Cr2O3	0.01	0.02	0.02	0.06	<0.01	0.05	<0.01	0.03
V2O5	0.01	0.01	0.01	0.05	<0.01	0.02	<0.01	<0.01
LOI	0.23	-0.92	-0.98	9.30	26.30	2.33	0.00	-0.34
Total	100.0	100.6	100.4	99.2	98.2	99.7	100.1	100.5
(ppm)								
Cr	79.7	77.0	138	303	47.9	228	15.1	133
Ni	31.3	33.5	42.1	109	482	58.5	25.6	41.2
Co	52.7	69.3	74.0	16.5	112	87.1	23.6	60.5
Sc	14.8	9.29	9.80	30.1	4.23	27.6	1.37	17.8
V	97.7	71.6	79.3	334	67.8	106	29.8	74.9
Cu	5.18	25.3	10.4	289	333	12.6	6.65	40.0
Pb	14.3	39.7	7.49	7.88	8.88	28.2	0.73	9.94
Bi	0.12	0.21	0.07	0.08	0.45	0.39	0.02	0.63
Zn	135	116	111	655	67.8	236	52.9	140
Cd	0.04	0.17	0.13	4.64	0.08	0.10	0.53	0.13
Sn	1.92	2.04	1.36	1.73	2.46	3.44	0.38	2.25
W	0.34	0.58	0.96	4.33	2.75	0.87	0.13	1.71
Mo	0.57	2.95	2.17	26.9	58.7	1.15	2.42	1.92
Ag	0.05	0.12	0.09	0.72	1.98	0.09	0.02	0.07
Sb	0.51	0.53	1.86	0.83	0.03	0.07	0.72	0.01
Rb	128	5.12	4.38	28.7	2.74	162	0.43	102.41
Cs	24.7	0.87	1.20	1.14	0.42	13.39	0.03	15.2
Ba	1137	124	99.1	150	48.0	1180	17.7	2929
Sr	117	28.7	15.5	120	2.69	28.6	11.5	15.7
Li	52.0	17.3	16.5	11.0	2.88	120	11.0	21.3
Be	0.77	0.42	0.55	1.01	0.05	1.05	0.72	1.30
Ge	6.06	7.52	8.55	3.77	ud	5.27	2.57	5.12
As	2.49	1.91	18.0	37.3	3.64	4.23	86.8	ud
Ta	0.73	0.49	0.96	0.31	0.19	1.57	0.04	1.12
Nb	13.2	6.10	9.70	5.50	1.77	16.9	0.78	14.1
Hf	2.65	1.63	2.02	2.38	0.43	3.31	0.11	2.46
Zr	79.0	50.7	78.8	70.9	14.4	91.2	5.55	72.6
Y	7.32	5.2	6.81	1.55	1.50	14.8	0.35	10.51
Th	0.67	0.90	1.12	8.95	10.9	1.51	0.24	1.33
U	9.80	15.4	11.9	19.8	5.75	27.8	9.30	18.4
La	3.58	37.6	8.49	9.27	2.89	39.5	5.48	14.6
Ce	12.8	114	32.3	20.5	6.05	119	13.4	44.9
Pr	0.99	9.79	2.46	2.9	0.88	9.92	1.29	3.60
Nd	3.99	37.1	9.64	13.0	3.52	35.8	5.34	13.7
Sm	0.83	6.36	2.45	3.31	0.85	7.04	1.07	3.54
Eu	0.21	1.31	0.87	1.10	0.22	1.48	0.28	1.13
Gd	1.35	5.15	3.02	3.95	0.95	7.30	1.26	4.95
Tb	0.26	0.64	0.47	0.60	0.16	1.04	0.21	0.68
Dy	2.07	3.59	2.79	3.71	1.08	6.45	1.49	4.17
Ho	0.48	0.72	0.61	0.78	0.24	1.20	0.34	0.81
Er	1.44	2.10	1.71	2.33	0.84	3.30	1.23	2.38
Tm	0.23	0.32	0.28	0.34	0.13	0.46	0.18	0.37
Yb	1.61	2.08	1.96	2.18	0.84	3.06	1.34	2.53
Lu	0.22	0.29	0.28	0.36	0.16	0.47	0.21	0.35

LOI, loss on ignition. ud, undetected. SFIF, silicate facies iron formation.

Two samples of the distinctive, fragmental sulphidic boulders (Figure 2-12a) were analyzed. One sample had a matrix dominated by pyrrhotite and accordingly had a high FeO value of 60.7 wt% and low Al_2O_3 value of 1.12 wt%. The other sample, which had a matrix dominated by graphite with minimal pyrrhotite, had a much lower FeO value, 18.6 wt%, and higher Al_2O_3, 10.6 wt%. Thus, the differences observed in thin section are also seen chemically.

Three clastic samples were analyzed to allow for comparison with the chemical sedimentary rocks. Two of the samples are medium-grained biotite + garnet semi-pelite and one a fine-grained biotite psammite. The clastic samples have the highest Al_2O_3 values, average 14 wt%, the lowest FeO values, average 13.5 wt%, and much greater SiO_2 values, average 59%, than the chemical sedimentary rocks, values from 26-38 wt%. This supports the assumption that Fe is dominantly hydrothermally sourced and that Al is detritally sourced.

It can be seen that most samples display LREE enrichment over the HREE, a positive Ce anomaly, and a negative Eu anomaly (Figure 3-6). The exceptions are the two sulphide boulder samples, as these lack the above-mentioned Ce and Eu anomalies. Clastic sedimentary rocks show the greatest LREE enrichment with an average La/Yb_{cn} value of 9.47, the chemical sedimentary rocks show a decreasing La/Yb_{cn} with increasing FeO, such that Group I has an average La/Yb_{cn} of 5.98, Group II 5.78, Group III 2.75, and the sulphide boulders 2.79. Given the similar REE patterns between the different lithologies, it appears that all of the chemical sedimentary rocks share a common source.

3.4 Discussion

One of the most important goals of this MSc research was to determine if the volcanic rocks and the chemical sedimentary rocks found throughout the length of the North Touak-Cape Dyer volcanic belt are correlative and, in so doing, determine whether it is appropriate to designate formational status based upon all available stratigraphic, petrologic, and geochemical data. The formal definition of a formation being "… a body of rock identified by lithic

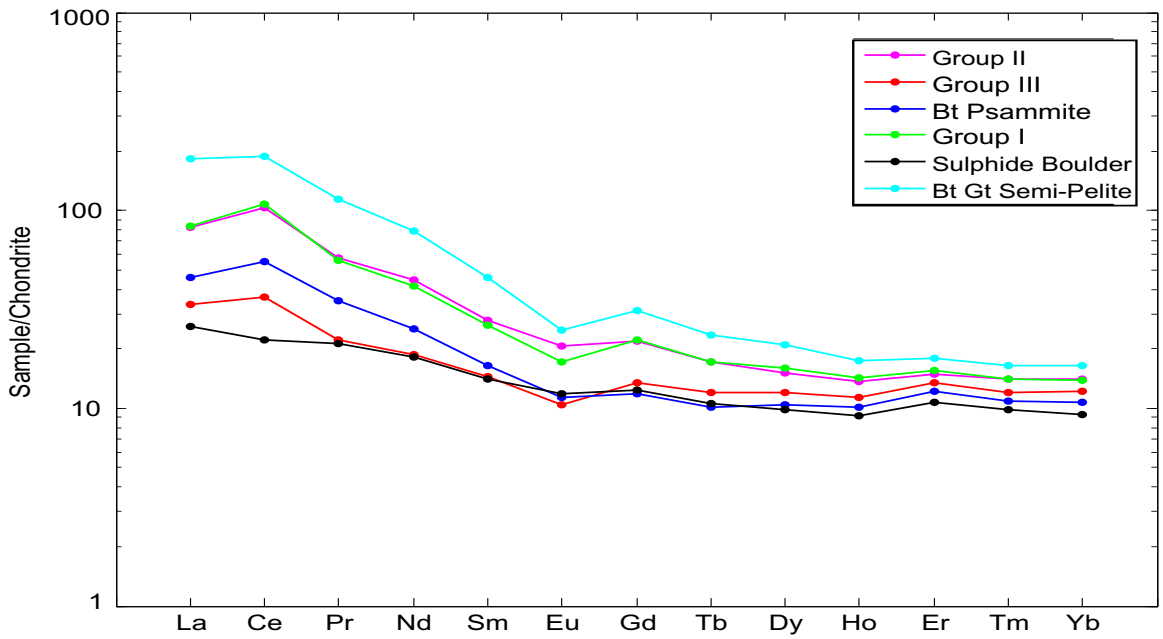

Figure 3-6. Chondrite (Sun and McDonough, 1989) normalized REE plot for the chemical and clastic sedimentary rocks. Notice similarity in pattern between all the groups of chemical sedimentary rocks, including LREE enrichment, positive Ce and negative Eu anomalies.

characteristics and stratigraphic position; it is prevailingly but not necessarily tabular and is mappable at the Earth's surface…" (North American stratigraphic code).

The volcanic rocks of the North Touak-Cape Dyer volcanic belt can be classified as a suite of komatiites, komatiitic basalts, and tholeiites. Despite the geochemical and petrologic differences between the ultramafic and mafic rocks, they occupy the same stratigraphic position, namely, beneath the chemical sedimentary rocks. Komatiite-tholeiite associations have been well-known and well-documented from greenstone belts for years (Anhaeusser, 1975; Arndt, et al., 1979; Fan and Kerrich, 1997). This association of mafic-ultramafic volcanic rocks is believed to stem from differing thermal conditions within mantle plumes, such that the bulbous head of the plume incorporates cooler mantle material, whereas the central axis remains hot; thus tholeiites are sourced from the plume head and komatiites the tail (Campbell et al., 1989). Therefore the differences in major element geochemistry between the tholeiites and komatiitic rocks are better explained as a result of plume dynamics, rather than differing sources.

Despite the differences in major element concentrations, all of the volcanic rocks, including the olivine-blastoporphyritic sills, possess parallel trace element patterns. Although absolute concentrations of the HFSE vary, the entire volcanic suite exhibits a fractionated pattern, enrichment compared to 'classic' komatiites, and a negative Zr-Hf anomaly (Figure 3-3). All of the samples show LREE enrichment over HREE and strongly fractionated patterns (Figure 3-4). Both mineralogically and geochemically, the olivine-blastoporphyritic sills are similar to the volcanic rocks; strong evidence that they represent feeders to the volcanic rocks of the North Touak-Cape Dyer volcanic belt.

Given the stratigraphic and geochemical similarities between all of the volcanic rocks within the North Touak-Cape Dyer volcanic belt it is proposed that they all be grouped under one formation name. Due to the spectacular exposure at the Totnes Road Fiord locality, it is suggested that the volcanic rocks be referred to as the Totnes Road formation. Defining aspects of the Totnes Road formation are that it:

1. consists of green-weathering komatiites, komatiitic basalt, and olivine-blastoporphyritic feeder sills and black-weathering tholeiites.
2. is located within the Paleoproterozoic Hoare Bay group of Baffin Island, Canada.
3. is exposed in the east-central portion of the Cumberland Peninsula within the ~150km long NE-SW trending North Touak-Cape Dyer volcanic belt.
4. has a lower contact with a clastic sequence and an upper contact with the chemical sedimentary rocks.
5. possesses well-preserved primary textures dominated by fragmental units, but including massive, pillowed, and variolitic units.
6. is ~20-200m thick; seen to pinch-out along strike.
7. is composed of a secondary mineral assemblage dominated by amphiboles, plagioclase, titanite, chlorite, and ilmenite.
8. exhibits Ti and HFSE enrichment compared to 'classic' komatiites.

The chemical sedimentary rocks also display large variations in their major element concentrations but have similar trace element patterns. All of the groups show LREE enrichment, strongly fractionated patterns, and with the exception of the sulfide boulders, a positive Ce anomaly and negative Eu anomaly (Figure 3-6). This, coupled with the observation that the chemical sedimentary rocks are almost always found stratigraphically above the Totnes Road formation, supports the field-based interpretation that they represent one main period of hydrothermal activity. Excellent exposure, due to shallow dip and steep topography, of the chemical sedimentary rocks was noted to occur in the vicinity of Clephane Bay Fiord by other members of the CPIG mapping team; therefore it is proposed that the chemical sedimentary rocks overlying the Totnes Road formation be referred to as the Clephane Bay formation. Defining aspects of the Clephane Bay formation are that it:

1. consists of a variety of chemical sedimentary rocks with an exhalative origin.
2. is located within the Paleoproterozoic Hoare Bay group of Baffin Island, Canada.
3. has a lower contact with the volcanic Totnes Road formation and an upper contact with the clastic rocks of a yet undefined formation.
4. is composed of interbedded silicate and sulfide facies iron formation, deformed semi-massive sulfide boulders, and chert.
5. is composed of individual units <10m thick, with the overall package being <200m thick.
6. is moderately deformed and is delineated by zones of gossan.
7. has a variable mineralogy which is dominated by magnetite, grunerite, garnet, biotite, pyrite, pyrrhotite and graphite.
8. has varying Al and Fe concentrations between units, this is likely indicative of differing degrees of hydrothermal versus clastic input.
9. possesses consistent REE patterns for all of its lithologies, indicating deposition was co-genetic throughout one basin.

3.5 Conclusions

Geochemical analysis has confirmed the field-based interpretation that the green-weathering volcanic rocks and olivine-blastoporphyritic sills are ultramafic in composition and the black-weathering volcanic rocks are mafic. Despite the differences in their major element geochemistry, both groups of rocks exhibit enrichment in the HFSE compared to 'classic' komatiites, possess negative Zr-Hf anomalies, and display fractionated REE patterns (Figure 3-4). These geochemical similarities, combined with their consistent stratigraphic location, has led to the interpretation that all of the volcanic rocks within the North Touak-Cape Dyer volcanic belt can be considered co-genetic and therefore can be considered as one formation, herein designated the Totnes Road formation.

Associated chemical sedimentary rocks that overlie the Totnes Road formation show variation among the major elements but exhibit consistent REE patterns and stratigraphic position. Thus, the chemical sedimentary rocks are herein designated the Clephane Bay formation.

Consideration of field, petrologic, and geochemical data has underscored the presence of two diagnostic formations within Cumberland Peninsula's Paleoproterozoic Hoare Bay group: the volcanic Totnes Road formation, and the chemical sedimentary-dominated Clephane Bay formation.

CHAPTER 4

TECTONIC SETTING, PETROGENESIS, AND REGIONAL CORRELATIONS OF THE TOTNES ROAD FORMATION AND CLEPHANE BAY FORMATION, CUMBERLAND PENINSULA, BAFFIN ISLAND

4.1 Introduction

The establishment and characterization of the Totnes Road formation and Clephane Bay formation in Chapters 2 and 3 allows for interpretations regarding the geological history of the North Touak-Cape Dyer volcanic belt. Trace element geochemical analysis of the Totnes Road formation provides constraints on tectonic setting, mantle source, and shallow-level processes. Analysis of the geochemical characteristics of the Clephane Bay formation yields insight into the source of these rocks, as well as their environment of deposition. Collectively, these analyses will provide valuable insights regarding the assembly of the Hoare Bay group.

As the Canadian Arctic experiences warmer temperatures exploration companies are increasingly turning their interest to the under-explored north. The North Touak-Cape Dyer volcanic belt hosts economically prospective lithologies, especially the Clephane Bay formation, and therefore the economic potential of the belt will be briefly discussed.

As mentioned in Chapter 1, the geology of the Cumberland Peninsula was poorly understood prior to CPIG, resulting in a lack of sound region correlations. The increase in the data available, and the resultant enhanced knowledge of the Totnes Road formation now allows informed regional correlations to be made. Mafic-ultramafic volcanic sequences surrounding the Cumberland Peninsula shall be compared with the Totnes Road formation to determine if correlations exist among the volcanic rocks of the region.

4.2 Interpretation of the Totnes Road formation

4.2.1 Tectonic Setting

Tectonic discrimination diagrams have been used extensively to interpret the tectonic setting of mafic and ultramafic rocks. It is generally agreed upon that high-Mg komatiitic magmas, which require large degrees of partial melting at high temperatures, are the product of melting in the central axis of a mantle plume where temperatures are the hottest, and that associated basalts are sourced from the larger, cooler plume head (Bickle, 1993; Campbell et al., 1989; Arndt et al., 1997; Condie, 2001; Arndt, 2008). Plume-sourced volcanic rocks are expected to have a within-plate signature on Wood et al. (1979)'s tectonic discrimination diagram because mantle plumes are not associated with any particular tectonic setting, they are therefore, most likely to erupt in a within-plate setting, due to the geographically restricted nature of all other tectonic settings in comparison. The Totnes Road formation is no exception, with all samples exhibiting a within-plate signature (Figure 4-1).

The use of classic discrimination plots for altered and metamorphosed samples was questioned by Agrawal et al. (2008) who were concerned (1) that the field boundaries in classic discrimination plots were drawn in by eye, (2) the constant sum problem is not taken into consideration, and (3) that the samples used to create the diagrams were not statistically representative. They addressed these concerns by using linear discriminant analysis to create the field boundaries, by using log-transformed ratios instead of individual elements to overcome the constant sum problem, and by using a large dataset of samples to create the diagrams. With these new criteria, they found that their discrimination diagram (Figure 4-2a) has a 91-96% success rate at correctly placing samples in their appropriate tectonic setting. They also found that by using immobile trace elements, including Th, Nb, La, Sm, and Yb that the discriminant plots are also highly successful for samples that have experienced alteration and metamorphism.

When plotted on the tectonic discrimination diagram of Agrawal et al. (2008) the Totnes Road formation samples plot within the mid-ocean ridge basalt (MORB) and continental rift basalt + oceanic island basalt (CRB+OIB) fields along a trend that parallels the line joining

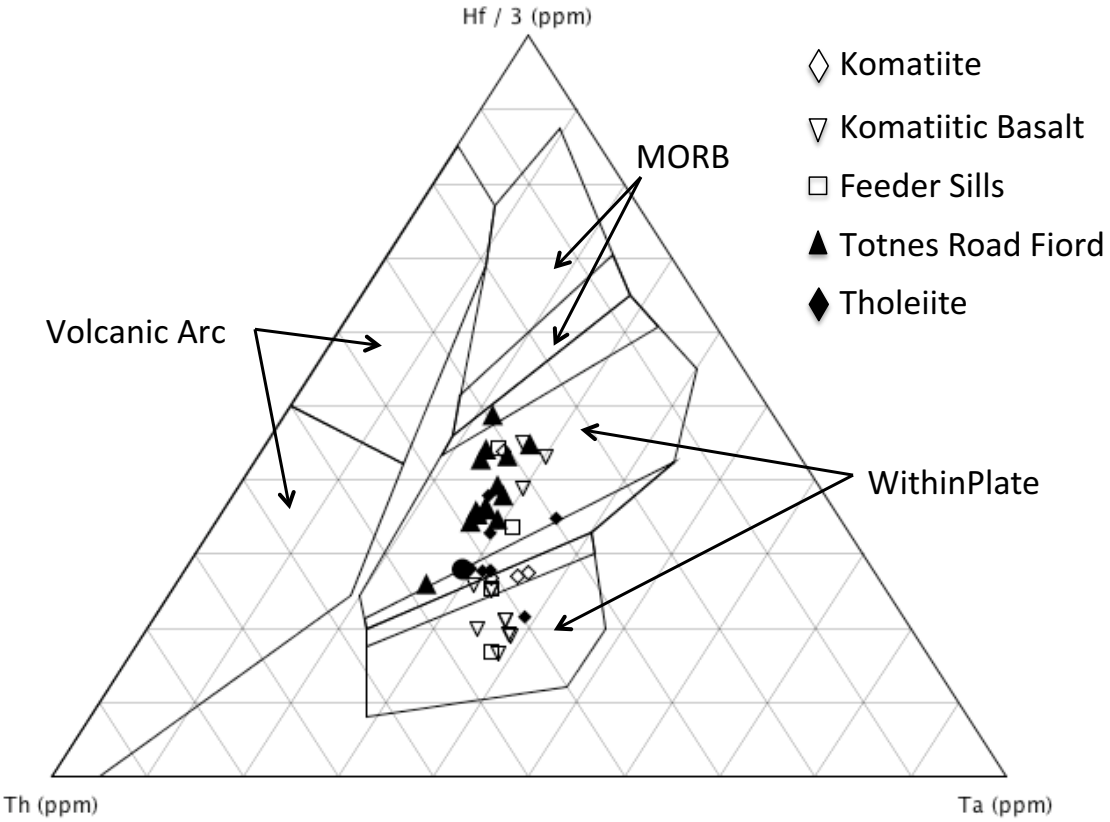

Figure 4-1. Wood (1980) tectonic discrimination diagram. Samples from Totnes Road formation plot in within-plate fields.

mean-MORB and mean-OIB (Figure 4-2b). This suggests that the Totnes Road formation may have been derived in a tectonic setting in which an OIB source interacted with a rift or a ridge where rising MORB material could be incorporated. This setting has been referred to as a plume-ridge interaction, and is seen in Iceland today. Another possible interpretation of the data is that there are two distinct sources for the volcanic rocks on the Cumberland Peninsula: some with a MORB source and some with an OIB source. However, samples from the Totnes Road locality, which are contained within one contiguous unit, also plot within the MORB and CRB+OIB fields, which indicate that the MORB-OIB signature is real. An OIB signature indicates that a plume was the most likely source for the volcanic rocks, whereas a MORB signature indicates the presence of a more depleted mantle source, possibly originating during local rifting. The occurrence of a MORB signature for some of the samples in the diagram of Agrawal et al. (2008) could also be due to the incorporation of some depleted mantle material that was entrained in the plume during its ascent through the upper mantle. The dominant control on the geochemical characteristics of the Totnes Road formation appears to be its plume source, as evidenced by the rocks highly-magnesian nature and within-plate setting signature. Therefore, when interpreting the petrogenesis of this formation emphasis will be placed on its similarity to OIB.

4.2.2 Source and Melting

The Totnes Road formation exhibits several unusual geochemical characteristics in comparison to 'classic' komatiites. These include: strongly fractionated REE patterns with LREE enrichment over the HREE, negative Zr-Hf anomalies, and enrichment in HFSE, such as Th and Nb. Given the immobility of these elements during alteration, these characteristics are suspected to be the result of primary processes and must be taken into consideration when interpreting the petrogenesis of these rocks.

The negative Zr-Hf anomalies and HREE depletion relative to the LREE, are characteristics that, when combined with Al-depletion, are easily explained by deep-mantle melting in the presence of majorite garnet at depths >250km (Nesbit et al., 1979; Herzberg, 1995). Majorite garnet preferentially takes up aluminum, Zr, Hf, and the HREE and retains them

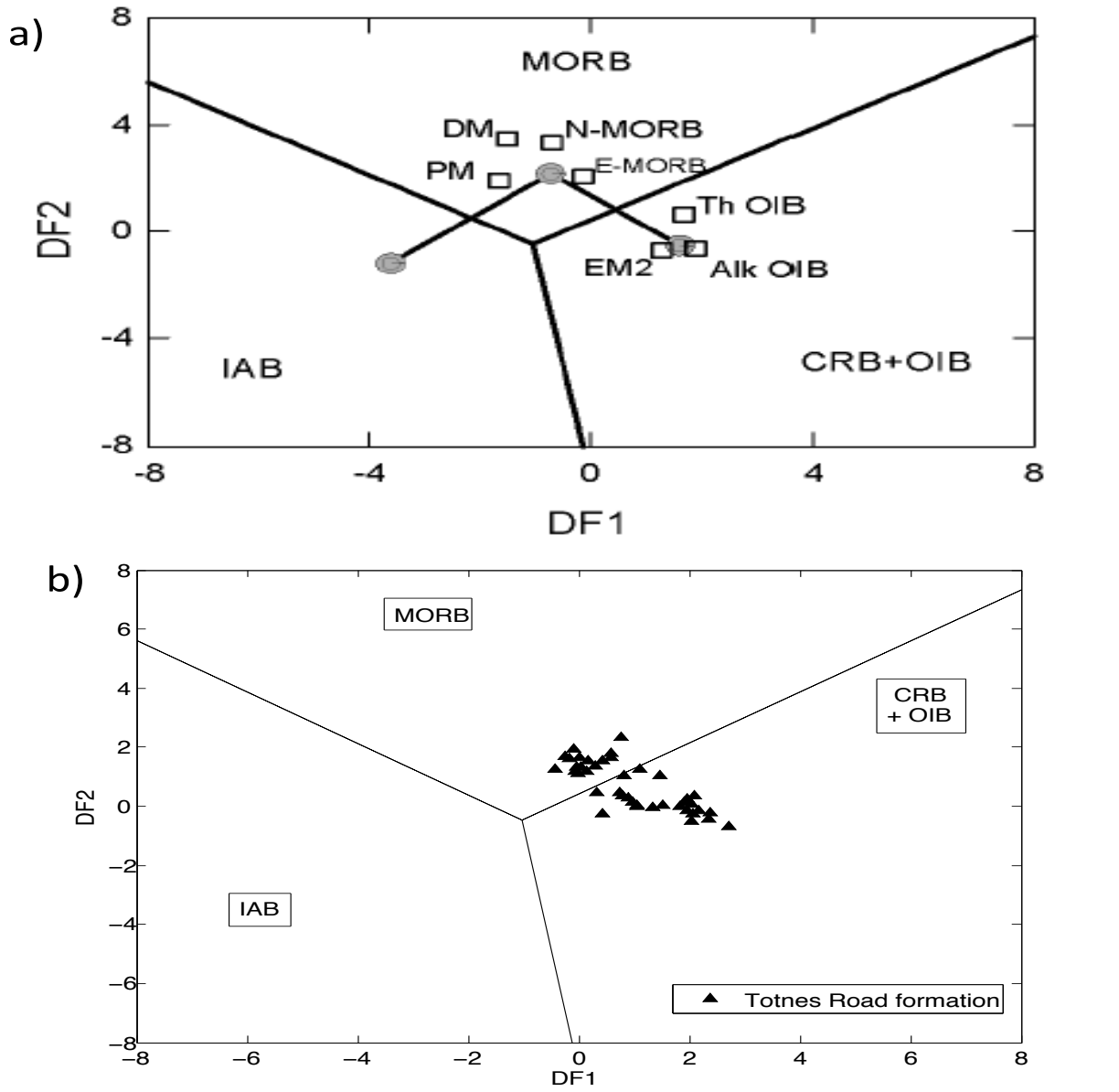

Figure 4-2. a) Plot from Agrawal et al., (2008) depicting the tectonic discrimination plot they created and where classic mafic volcanic rock types plot. The filled in circles in each field represent the mean sample for each field and the lines connecting them the trends along which samples with a mixture of the two end-members will plot. b) A plot of the Totnes Road formation on the same diagram. The samples plot on a trend line which is parallel to that connecting the average MORB and average CRB+OIB sample in a) indicating a setting in which an OIB source (plume) interacted with a MORB source (ridge). DF1 and DF2 are discriminant function whose equations can be found in Agrawal et al. (2008) along with the points used to define the field boundaries.

in the mantle as it remains in the residuum during melting. However, as documented in section 3.3.2, the Totnes Road formation samples do not exhibit Al-depletion (Figure 3-2b) and therefore it is unlikely that deep-mantle melting accounts for their Zr-Hf anomaly and HREE depletion.

The Totnes Road formation possesses trace-element characteristics similar to OIBs on tectonic discrimination plots and shows similar levels of enrichment in the HFSE and LREE compared to OIBs (Figure 4-3). There has been controversy when attempting to explain the HFSE-enriched nature of OIB, however, all theories invoke an enriched deep-mantle source. Hofmann and White (1989), Weaver (1991), Prytulak and Elliott (2007), and White (2010) propose that the mantle source from which OIB plumes formed contains recycled basaltic oceanic crust. This oceanic crust would be enriched with HFSE relative to normal mantle peridotite given that it is a product of partial melting. During the partial melting process incompatible elements, including the HFSE, preferentially enter into the melt, which will eventually erupt to form oceanic crust. Weaver (1991) proposes that OIB melts form from a mantle composed dominantly of peridotite containing stringers or blobs of recycled oceanic crust. Niu and O'Hara (2003) and Pilet et al. (2005) advocate for recycled oceanic lithosphere that was subducted and eventually added incompatible elements, such as the HFSE, to the lower mantle by low degrees of melt. These low degrees of melt concentrated the incompatible elements and metasomatised the surrounding mantle creating the enriched source for OIB. Dasgupta et al. (2010) suggest that it is a combination of peridotite, carbonated eclogite, and volatile-free silica-excess eclogite that give rise to OIB melts.

Alternatively, Niu et al. (2011) proposed that the thickness of the overlying lithosphere exerts a first-order control on the geochemistry of OIB and termed this the 'lid effect'. They pointed out that melts originating beneath thick lithosphere experience low degrees of melting at high pressures, whereas melts beneath thin lithosphere experience high degrees of low-pressure melting. Low degrees of melt would concentrate incompatible elements and as degree of melting increased, this incompatible element enrichment would be diluted as more compatible elements began to enter into the melt.

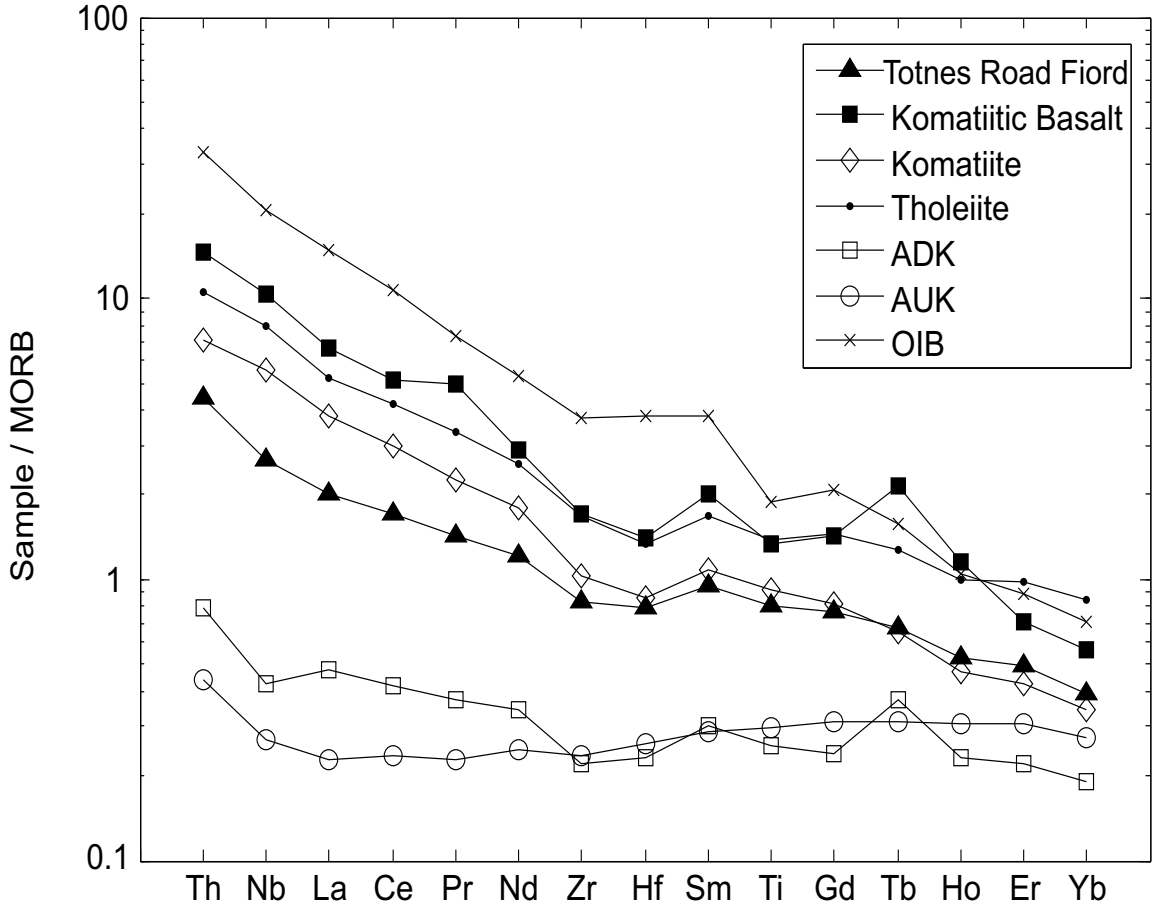

Figure 4-3. MORB (Sun and McDonough, 1989) normalized plot of select HFSE for the Totnes Road formation, ADK, AUK, and OIB showing the similarity in HFSE enrichment and strongly fractionated patterns between the Totnes Road formation and OIB. Data for AUK and ADK same as Figure 3-3, OIB data is a global average from Sun and McDonough (1989).

As explained above, the enriched nature of OIB's has been broadly attributed to melting of a heterogeneous mantle source that is dominated by mantle peridotite but contains portions of recycled, enriched, mafic material. The combination of numerous processes occurring at a subduction zone could create a mafic source, which, if it contributed to a mantle plume melt could account for the unusual geochemical characteristics seen within the Totnes Road formation.

Three distinctive features that characterize the Totnes Road formation need explanation: enrichment in HFSE, strong fractionation of the LREE from the HREE, and negative Zr-Hf anomalies.

Enrichment in the HFSE can be explained through the process of mantle metasomatism during subduction. The HFSE are highly incompatible and therefore will preferentially enter into melt. Jackson et al. (2008) suggest that melting of eclogite during subduction, especially in the hotter Archean, produced a rutile-bearing material. Studies have shown Ti, Ta, and Nb are strongly partitioned into rutile during high-pressure melting (Jackson et al., 2008 and references therein) therefore rutile-bearing recycled slab material would contain high concentrations of Ti, Ta, and Nb due to subduction zone melting. Peridotite xenoliths from the sub-continental mantle lithosphere show that Ti-rich minerals (e.g. rutile) that have been produced by mantle metasomatism are enriched in HFSEs (Kalfoun et al. 2002 in Gangopadhyay et al. 2005). Wagner & Grove (1997) have shown experimentally that Ti-oxide minerals will melt faster than other mantle phases such as clinopyroxene (Gangopadhyay et al. 2006). Therefore if a mantle plume incorporated some of this recycled, metasomatised material, minerals enriched in Ti could be preferentially melted within the ascending magma, thereby increasing its Ti and HFSE concentrations.

Processes operating within a subduction zone can also explain the strong fractionation of the REE, with enrichment of the LREE over the HREE. During subduction, high pressure, low temperature metamorphism of basaltic oceanic crust to form eclogite occurs. It has been shown that fluids can mobilize the LREE during this type of metamorphism (John et al., 2004). Fluids released during dehydration of the subducting oceanic lithosphere trigger the eclogitization process within the basaltic crustal material. These fluids can mobilize the LREE, causing

fractionation from the HREE. Infiltration of these fluids, which have previously scavenged LREE, into the eclogite, can result in incorporation of LREE by minerals such as epidote, allanite, and apatite, thus resulting in LREE-enriched eclogitic material (John et al., 2004). This process is thought to require high fluid-rock ratios of up to 80% (John et al., 2004).

The negative Zr-Hf anomalies displayed by the Totnes Road formation samples may be attributable to the presence of group A eclogitic material in their source region. It has been shown that Zr and Hf, which are generally incompatible, become compatible in garnet with >19 mol% Ca (grossular). Garnet of this composition is commonly found in group A eclogites (van Westrenen et al., 2001). Melting of an eclogite containing garnet of this composition would result in a negative Zr-Hf anomaly because instead of behaving as incompatible elements, like normal, they would preferentially remain within the crystal structure of the garnet while the other incompatible elements (e.g., REE, Ti, Nb, Ta) entered the melt.

Accordingly, all three unusual geochemical characteristics of the Totnes Road formation are consistent with the incorporation and melting of subduction-zone processed garnet-bearing eclogitic material. This material would have a lower solidus than the surrounding mantle and therefore would have a large contribution to the melt even if it is volumetrically small (van Westrenen et al., 2001). Melting during subduction will concentrate HFSE such as Ti, Ta, and Nb into rutile, which will preferentially melt out within the plume. The LREE can be fractionated from the HREE by the same fluids that contributed to the initial eclogitization process. Zr and Hf becoming compatible in garnet with >19 mol% Ca, a composition found within group A eclogites, will cause the negative Zr-Hf anomaly.

The presence of Archean basement on the Cumberland Peninsula points to the existence of Archean continental crust, which the plume would have melted beneath. Thus, the lid effect also likely contributed to the geochemistry of the Totnes Road formation, as only small degrees of melt would have occurred, further increasing the contribution of the incompatible element enriched eclogite. Further evidence for low degrees of partial melting comes from the Ti-Yb proxy, which has been used by Pearce (2008) to determine the melting depth of recent oceanic volcanic rocks, with shallow melting generating MORB and deeper melting generating OIB. The

basis for this proxy is that Yb is much more strongly partitioned into majorite garnet than Ti, and therefore an increasing Ti/Yb indicates deeper melting as more Yb remains in the majorite garnet-bearing residuum. However, most komatiites possess low (<0.6) Ti/Yb values, even though they have been sourced from a deep-seated mantle plume, therefore, this proxy cannot be used to make tectonic interpretations for komatiites as OIB (within-plate setting) and MORB (ridge setting) cannot be distinguished. This is likely due to the Archean-early Paleoproterozoic age of most komatiitic rocks, as high degrees of melting in the Archean result in lithosphere thickness, an indicator of tectonic setting, to no longer be the controlling factor for Ti-Yb fractionation. The fractionation is instead controlled by the degree of melting, with less melting resulting in stronger fractionation; hence high Ti values indicate low degree of melt for ancient rocks. The majority of the samples from the Totnes Road formation possess high Ti/Yb ratios, similar to OIB, indicating that they likely experienced lower degrees of melting relative to AUK and ADK, which have much lower Ti/Yb ratios (Figure 4-4).

4.2.3 Crustal Contamination

Field evidence that the plume which sourced the Totnes Road formation passed through Archean crustal material includes feeder sills within the basement rocks and clasts of intermediate Archean rocks within the Totnes Road formation. Contamination of the mantle plume by crustal material is anticipated, given that the plume material would be much hotter than the crust and therefore likely caused melting and subsequent incorporation of this crustal material. This contamination usually manifests itself as a negative Nb anomaly inherited from the continental crust. Continental crust possesses a negative Nb anomaly due to the process of subduction zone dehydration, which fractionates Th, as it is preferentially mobile in fluids, from Nb. Nb is preferentially recycled into the mantle and Th gets incorporated into melts, which form crustal material. Therefore crustal material is enriched in Th resulting in a negative Nb anomaly. Pearce (2008) developed a plot that makes use of the Th-Nb proxy to determine if an oceanic volcanic rock has experienced any crustal input. It has been found that 98% of modern oceanic basalts plot within a narrow swath on this plot termed the MORB-OIB array (Figure 4-5). If the rocks have experienced crustal input then they plot above the array as interaction with continental crust will increase the Th content of a magma relative to its Nb content. The Totnes Road formation, OIB, ADK from Barberton, and AUK from Munro Township fall within the

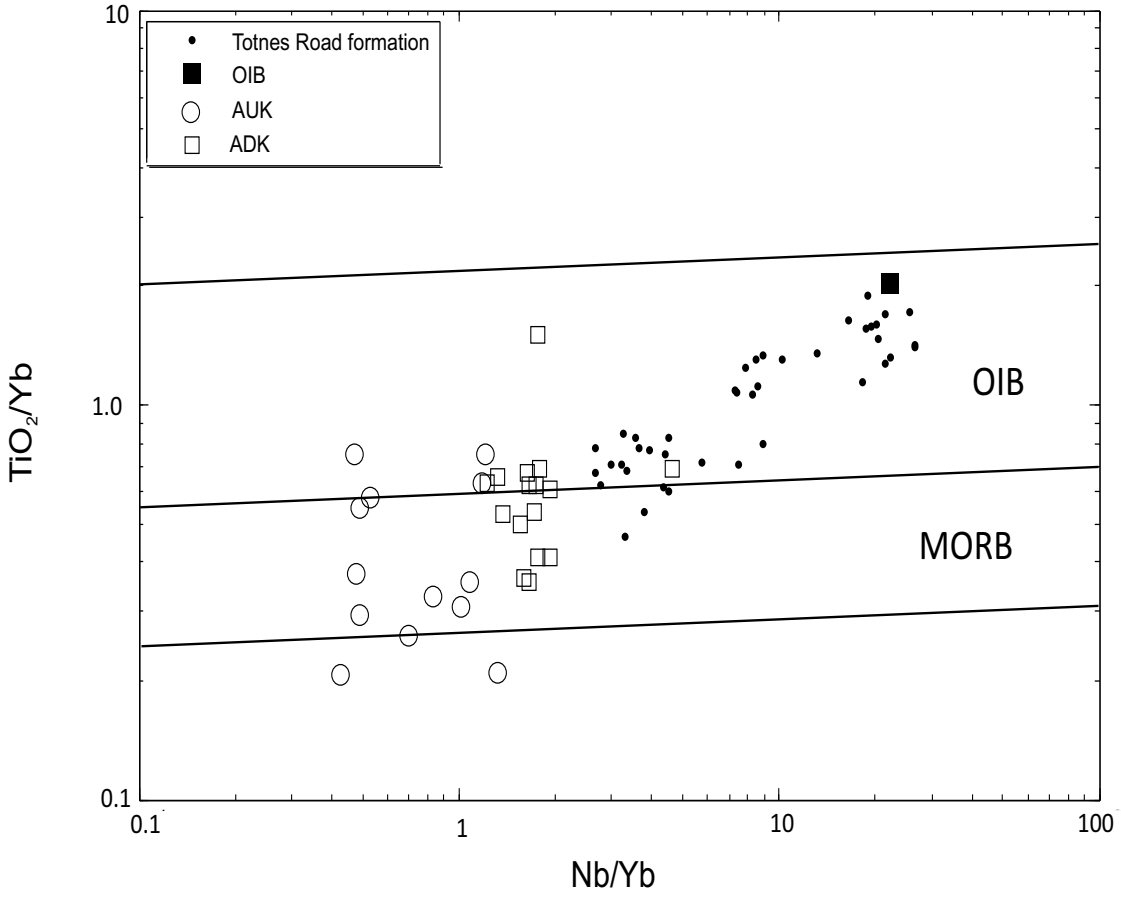

Figure 4-4. MORB-OIB array after Pearce (2007) of TiO_2/Yb versus Nb/Yb. AUK and ADK plot mainly within the MORB array. The Totnes Road formation straddle the boundary between OIB and MORB but plot mainly within the OIB array. Data same as Figure 2-9, OIB from Sun and McDonough (1989).

array (Figure 4-5) and therefore do not appear to have interacted with continental crust and are oceanic in origin. This apparent lack of an anomaly may be due to the enriched nature of the Totnes Road formation. If the plume incorporated eclogitic material with TITAN-enriched rutile, then it is possible that the Nb concentration was high enough in the melt that contamination by crustal material could not enrich the melt with Th enough to create a negative Nb anomaly. It is also possible that the crustal material, at the time of eruption, was relatively thin and only small amounts of contamination occurred.

4.2.4 Surface Processes

Textures, such as pillows, indicate that the environment of deposition was subaqueous. The fragmental character of the Totnes Road formation is distinctive and somewhat unusual, given that komatiites usually erupt at such high temperatures and with such low viscosities that they tend to form thin flows (Arndt, 2008). Their fragmental nature may be explained by a process of steam explosivity – the expansion and subsequent collapse of steam formed at the magma-water interface (Kokelaar, 1986). This process may be enhanced if the komatiitic magma increased its water content on ascent through hydrated continental crust. Thus the fragmentation may be caused by a combination of steam and magmatic explosivity, the latter being the release of magmatic volatiles upon approaching the surface (Kokelaar, 1986). All fragmentation processes are controlled by volatile content and water depth (hydrostatic pressure), and Kokelaar (1986) suggested that the maximum depth for fragmentation of mafic magmas is approximately 200 m. A recent discovery on the ultraslow-spreading Gakkel ridge has shown that explosive volcanism can occur at depths as great as 4000m, however, it was calculated that the magma would have to contain at least 13 wt% CO_2 in order to fragment at such high hydrostatic pressure (Sohn et al. 2008). Accordingly, all available data suggests that essentially anhydrous komatiitic magmas will fragment at shallower depths, on the order of < 200m.

The current understanding of the stratigraphy within the volcanic belt indicates that clastic sedimentation was interrupted by a period of volcanic and hydrothermal activity. Given the association with plutonic Archean basement, the volcanic rocks most likely erupted on a

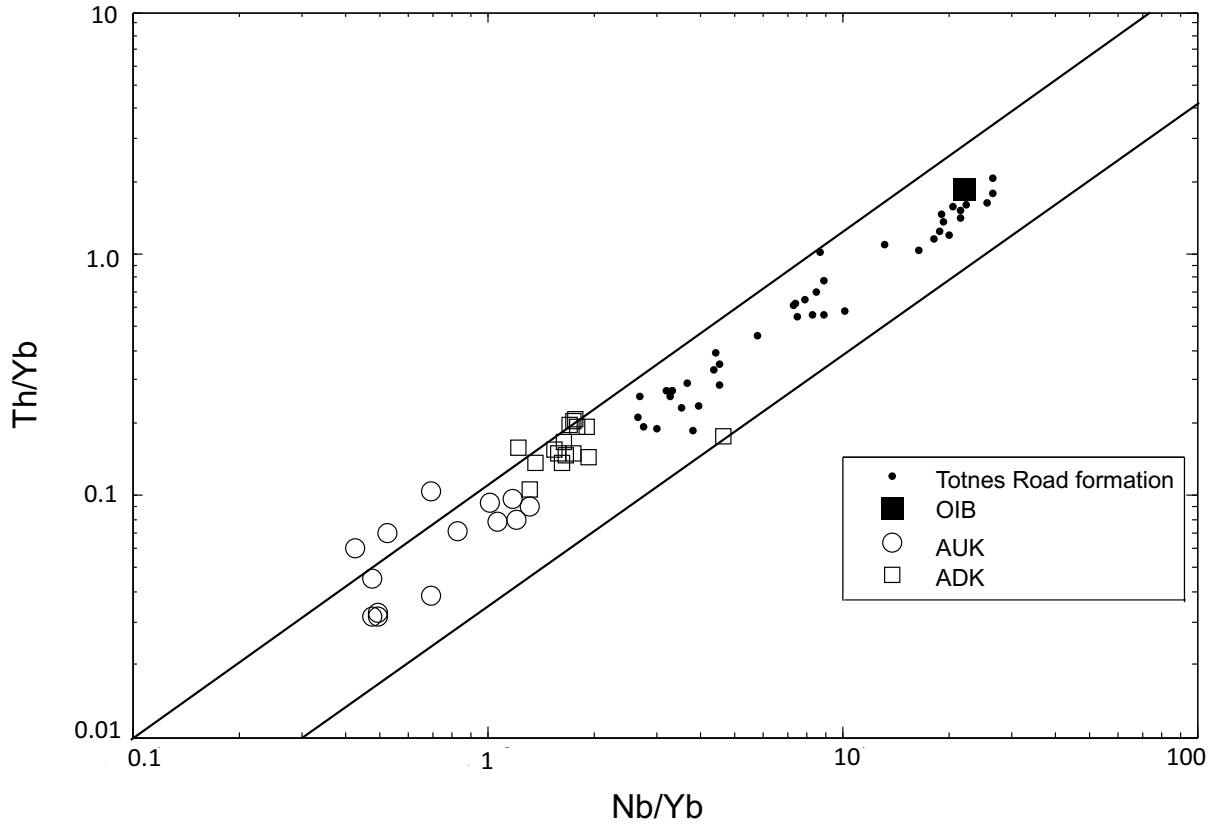

Figure 4-5. MORB-OIB array after Pearce (2007) of Th/Yb versus Nb/Yb. AUK, ADK, and Totnes Road formation plot entirely within array. Data same as Figure 2-9, OIB from Sun and McDonough (1989).

rifted continental margin. Interaction between the komatiitic magma and the Archean crust may have contributed small amounts of water to the initially anhydrous magma, increasing the likelihood for an explosive eruption. Rifting may have been initiated by the arrival of the mantle plume that sourced the komatiitic suite. Rifting would have thinned the overlying crust, which may explain that lack of a Nb anomaly. Hydrothermal activity followed volcanism due to continued high heat flow in the region. Clastic sedimentation, in the form of deeper water turbidites, resumed following the cessation of hydrothermal activity.

4.3 Interpretation of the Clephane Bay formation

4.3.1 Source of the chemical sedimentary rocks

As described in Chapter 2, a variety of chemical sedimentary rock types were mapped throughout the North Touak-Cape Dyer volcanic belt. One possibility for this variation is varying influence from hydrothermal and detrital sources. Boström (1973) developed a discrimination diagram (Fe/Ti versus Al/(Al+Fe+Mn)) that could be used to distinguish between rocks with a hydrothermal source and rocks with a detrital source, by assuming that Fe could be used as a proxy for the hydrothermal component, and Al for the detrital component. Boström (1973) developed his curve by theoretically mixing sediment from an active ridge (22% Fe, 8.8% Mn, 0.5% Al, and 0.02% Ti) with an average of continental crust (5.4% Fe, 0.095% Mn, 8.3% Al, and 0.52% Ti). More recently, this discrimination diagram was used by Peter (2003) as a vector to ore in the Bathurst Mining Camp.

Samples of chemical sedimentary rocks of the Clephane Bay formation and clastic sedimentary rocks from the North Touak-Cape Dyer volcanic belt were compared with global samples of hydrothermal and detrital sediments (Figure 4-6). The samples from the volcanic belt define a smooth curve that closely approximates Boströms curve. This demonstrates that the presence of such a variety of chemical lithologies is probably related to a mixing of hydrothermal and detrital inputs. The grunerite-magnetite iron formation (group III) and the sulphide-rich boulders record 80-100% hydrothermal input, the group I and II iron formations, with garnet and biotite, record 40-80%, the clastic samples in contact with the chemical

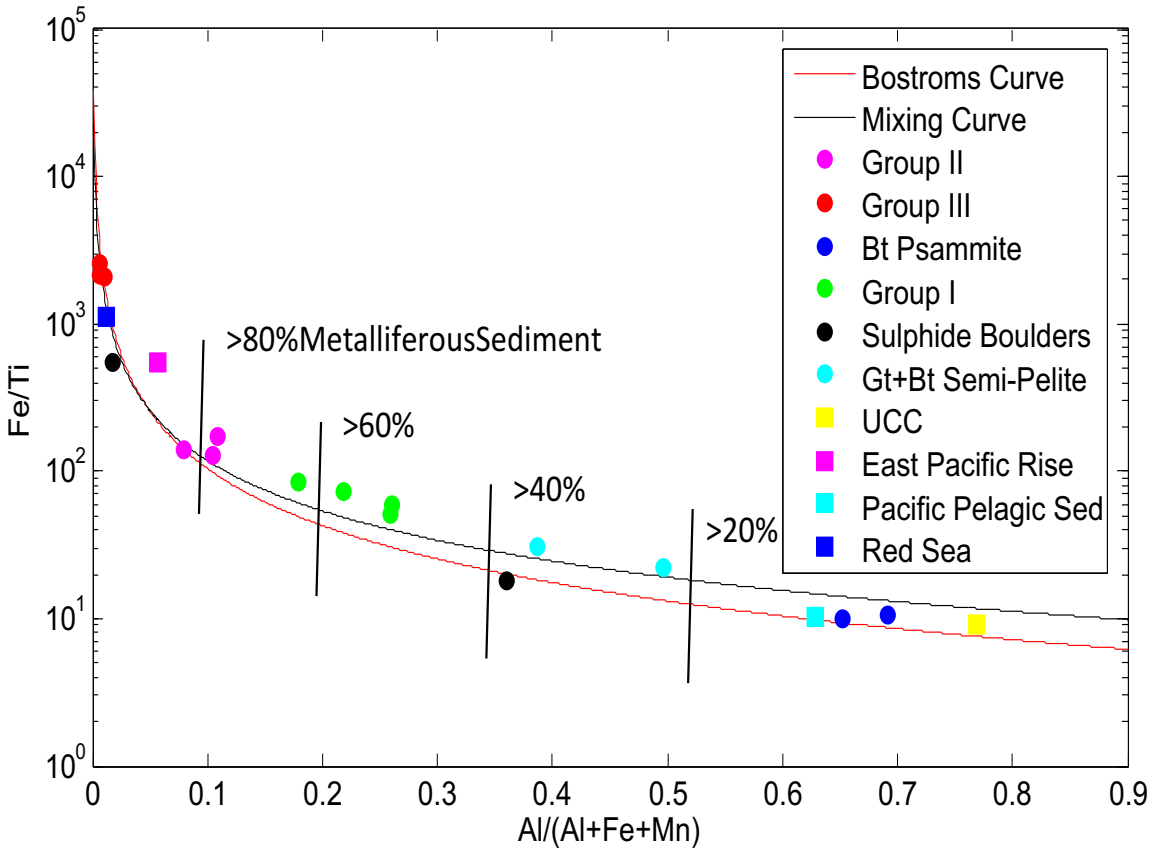

Figure 4-6. Plot of Fe/Ti versus Al/(Al+Fe+Mn) after Broström (1973) and Peter (2003). Mixing curve is fit through the Cumberland samples. Vertical lines represent approximate proportion of hydrothermal input. UCC = upper continental crust (Cronan, 1976 and references therein), East Pacific Rise (Broström and Peterson, 1968), Pacific Pelagic Sediment (Cronan, 1976), Red Sea (Marchig et al., 1982).

sedimentary rocks record 20-40%, and the purely clastic samples <20% hydrothermal input.

4.3.2 Environment of Deposition

The variation in major element composition within the Clephane Bay formation records the proportion of detrital and hydrothermal input, as described above. Trace elements, and specifically the REE, were used to provide constraints on the environment of deposition. It can be seen that although the concentrations vary between lithologies the patterns are identical with the exception of the sulphide boulders (Figure 3-6). This provides evidence that all of the chemical sedimentary rocks within the North Touak-Cape Dyer volcanic belt were deposited within the same basin and received the same hydrothermal and detrital inputs. All units display LREE enrichment, a positive Ce anomaly, and a negative Eu anomaly. Both Ce and Eu can occur in two valence states, Ce as Ce^{3+} and Ce^{4+} and Eu as Eu^{2+} or Eu^{3+}, which makes them unique among the REE. In modern oxic seawater, Ce^{3+} is oxidized to Ce^{4+} which is highly insoluble and thus is incorporated into the crystal structure of Mn-nodules and Fe-Mn crusts, resulting in a depletion of Ce in the seawater, and nil to negative Ce anomalies in chemical sediments deposited into this oxic environment (Peter, 2003). Therefore it seems that the location in the basin in which these chemical sedimentary rocks were deposited was anoxic in order to produce a positive Ce anomaly. Eu anomalies are mainly related to temperature (Peter, 2003). Eu exists as Eu^{2+} under high-temperature (>250°C), reducing conditions. Given that all samples exhibit a negative Eu anomaly, it would appear that the hydrothermal fluids involved never exceeded 250°C.

4.4 Economic Potential

As mentioned above, given the abundance of Fe and sulphides within the lithologies of the Clephane Bay formation, this appears to be one of the most economically prospective formations on the Cumberland Peninsula. The ultramafic volcanics could be prospective for Ni-Cu-PGE massive sulphide type mineralization but, to date, no mineralized zones have been found within the volcanic rocks. Ni and Cu values up to 1722ppm and 1032ppm respectively (Table 3-1) throughout all the samples, indicate that Ni and Cu were likely not scavenged from

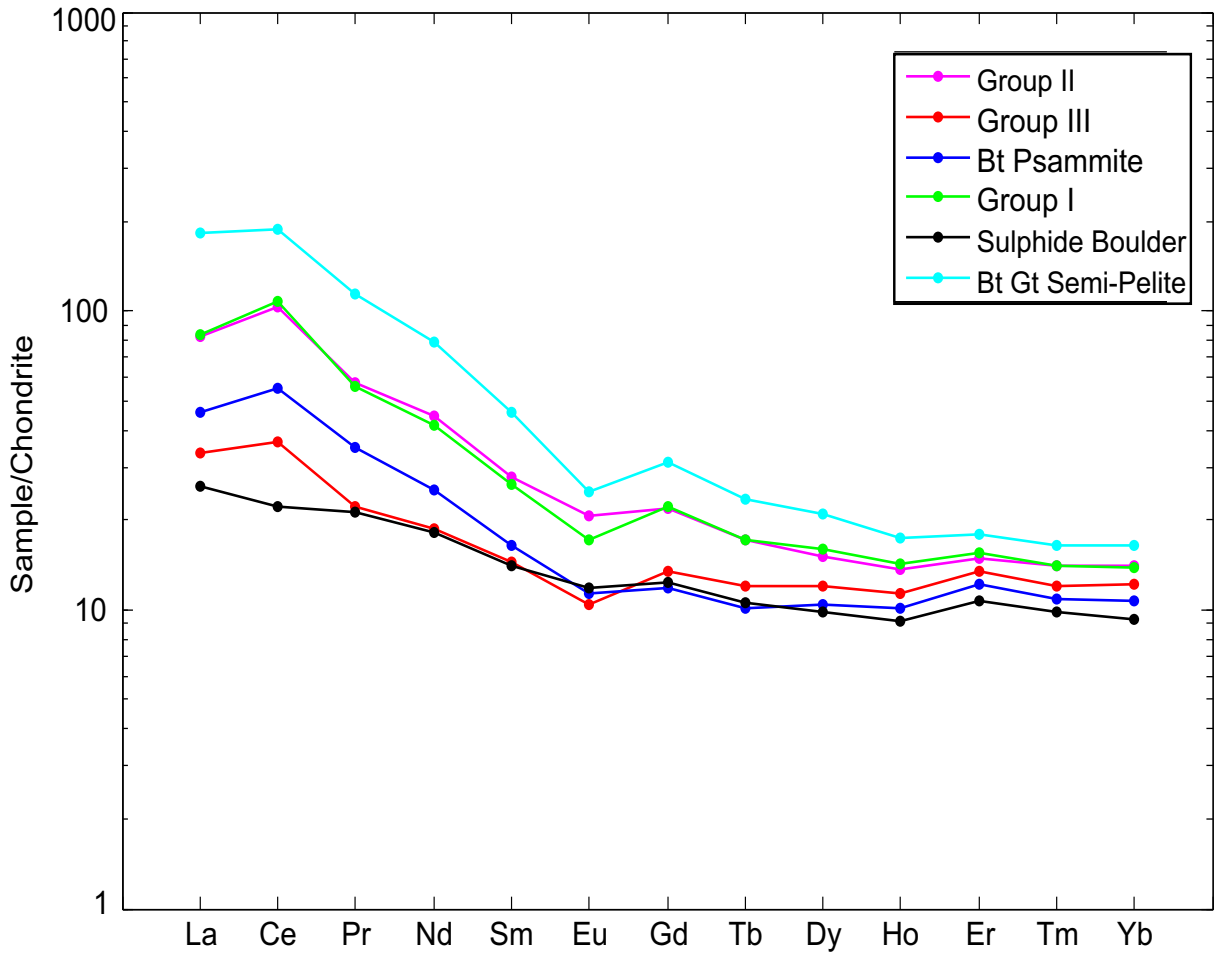

Figure 4-7. Chondrite (Sun and McDonough, 1989) normalized REE plot for the chemical metasedimentary rocks. Notice similarity in pattern between all the groups of chemical sedimentary rocks, including LREE enrichment, positive Ce and negative Eu anomalies.

the magmas. Fe-rich hydrothermal exhalite deposits, such as iron formations, are indicative that hydrothermal precipitation of minerals was taking place within the basin, therefore the possibility of a VMS-type deposit needs to be considered.

The exhalite deposits currently found on the Cumberland Peninsula occur in a thin and discontinuous belt, as seen on surface, along the southern edge of the volcanic belt. The lithologies mapped thus far are dominated by Fe-rich minerals such as magnetite, pyrite, and pyrrhotite, which are generally considered lower temperature, distal minerals. High temperature minerals such as chalcopyrite and sphalerite were only found in trace amounts. This may indicate that all samples examined thus far are merely distal and the high temperature, economic minerals exist in a localized zone around a vent somewhere that has not been sampled to date. It may also indicate that only low-temperature hydrothermal fluids were ever present in the basin. This second possibility is supported by the negative Eu anomaly which suggests that the hydrothermal fluids never exceeded more than about 250°C (Peter, 2003). Notwithstanding, the Wolverine iron formation deposit in the Yukon Territory, which exhibits a negative Eu anomaly, is associated with an economic polymetallic massive sulfide deposit (Lydon et al., 2000).

Given the current available database, the economic potential of the Clephane Bay formation appears somewhat low given the thin and discontinuous nature of the formation, the lack of high-temperature, economic metals in sufficient quantity, the negative Eu anomaly indicative of low-temperature fluids, and the challenges of working in northern frontier regions. Notwithstanding, it could be possible that high-temperature vent deposits do exist and have not been mapped or sampled to date given the 1:200 000 scale of the Cumberland mapping project. Given the mafic-ultramafic volcano-sedimentary nature of the North Touak-Cape Dyer belt and its low to mid metamorphic grade, it appears to fall under the greenstone belt family. Therefore, there is also the potential for greenstone-hosted quartz-carbonate vein gold mineralization, given that this deposit type is especially prevalent in greenstone belts that host variolitic, tholeiitic basalts and komatiites (Dubé and Gosselin, 2007). However, quartz veins have not been abundantly mapped within in the belt to date and no high Au values have been returned in the current, limited, suite of assay samples (Sanborn-Barrie & Young, 2011).

4.6 Regional Correlations

In the past, due to the lack of knowledge regarding the geology of the Cumberland Peninsula and surrounding areas, regional correlations have been tentative and uncertain. Projects like CPIG aim to fill in knowledge gaps in order to establish stronger regional correlations, to help better interpret the geologic history of the Arctic region. Given the increased geologic knowledge for the Totnes Road formation, regional correlations will focus on other mafic-ultramafic volcanic sequences in the eastern Arctic. Mafic-ultramafic volcanic sequences have been reported from regions surrounding Cumberland Peninsula: to the northwest (Bravo Lake Formation), east (Karrat Group and Nunatarsuaq supracrustal belt) and southwest (Schooner Harbour Sequence, Chukotat and Povungnituk Groups) (Figure 4-8). Any possible correlations will be important in expanding the knowledge available concerning the evolution of, and correlations between, the Paleoproterozoic orogenic elements in this region.

As mentioned in the regional geology section (2.2) correlations are problematic in the Canadian Arctic due to the limited amount of geological data. One interpretation is that the Piling Group of central Baffin Island and the Hoare Bay group are correlative (St-Onge et al., 2009). This would imply that the Bravo Lake Formation of the Piling Group might be correlative with the Totnes Road formation. Fortunately, the Bravo Lake Formation is one of the few regional volcanic sequences that has received geochemical analysis. Johns et al. (2006) described the Bravo Lake Formation as a mafic volcanic sequence possessing amygdaloidal and pillowed flows, hydroclastic breccia, dyke swarms, laminated mafic sediments, and both massive and fragmental flows. Geochronological work indicates that the volcanic rocks are older than 1916 ± 35 Ma, and geochemical analyses delineated both alkalic and tholeiitic basalts, that were interpreted to have erupted in a local rift environment, that was not related to a mantle plume (Johns et al., 2006). The Bravo Lake Formations mafic character, with MgO values between 2.34–16.43 wt% (one anomalous value of 20.14 wt%), as well as its greater enrichment in the REE and HFSE (Figure 4-9) does not strongly support a correlation with the dominantly ultramafic Totnes Road formation.

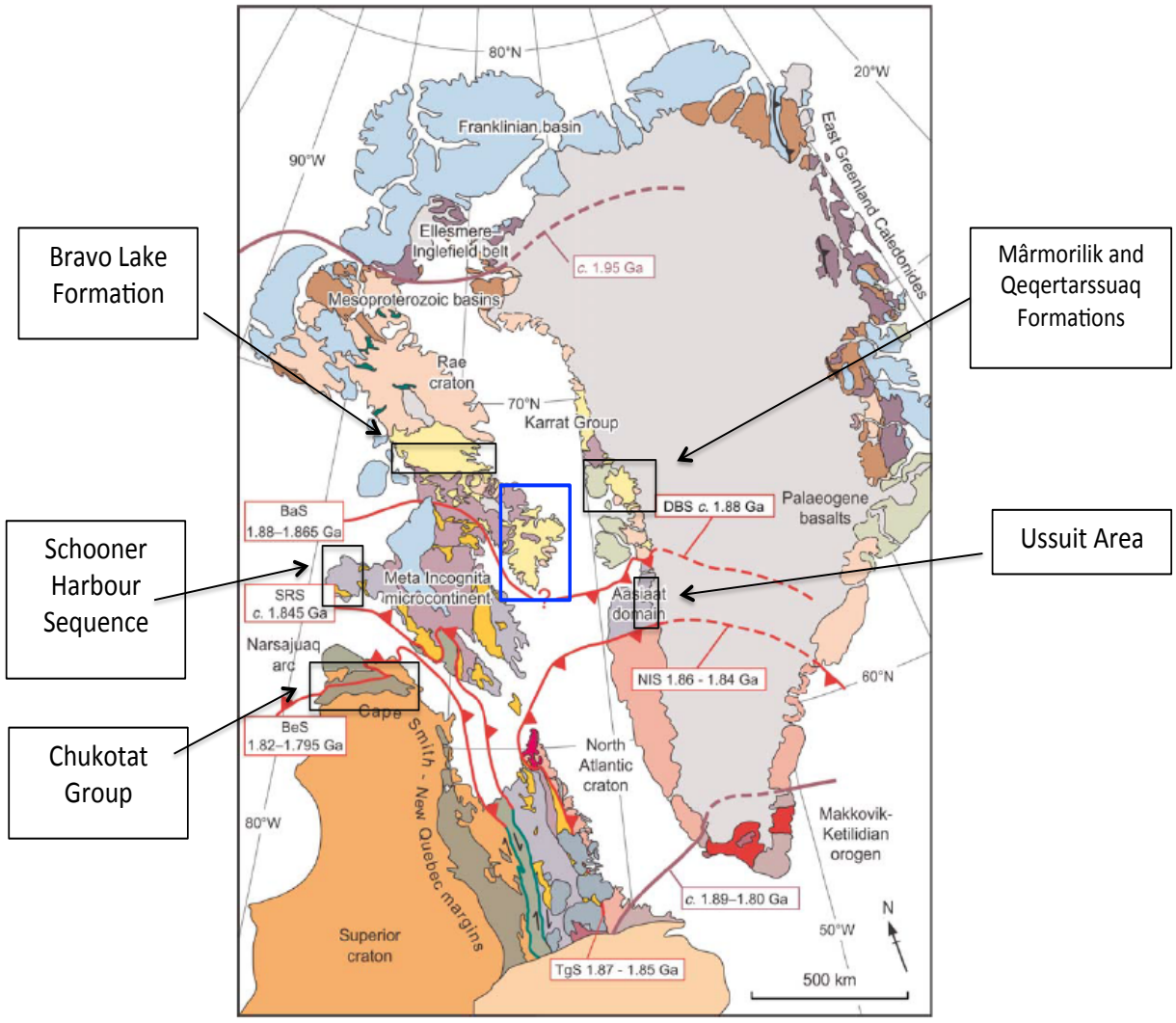

Figure 4-8. Map of regional occurrences of mafic-ultramafic volcanic rocks. Publications which mention the volcanic rocks as follows: Bravo Lake Formation (Johns et al., 2006), Schooner Harbour Sequence (Sanborn-Barrie et al., 2008), Chukotat Group (St-Onge et al., 1992 and St-Onge et al., 2000), Mârmorilik and Qeqrtarssuaq Formations (Henriksen et al., 2009), and the Ussuit area (Connelly et al., 2006 and Kalsbeek and Manatschal, 1999). Cumberland Peninsula highlighted by blue box.

However, samples from the Bravo Lake Formation do exhibit HFSE patterns almost identical to OIB and the Totnes Road formation, with a negative Zr-Hf anomaly, and HREE depletion (Figure 4-9). Both of these attributes are indicators of deep mantle-melting which most likely occurred in a plume. Therefore, it may be necessary to re-evaluate the tectonic setting proposed by Johns et al (2006) given that the basalts possess these geochemical indicators of plume involvement.

The Piling Group is currently considered correlative with the Paleoproterozoic Karrat Group of Greenland, which is interpreted to have been deposited in a passive-margin setting on the southern margin of the Rae Craton between ca. 2000 Ma and ca. 1870 Ma (Jackson and Taylor, 1972; Henriksen et al. 2009; St-Onge et al., 2009). Within the Karrat Group, mafic volcanic rocks displaying pillowed and fragmental textures have been observed in both the Mârmonlik and Qeqertassuag Formations (Henriksen et al., 2009; St-Onge et al., 2009). No further information is available concerning the volcanic rocks, however, given that the rocks are described as mafic in nature, it may be that they are more likely correlative with the Bravo Lake Formation than with the Totnes Road formation.

Another group of Paleoproterozoic supracrustal rocks occurs south of the Karrat Group within the Nagssugtoqidian Orogen. In the Ussuit area, Kalsbeek and Manatschal (1999) describe the occurrence of two ultramafic units within a supracrustal package believed to have been deposited between 1950-2100 Ma. The lower sequence is composed of depleted periodotite whereas the upper sequence is komatiitic. The upper komatiitic sequence has been metamorphosed to amphibolite grade and therefore is dominated by pale green amphiboles with some relict primary olivine, clinopyroxene, and orthopyroxene. Pillows were observed in the field confirming that the ultramafics are volcanic in origin. Kalsbeek and Manatschal (1999) hypothesize that the komatiites may be related to the opening of the Nagssugtoqidian Ocean but are unsure of how a mantle plume would fit into the history of the orogen. Chemically the two samples of the Ussuit komatiite are similar, though not identical to, the Totnes Road formation. The Ussuit komatiitic suite has MgO values of 21.37 and 20.68 wt% and displays enrichment in incompatible elements including the REE and HFSE when compared to alumina-depleted

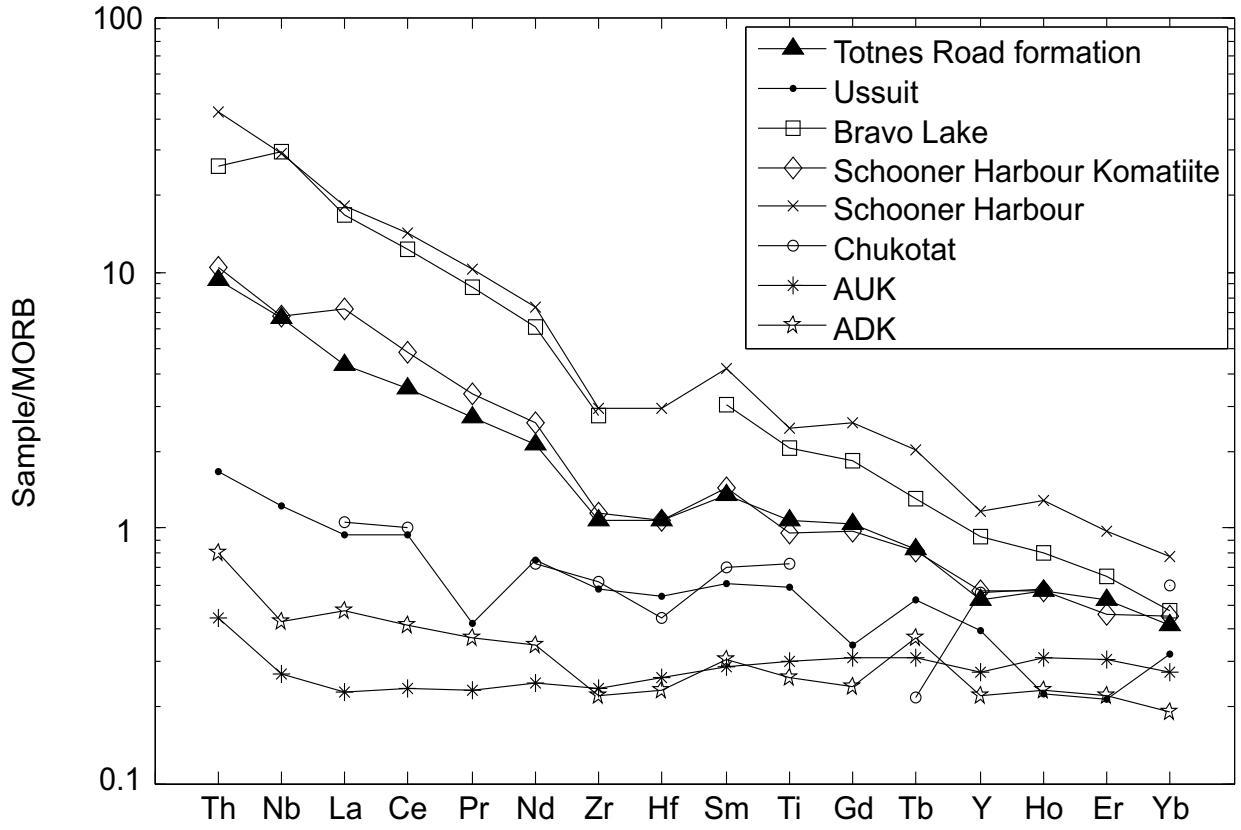

Figure 4-9. MORB (Sun and McDonough, 1989) normalized plot of selected HFSE for the Cumberland Peninsula Totnes Road formation, regional samples, ADK, and AUK. Samples from the Bravo Lake Formation and Schooner Harbour Sequence plot similarly, the Totnes Road formation and the Schooner Harbour Sequence komatiite plot almost identically, and the Chukotat and Ussuit samples plot uniquely. All the regional samples show enrichment in the HFSE relative to ADK and AUK. Data sources for regional volcanics as in Figure 4-7, ADK and AUK data sources same as Figure 3-2.

komatiites and alumina- undepleted komatiites (Figure 4-8). However, the suite does not reach the level of enrichment or fractionation of the Totnes Road formation, although concentrations of the HREE are almost identical between the two.

On southwest Baffin Island there is an occurrence of green, fragmental rocks interpreted to be ultramafic. The rocks, designated the Schooner Harbour Sequence, are interpreted to have been deposited on the Meta-Incognita micro-continent (Sanborn-Barrie et al., 2008). The sequence has tentatively been dated at ca. 1.88 Ga based on the age of a dyke interpreted to be a feeder to the volcanics (Sanborn-Barrie et al., 2008 and references therein). Four geochemical samples exist for the Schooner Harbour Sequence (Joe Whalen, personal communication, unpublished data), two from extrusive rocks and two from intrusive rocks. Three of the samples are basaltic in nature with MgO values of 5.54-7.47 wt% with the fourth possessing an anomalous value of 21.46 wt%. The three basaltic samples possess greater amounts of HFSE enrichment than the Totnes Road formation and are nearly identical to the samples from the Bravo Lake Formation and OIB (Figure 3-9). The ultramafic sample, classified as a pyroxenite, is undistinguishable from the Totnes Road formation samples. Again, all the samples display a negative Zr-Hf anomaly and exhibit depletion in the HREE relative to the LREE (Figure 4-9); thus it is seems likely that the Schooner Harbour Sequence rocks were also sourced from a mantle plume.

The final notable occurrence of ultramafic volcanic rocks in the region occurs on the Ungava Peninsula of Northern Québec. The Chukotat and Povungnituk Groups record rifting on the northern margin of the Superior Province that resulted in the creation of the Meta-Incognita micro-continent (St-Onge et al., 2000). The Povungnituk Group is postulated to represent the early stages of rifting between 2038 +4/-2 Ma and 1959 +3.1/-2.7 Ma whereas the Chukotat Group is postulated to record a final pulse of rifting between 1918 +9/-7 Ma and 1870 ± 4 Ma (St-Onge et al., 2000). Basaltic volcanism represented by thick, massive flows and pyroclastic deposits dominate the early stages of rifting, whereas komatiitic volcanism and banded iron formation deposition dominate the later stages (St-Onge et al., 1992); therefore it appears that both temporally and lithologically the Chukotat Group closely resembles the Totnes Road formation. Arrival of the Ungava mantle plume has been suggested as the driving force behind

the rifting and komatiitic volcanism (St-Onge et al., 2000). The age of the Ungava plume is bracketed by the age of a radiating dyke swarm on the northeastern Superior margin at 2220-2210 Ma (Ernst and Bleeker, 2010) therefore, St-Onge et al (2000) proposes that the plume migrated from the northeastern to the northwestern margin of the Superior province and was thus able to produce the younger komatiitic volcanism of the Chukotat Group and initiate rifting. The Chukotat volcanic rocks are not ultramafic, but are highly-magnesian in nature, with values ranging from 11.19-16.81 wt%. The rocks have REE contents similar to the Ussuit suite (Figure 4-9) with flatter, less-enriched patterns compared to the Totnes Road formation but enrichment compared to 'classic' alumina-undepleted and alumina-depleted komatiites (Figure 4-9).

Trace element geochemistry defines three clear groupings of the above mafic-ultramafic volcanic rocks: (1) strongly-enriched (30-40x MORB), fractionated, with a negative Zr-Hf anomaly (2) moderately-enriched (10x MORB), fractioned, with a negative Zr-Hf anomaly and (3) non-enriched and weakly fractioned (Figure 4-9). The first group consists of the basaltic Bravo Lake Formation and Schooner Harbour Sequence, the second group comprises komatiites from the Totnes Road formation and the komatiitic sample from the Schooner Harbour Sequence, and the final group consists of the komatiites from the Ussuit region and komatiitic basalts from the Chukotat Group.

The komatiitic sample from the Schooner Harbour Sequence and the Totnes Road formation are the most similar as they exhibit near-identical trace element patterns (Figure 4-9). The basaltic samples from the Schooner Harbour Sequence and Bravo Lake Formation are more enriched than the komatiitic Totnes Road formation and Schooner Harbour Sequence sample. However, both groups share a strongly fractionated smooth pattern from Th to Nd, a negative Zr-Hf anomaly, a curving depletion from Ti to Y, a negative Y anomaly, and a curving depletion from Ho to Yb (Figure 4-9). Given the similarity between the Totnes Road formation, Bravo Lake formation, and Schooner Harbour Sequence it is possible that they shared a source, likely a plume, given the ultramafic nature of some samples. The basaltic rocks may have been sourced from the cooler plume head where lower degrees of melting occurred, resulting in greater incompatible element enrichment and the komatiitic samples may have been sourced from the hotter plume axis where higher degrees of melting would have occurred and diluted the

incompatible enrichment by addition of compatible elements. The rock suites also possess similar ages of between ca. 1880-1990 Ma. It may be possible that all of the above suites are related to the same volcanic period caused by melting of the Ungava plume, after it migrated to the northwest. Geochronological data and more robust geochemical datasets will be needed to assemble an accurate regional history of volcanism in the eastern Canadian Arctic.

4.7 Discussion

The enriched nature of the Totnes Road formation is comparable to the enrichment seen in oceanic island basalts. In the case of OIBs the enrichment is believed to be due to a source region that contains subducted oceanic material, combined in some cases with low degrees of melting beneath thick lithosphere. The combination of HFSE enrichment, strongly fractionated REE patterns, and negative Zr-Hf anomalies can be explained if subduction zone-processed eclogitic material was incorporated into the mantle plume which sourced the Totnes Road formation.

The lithological variety seen within the Clephane Bay formation can be explained by mixing of a purely hydrothermal source with a purely detrital source. Parallel REE patterns indicate that the chemical sedimentary rocks were deposited co-genetically within one basin. A positive Ce anomaly indicates that this basin was anoxic at the time of deposition and a negative Eu anomaly indicates that the fluids sourcing the Clephane Bay formation likely never exceeded temperatures of 250°C.

The discontinuous nature of the North Touak-Cape Dyer volcanic belt, lack of economic minerals present within the Totnes Road formation and Clephane Bay formation, and remoteness of the region all combine to a current understanding of a low economic potential for the volcanic belt, however, the small-scale nature of the CPIG mapping program means that large swaths of the North Touak-Cape Dyer volcanic belt remaining unexplored.

Regionally, plume volcanism is also a likely source for the Bravo Lake Formation, Schooner Harbour Sequence, komatiites from the Ussuit Region, and the Chukotat Group. All of these mafic-ultramafic volcanic rocks are similar in age and therefore may have been erupted during the same period of volcanism from different portions of the same mantle plume. The samples from the Schooner Harbour Sequence and Bravo Lake formation are the most similar to the Totnes Road formation with parallel HFSE patterns, possibly indicating that they all belong to a regional co-genetic suite. Overall, the geochronological control on these volcanic sequences needs to be improved to fully unravel the relationship between all of these volcanic units in the eastern Canadian Arctic.

CHAPTER 5

REFINING THE CLASSIFICATION OF KOMATIITIC ROCKS USING CONSTRAINTS FROM THE TOTNES ROAD FORMATION, CUMBERLAND PENINSULA, EASTERN BAFFIN ISLAND

5.1 Introduction

Unusual packages of fragmental komatiitic rocks have been found in a number of localities worldwide (Figure 5-1) including the Karasjok greenstone belt of Norway (Barnes and Often, 1990), the Central Lapland greenstone belt of Finland (Hanski et al., 2001; Gangopadhyay et al., 2006), the Inini greenstone belt of French Guiana (Capdevilla et al., 1999), the Steep Rock and Lumby Lake greenstone belts of the Superior Province of Canada (Tomlinson et al., 1999), the Murchison Terrane of the Yilgarn Craton of Australia (Barley et al., 2000), and most recently the Totnes Road formation of Baffin Island (this M.Sc. thesis). In addition, these komatiites all lack the characteristic spinifex texture of most komatiite sequences, are Ti and HFSE-enriched, and have erupted through older continental or island arc crustal material. The wide geographic spread and strong similarities between these Ti-enriched komatiites prompted Barley et al. (2000) to propose a new komatiite sub-type named after the greenstone belt from which they were first described, the Karasjok Greenstone Belt of Finland (Barnes and Often, 1990).

The Boston Creek flow from the Abitibi greenstone belt of Canada, initially interpreted as an unusual Fe-rich basalt (Stone et al., 1987) but reinterpreted as a ferropicrite (Stone et al., 1995), has been incorrectly grouped with the above mentioned Ti-rich komatiites (Arndt, 2008). This has led to confusion and misconceptions regarding the definition of Karasjok-type komatiites (Arndt, 2008) The aim of this paper is to use new insights from the Totnes Road formation of the Paleoproterozoic Hoare Bay group, eastern Baffin Island, to refine the definition for Karasjok-type komatiites, and to propose a model for their formation and subsequent eruption that is consistent with petrogenetic interpretations of all known localities.

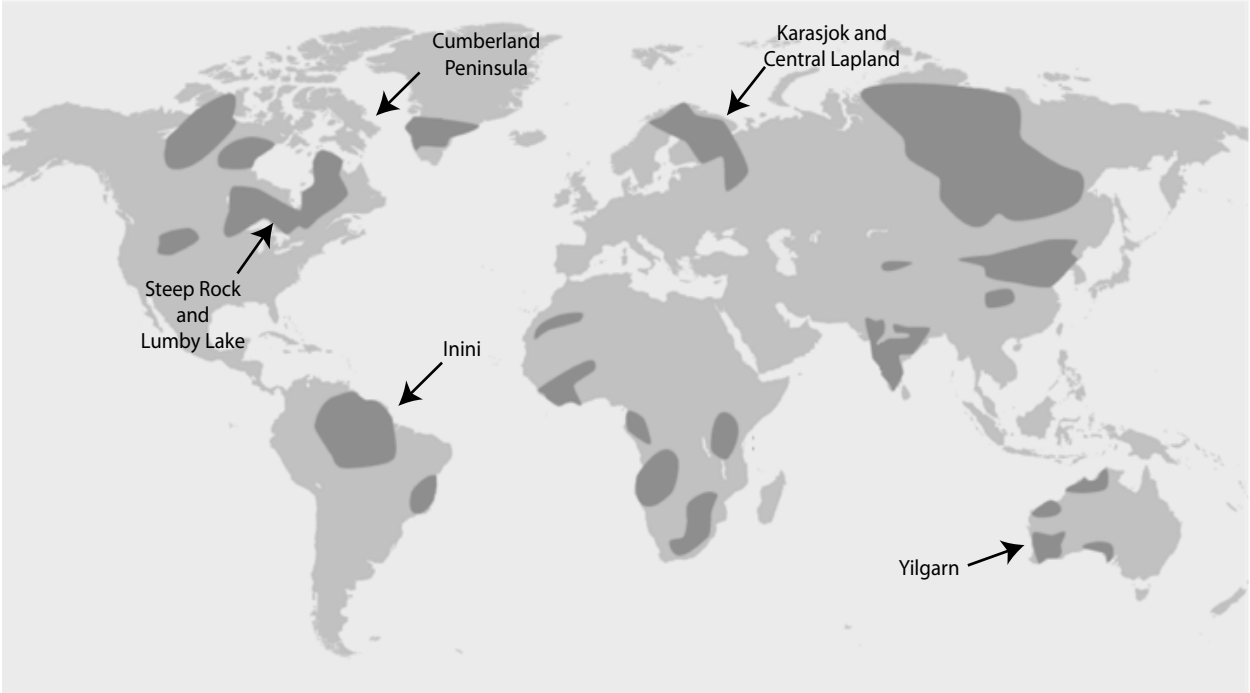

Figure 5-1. Map showing global distribution of Karasjok-type komatiites, which are typically associated with older crustal material as shown by the location of Archean cratons (dark grey). Modified from Petit (2010).

5.2 Totnes Road formation

Karasjok-type komatiites have been determined to be a component of the Totnes Road formation, on Cumberland Peninsula, eastern Baffin Island, based on the fragmental and geochemically enriched nature of the komatiites. The Totnes Road formation is Paleoproterozoic in age and erupted through Archean crystalline basement, similar to other Karasjok-type komatiites. Although the rocks in the region have been subject to amphibolite-facies metamorphism, primary textures are well preserved. Fragmental units, including hyaloclastite (Figure 5-2), are intercalated with fine-grained layered units believed to represent bedded-tuffaceous material, pillowed flows with variolitic rims, and fine to medium grained schistose units are believed to represent flows. The thickest fragmental unit (10's of meters) contains the largest and most well-rounded fragments, up to 20cm in length, possibly indicative of a volcaniclastic origin. Thinner fragmental units (2 to10m) contain much smaller, angular fragments, < 5cm in length, within a very fine-grained groundmass, more suggestive of a hyaloclastite origin.

5.3 Fragmentation

The fragmental character of Karasjok-type komatiites is distinctive and somewhat unusual, given that komatiites usually erupt at such high temperatures and with such low viscosities that they form flows (Arndt, 2008). Their fragmental nature may be explained by a process of contact-surface steam explosivity – the expansion and subsequent collapse of steam formed at the magma-water interface (Kokelaar, 1986). This process may be enhanced if the komatiitic magma increased its water content on ascent through hydrated continental crust. All fragmentation processes are controlled by volatile content and water depth (hydrostatic pressure), and Kokelaar (1986) suggested that the maximum depth for fragmentation to take place for a mafic magma, with a volatile content of 0.5 wt%, is approximately 200 m. A recent discovery on the ultraslow-spreading Gakkel ridge has shown that explosive volcanism can occur at depths as great as 4000m, however, it was calculated that the magma would have to contain at least 13 wt% CO_2 in order to fragment at such high hydrostatic pressure (Sohn et al. 2008). Accordingly, all available data suggests that essentially anhydrous komatiitic magmas will only fragment at shallower depths, on the order of < 200 m.

The fragmental nature of the rocks also likely explains the absence of spinifex texture. Spinifex requires a komatiitic lava to form flows at the surface within which bladed olivine can crystallize during cooling (Nesbitt, 1971). Thus spinifex requires a passive flow-forming eruption as compared to an explosive fragmenting eruption, such as those experienced by Karasjok-type komatiites. This calls into question the use of spinifex texture as a defining characteristic of komatiites, as it is strongly related to cooling conditions. This will be discussed further in section 5.6.

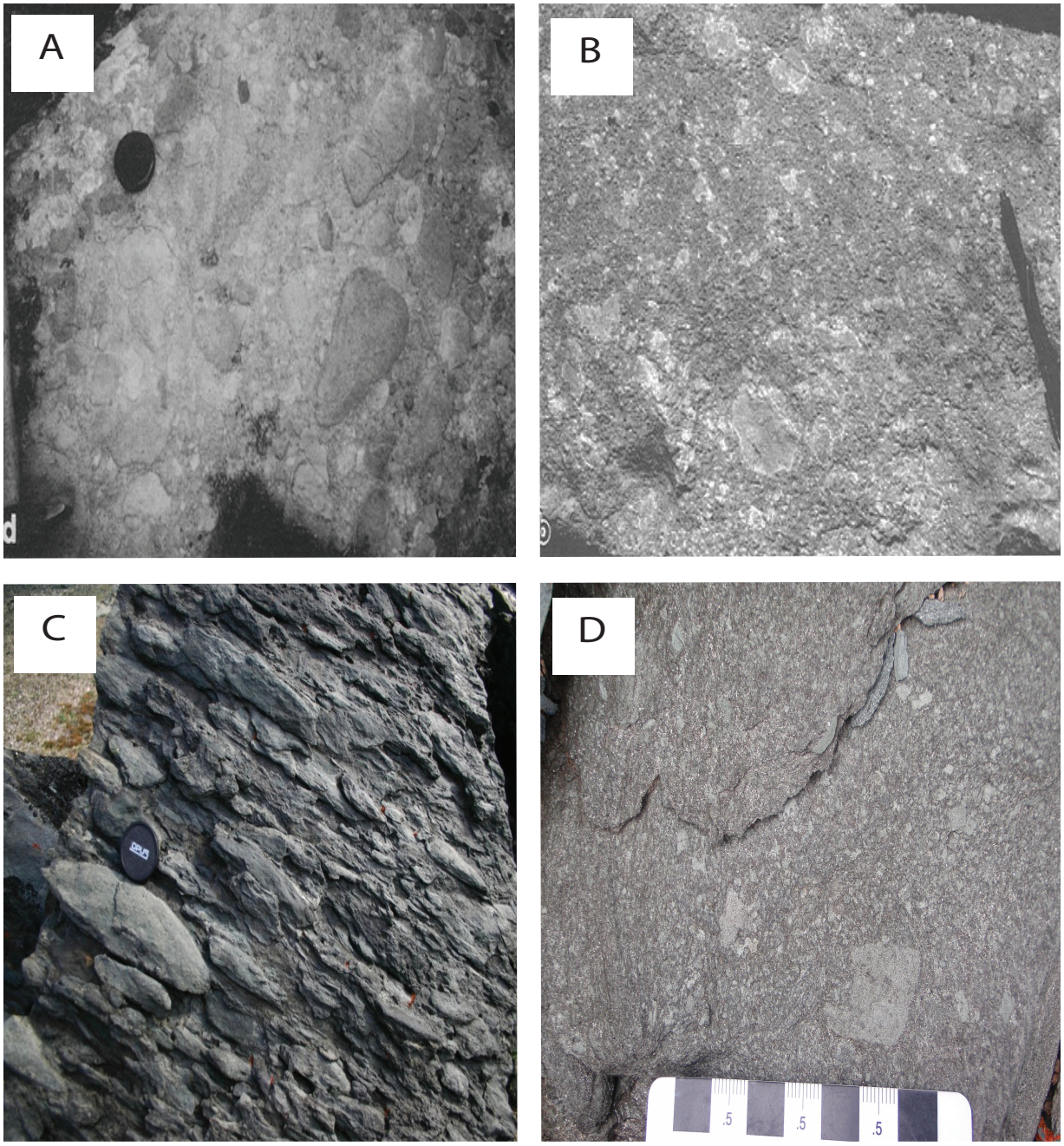

Figure 5-2. Field photographs showing the fragmental nature of Karasjok-type komatiites. Figures A and B are a volcaniclastic and pyroclastic unit, respectively, from the Karasjok Greenstone Belt of Norway (Barnes & Often, 1990). Figures C and D are a likely volcaniclastic and a pyroclastic unit, respectively, from the Totnes Road formation, Cumberland Peninsula of Baffin Island.

5.4 Geochemistry

In addition to being texturally unusual, Karasjok-type komatiites possess unusual geochemical characteristics for komatiitic rocks. Komatiites are characterized by their high-MgO content; however, Karasjok-type komatiites have lower MgO values than the 'classic komatiites' of the Barberton greenstone belt and Munro Township within the Abitibi greenstone belt. The range of MgO values for Karasjok-type komatiites (8.52-36.25 wt%) overlaps with that of 'classic' komatiites (11.98-38 wt%) however, their average MgO concentrations are notably lower at, 18.6 wt% for Karasjok-type komatiites, compared with 25.5 wt% and 26.6 wt% for komatiites from Barberton (Viljoen et al., 1983) and Munro (Fan and Kerrich, 1997), respectively.

Komatiites are conventionally classified on the basis of their alumina content, as proposed by Nesbit et al. (1979), given the understanding that the depth of the melt source is the dominant control of alumina content. Alumina depleted komatiites (ADK) were first described from the Barberton Greenstone Belt in South Africa (Viljoen & Viljoen, 1969), and characterized by CaO/Al_2O_3 (~ 1.5), low Al_2O_3 / TiO_2 (~ 11), and HREE depletion (Nesbit, 1979). Depletion in alumina and the HREEs, as well as negative Zr-Hf anomalies (Stone et al., 1995), is consistent with majorite garnet being present in the residue during melting. Alumina undepleted komatiites (AUK) were first described from the Munro Township in the Abitibi Greenstone Belt (Pyke et al., 1973) and are characterized by chondritic ratios of CaO/Al_2O_3 (~ 1) and Al_2O_3 / TiO_2 (~20), with flat chondrite-normalized REE patterns (Nesbit et al., 1979). Majorite garnet is only stable in the mantle at depths of > 250km, therefore ADK is considered to reflect deep-mantle melting, whereas AUK reflect relatively shallow melting.

All of the early studies on Karasjok-type komatiites (Barnes & Often, 1990, Capdevila et al., 1999, Tomlinson et al., 1999, and Barley et al., 2000) concluded that they were Al-depleted komatiites based on Nesbit et al.'s (1979) komatiite classification. However, use of the Al_2O_3/TiO_2 ratio as a proxy to determine alumina depletion is unsuitable for Karasjok-type komatiites due to their high levels of TiO_2 (values >0.5 wt%). Average Al_2O_3/TiO_2 values for the

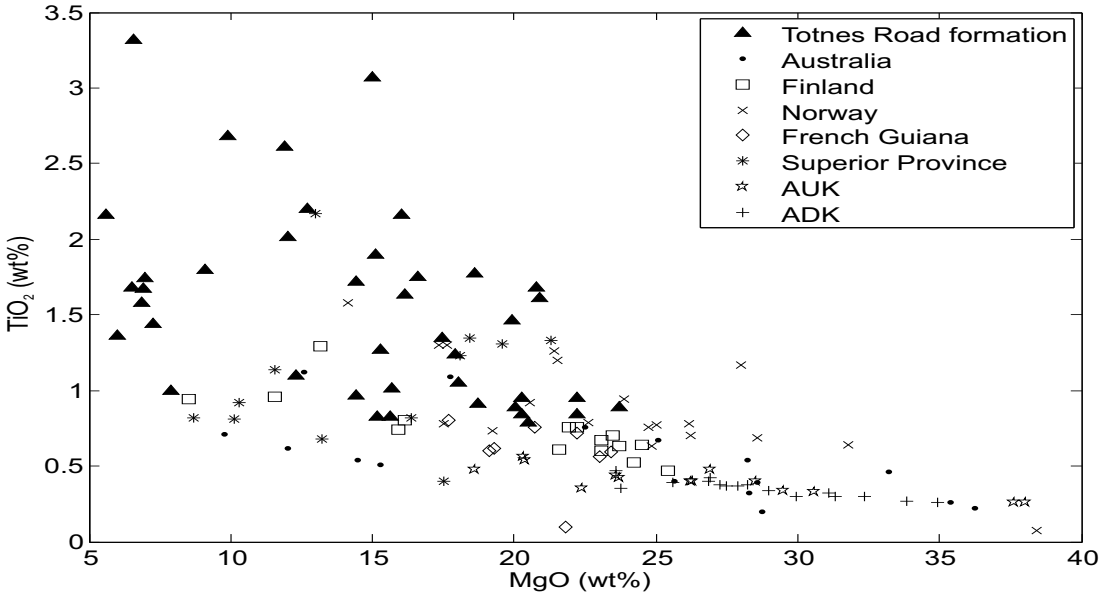

Figure 5-3. Plot of TiO_2 vs. MgO for Karasjok-type komatiites showing enrichment in TiO_2 for the Karasjok-type komatiites as compared to 'classic komatiites'. Data sources: Australia (Barley et al., 2000), Finland (Hanski, 2001), French Guiana (Capdevilla et al., 1999), Superior (Tomlinson et al., 1999), Al undepleted komatiites or AUK (Fan and Kerrich, 1997), and Al-depleted komatiites or ADK (Viljoen et al., 1983).

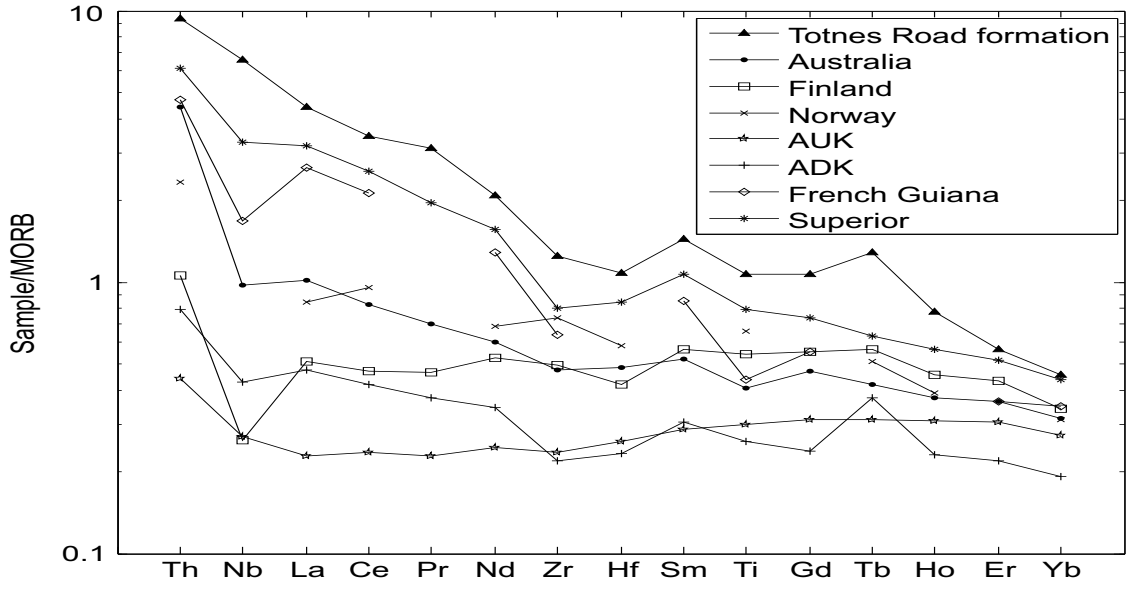

Figure 5-4. MORB (Sun and McDonough, 1989) normalized HFSE plot of Karasjok-type komatiites, ADK, and AUK showing that the Karasjok-type komatiites are enriched, with fractionated REE patterns, relative to 'classic' komatiites. Data sources same as Figure 5-3.

Karasjok-type komatiites are low and therefore more similar to the Al-depleted komatiite value than the Al-undepleted value. However, this is due to unusually high TiO_2 concentrations, not Al_2O_3 depletion. Comparison of TiO_2 concentrations between Karasjok-type komatiites, AUK, and ADK shows that Karasjok-type komatiites are enriched in Ti (Figure 5-3).

Karasjok-type komatiites are not only enriched in TiO_2, but other HFSE as well, such that Th, Nb, Hf, and Zr show enrichment compared to 'classic' komatiites (Figure 5-4). All of the Karasjok-type komatiites show weak to strong negative Zr-Hf anomalies, a characteristic usually associated with deep-mantle melting in the presence of majorite garnet. However, this process would also cause depletion in alumina, a characteristic not seen in the any of the Karasjok-type komatiites (Figure 5-3). In addition, with the exception of samples from Finland, all Karasjok-type komatiites show moderate to strong degrees of fractionation of the REE with LREE enrichment over the HREE (Figure 5-4). These are important, primary, characteristics of Karasjok-type komatiites and will be explained petrogenetically in section 5.6.

5.5 Karasjok-type Komatiite Classification

The IUGS utilizes a plot of Na_2O+K_2O vs. SiO_2 (wt%) for the classification of high-Mg volcanic rocks (Le Bas, 2000). Volcanic rocks with $SiO_2 < 52$ wt%, MgO values >18 wt%, and Na_2O+K_2O values of < 2 wt% are either komatiites or meimechites, with komatiites having TiO_2 values < 1 wt% and meimechites > 1wt%. Picrites have MgO between 12 wt% and 18 wt% and Na_2O+K_2O values < 3 wt%.

Kerr & Arndt (2001) responded to the new classification of high-Mg volcanic rocks (Le Bas 2000) with criticism over the distinction between picrites and komatiites being based only on MgO values. They argue that the true distinction between the two rock types is the presence or absence of spinifex texture. All komatiites should possess it whereas picrites should not. However, they do not propose a new name for volcanic rocks that have >18 wt% MgO and lack spinifex texture. They suggest that it is usually sufficient for volcanic rocks possessing these characteristics to be referred to as "the basal olivine-rich parts of differentiated flows or some such similar phrase." If this classification scheme were adopted, then all Karasjok-type

komatiites, distinguished by their lack of spinifex texture would be classified as the 'basal olivine-rich parts of differentiated flows". Le Bas (2001) answered Kerr & Arndt (2001) and upheld the IUGS Subcommission's view that chemical criteria be used to classify high-Mg volcanic rocks, but acknowledged that textural criteria can be important. Le Bas (2001) raises the very important point that spinifex texture only relates to how a lava crystallized at surface, whereas chemistry is related directly to the parental magma and its conditions of formation. Accordingly, should two chemically identical rocks (komatiites and picrites) be considered different rock types based entirely on the conditions under which they crystallized (Le Bas, 2001). He then raises the question of whether spinifex texture should be solely restricted to komatiites based on a plot by Kerr & Arndt (2001) that showed spinifex-textured komatiites plotting within the picrite field.

The IUGS classification scheme is inadequate for Karasjok-type komatiites in general and especially so for those of the Totnes Road formation. All Karasjok-type komatiite localities have some samples with Na_2O+K_2O values > 2 wt%, meaning they would be classified as picrobasalts and basalts even though they have >18 wt% MgO (Figure 5-5a). Some of the Totnes Road formation and Superior Province komatiite samples would classify as meimechites due to their elevated TiO_2, even though meimechites typically have higher TiO_2 and Na_2O+K_2O values (Figure 5-5b). Totnes Road komatiitic basalts, along with samples from Australia, French Guiana, and Finland would be classified as picrites due to their lower MgO values, as the IUGS does not make use of term komatiitic basalts. Arndt (2008) defines komatiitic basalts as any volcanic rock that has less than 18 wt% MgO but can be linked by petrography, texture, or geochemistry to associated komatiites.

A consensus on high-Mg volcanic rock classification obviously has yet to be reached. The IUGS scheme results in the incorrect classification of numerous samples and the suggested classification by Kerr and Arndt (2001) is inadequate. Therefore, I propose that the nomenclature already in place for Ti and HFSE-enriched, high-Mg volcanic rocks that display fragmental textures and lack spinifex texture should remain the same, and continue to be referred to as Karasjok-type komatiites. One possibility is that the upper limit of TiO_2 concentration for komatiites could be raised from 1 wt% to 2 wt%

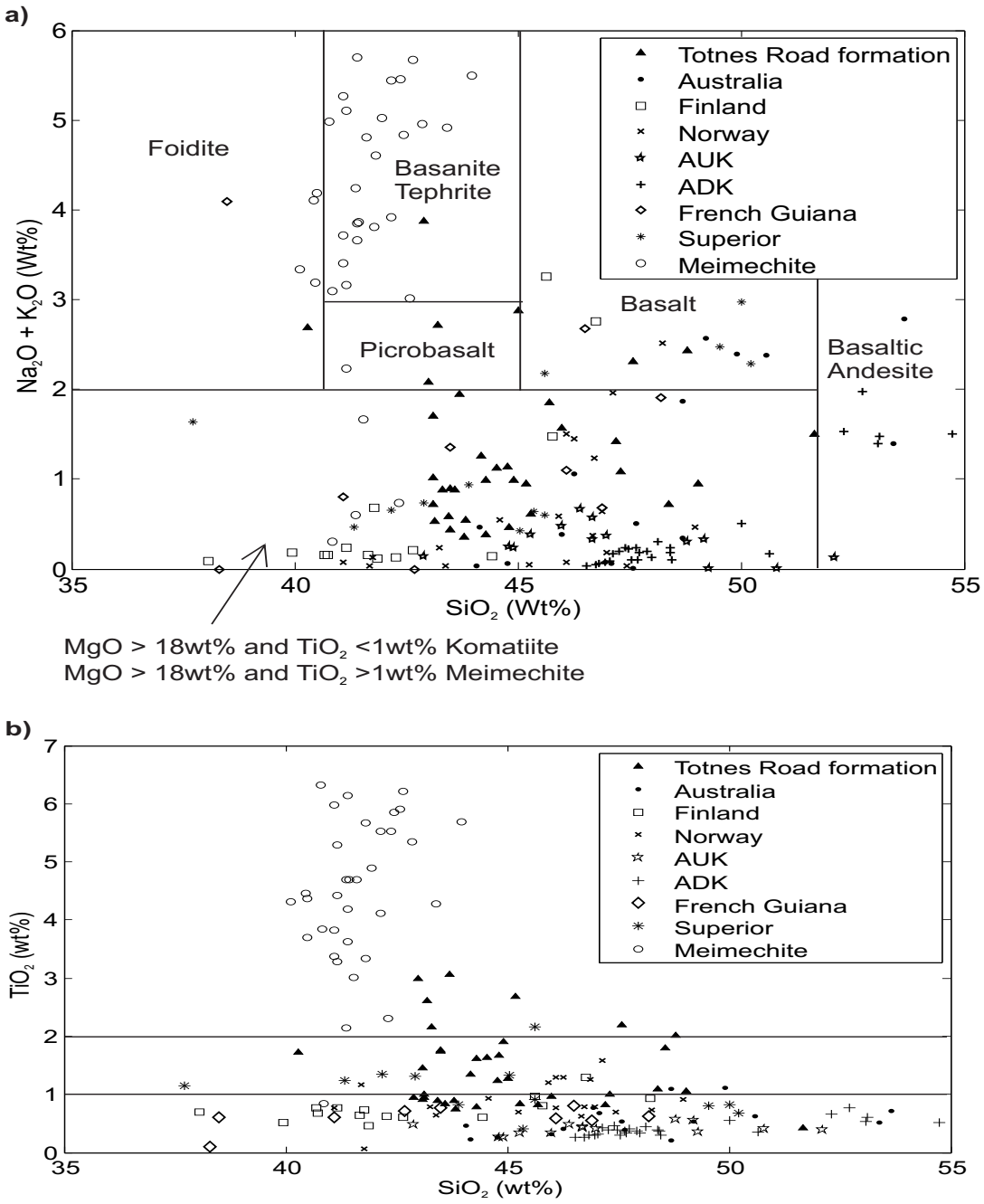

Figure 5-5. a) IUGS classification plot for high-Mg volcanic rocks of Na_2O+K_2O vs. SiO_2 (Le Bas, 2000) showing that most Karasjok-type komatiites plot with < 2 wt% Na_2O+K_2O but that all localities have samples that plot with >2 wt% Na_2O+K_2O. Meimechites plot to even greater values of Na_2O+K_2O than Karasjok-type komatiites. Data sources same as Figure 5-3, Meimechites (Sobolev et al., 2009). b) Plot of TiO_2 vs. SiO_2 for Karasjok-type komatiites and meimechites showing meimechites much greater enrichment in TiO_2 than any Karasjok-type komatiites.

5.6 Petrogenesis

Any petrogenetic model for Karasjok-type komatiites must explain the fragmental nature of the rocks (Section 5.3), their relatively low MgO values (18-25% MgO) compared to 'classic komatiites' (20-38% MgO), and their geochemical enrichment and fractionation. The HFSE and REE concentrations and MORB-normalized patterns exhibited by Karasjok-type komatiites are more similar to average OIB than AUK or ADK (Fig. 5.4 and 5.6), and so the subsequent discussion will focus on whether an OIB-like source could be involved in their origin.

Karasjok-type komatiites possess higher concentrations of MgO (average 18.6 wt%), than the global average of OIB (10.0 wt%; Sun and McDonough, 1989), likely due to lower degrees of partial melting in the younger OIB. Karasjok-type komatiites appear to be restricted to the period from the Neoarchean to Paleoproterozoic, whereas OIB have formed throughout geological time. Higher heat flow earlier in Earth's history is believed to be the reason why high-MgO volcanics, such as komatiites, are mainly restricted to ancient terranes. Therefore, higher MgO content in Karasjok-type komatiites, as well as classic komatiites, is believed to be a function of higher degrees of partial melting due to a hotter mantle in the Archean and early Paleoproterozoic when compared to modern systems.

Karasjok-type komatiites do not attain the same level of enrichment in the HFSE as OIB (Figure 5-6) but do exhibit similar fractionation patterns and greater enrichment than 'classic komatiites' (Figure 5-4). The rocks from the Totnes Road formation possess the highest levels of enrichment and most similar patterns to OIB, possibly indicating that they were sourced from very similar material. An enriched mantle source is invoked to explain the level of enrichment attained in OIB (Hofmann and White, 1982; Weaver, 1991; Niu and O'Hara, 2003; White, 2010). In this model, oceanic crust and/or lithosphere is processed at a subduction zone where the slab loses fluid soluble elements to dehydration. The now refractory material sinks into the deep mantle where it creates an "enriched zone". Additionally, Jackson et al. (2008) suggest that

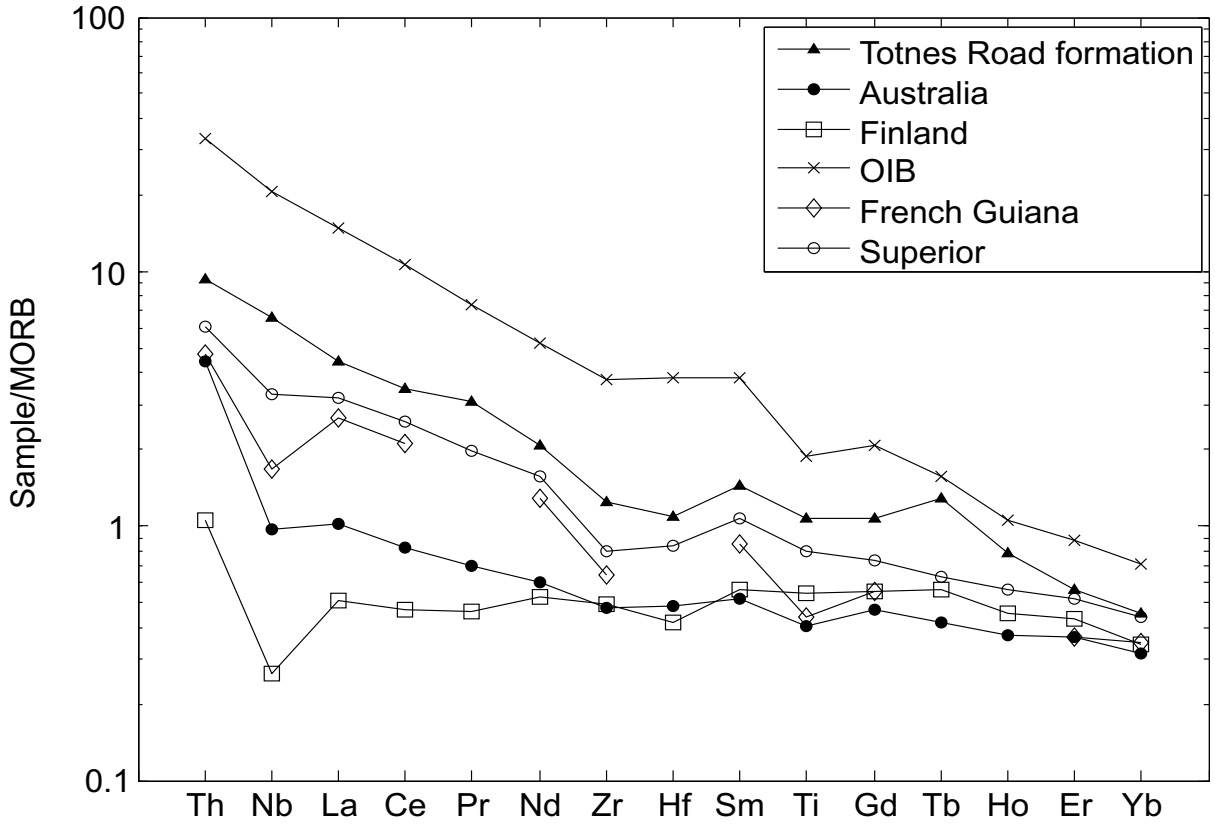

Figure 5-6. Plot of high-field strength elements normalized to MORB of Karasjok-type komatiites and OIB showing their similar fractionation patterns and enriched character. Data sources same as Figure 4-3, OIB (Sun and McDonough, 1989).

there is a global Ti, Nb, Ta (TITAN)-enriched reservoir sampled by OIB, characterized by high $^{3}He/^{4}He$, a signature associated with the deep mantle. The formation of this reservoir is thought to be due to the recycling of eclogitic material into the deep mantle. This material is believed to have experienced dehydration melting at a subduction zone, extracting the TITAN elements and concentrating them into rutile, which is conserved during subduction. This refractory eclogite will preferentially melt due to the elevated concentration of incompatible elements within it forming the parental magma of OIBs.

Karasjok-type komatiites, with their enrichment in the HFSE and specifically Ti, LREE fractionation, and negative Zr-Hf anomalies may have been sourced from similar, deep-mantle reservoirs in the late Archean to early Paleoproterozoic. The likely source for the Karasjok-type komatiites from the Totnes Road formation, to explain their unusual geochemical characteristics, includes recycled garnet-bearing eclogitic material (see Chapter 4). This material will have a lower solidus temperature than the surrounding mantle and therefore will provide a larger contribution to the melt even if it is volumetrically small (van Westrenen et al., 2001). The LREE can be fractionated from the HREE by the same fluids that contributed to the initial eclogitization process. Zr and Hf become compatible in garnet with >19 mol% Ca, a composition found within group A eclogites. If garnets with this composition exist within the eclogitic material, then melting within the source of Karasjok-type komatiites with garnet being preserved in the residuum, will lead to the preferential retention of Zr and Hf, resulting in a negative Zr-Hf anomaly in the resultant melt. The enrichment of the HFSE, such as Ti, Ta, and Nb, into the melt from this source results from the melting of rutile.

Recent work by Niu et al. (2011) has proposed that a strong control on OIB geochemistry is the thickness of the lithosphere through which OIB erupt; they term this control the "lid effect". They propose that the base of the lithosphere marks the final depth of melting for a rising mantle plume. A plume that erupts beneath thick lithosphere has a shorter distance to rise before melting ceases and therefore experiences deep, low degrees of melting. A plume that erupts through thin lithosphere has a greater distance to rise before reaching the lithosphere's base and thus experiences shallower, higher degrees of melting. Magmas generated from lower degrees of melting will be enriched in the incompatible elements compared to those that experienced higher

degrees of melt. Therefore, it seems plausible that Karasjok-type komatiites experienced lower degrees of melting than 'classic komatiites', yet still high enough to generate a high-MgO magma. This is supported by the observation that all Karasjok-type komatiites have erupted through continental crust or island arc material (French Guiana) as compared to 'classic komatiites', which are generally interpreted as erupting through oceanic crust. Since the base of the lithosphere is deeper beneath the continents than beneath the oceans Karasjok-type komatiites likely erupted through thicker lithosphere than their 'classic' counterparts.

Passage through continental crust by melts from a mantle plume usually results in contamination and the creation of a negative Nb anomaly (Arndt, 2008). All of the Karasjok-type komatiites, except the Totnes Road formation, possess this anomaly (Figure 5-4), confirming that they were contaminated by crustal material. This material may also have contributed water to the rising melt, which would have aided the fragmentation process by causing more explosive volcanism at surface. The lack of a negative Nb anomaly in the Totnes Road formation is not fully understood. Field evidence, in the form of feeder sills present within basement rocks and clasts of Archean material within the formation, suggest that the plume did pass through crustal material. The lack of an anomaly may be explained two ways: the Totnes Road formation exhibits the greatest levels of HFSE enrichment and thus it is possible that the crustal contamination signature is obscured by these high enrichment levels, or it is possible that at the time of eruption the underlying crustal material was quite thin and therefore contamination levels were low.

Plumes that were generated and ultimately melted beneath ancient continental crustal blocks would also be likely places for an enriched mantle source to exist, as subduction processes along the margins of the blocks could have supplied the necessary "enriched" material to the mantle (Figure 5-7). Therefore, all available data suggests that Karasjok-type komatiites were likely sourced from garnet-bearing eclogite-enriched mantle zones beneath thick lithosphere.

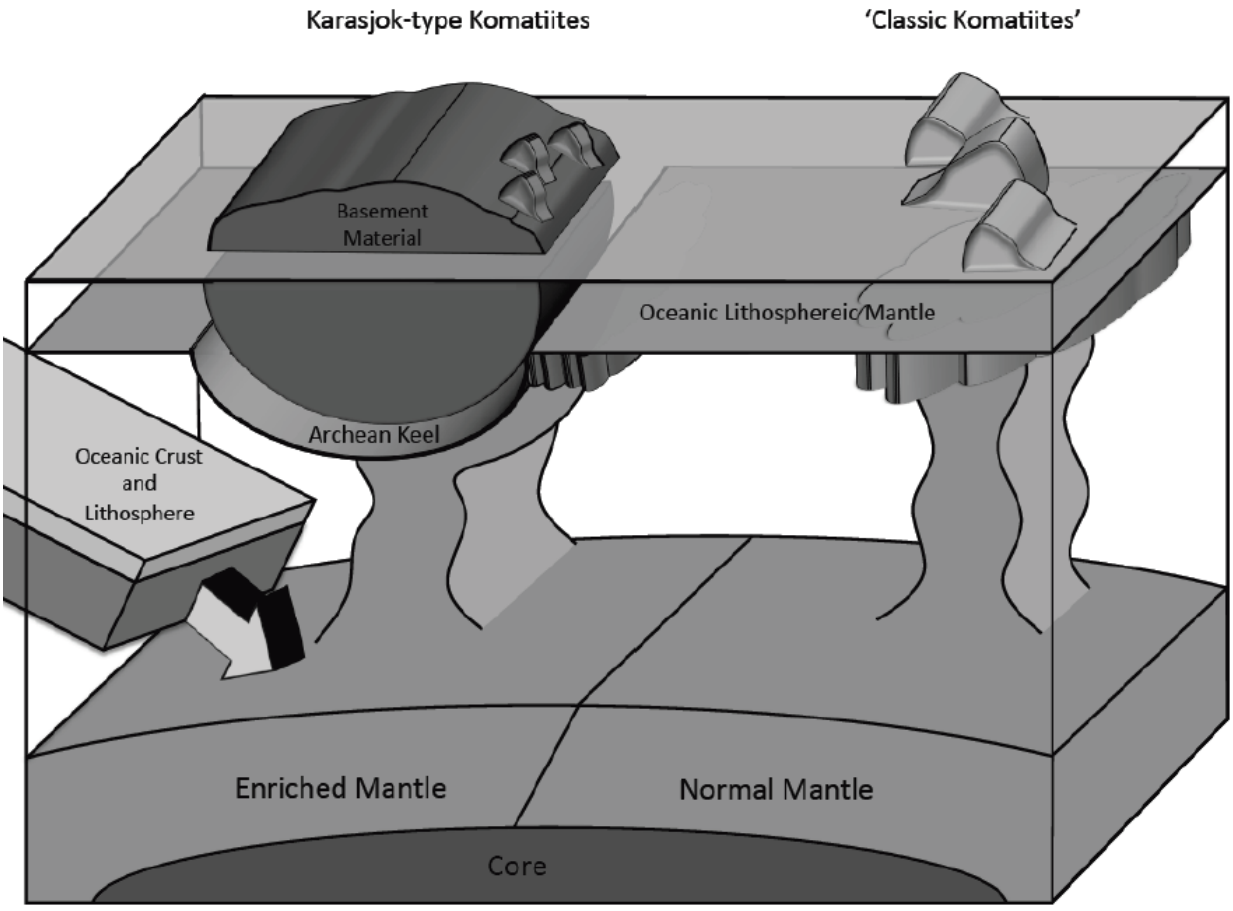

Figure 5-7. 3-D model illustrating proposed model for the petrogenesis of Karasjok-type komatiites as compared to 'classic komatiites'. Karasjok-type komatiites form from mantle enriched by subducted eclogitic material and melt beneath thick Archean lithosphere. 'Classic komatiites' form from normal mantle that has not been enriched by subducted material and are generated by melting below, and subsequently erupt through, comparatively thin oceanic crust.

5.7 Conclusions

Karasjok-type komatiites represent a distinct and unusual subset of komatiitic rocks. They are found in a few Neoarchean to mid Paleoproterozoic localities throughout the world. Classification of volcanic rocks as Karasjok-type komatiites should be based on the follow characteristics: dominantly fragmental units, lack of spinifex texture, high-MgO values of >18 wt% but likely lower than 'classic komatiite' values of 25-26 wt%, enrichment in Ti with TiO_2 values > 0.5 wt%, HFSE enrichment with values of at least 10x MORB, negative Nb anomalies, and negative Zr-Hf anomalies. The above characteristics are most likely caused by subaqueous eruption in water depths < 200m, melting of eclogite-enriched mantle, and eruption through older crustal material. Refinement of the definition for Karasjok-type komatiites based on new insights gained through the discovery and documentation of komatiitic rocks of the Totnes Road formation, Cumberland Peninsula, eastern Baffin Island has assisted in better-defining these unusual rocks and thereby providing insights into their formation.

Chapter 6

CONCLUSIONS

The overall goal of this M.Sc. thesis was to provide the first description of the volcanic rocks, now termed the Totnes Road formation, and the chemical sedimentary rocks, now termed the Clephane Bay formation, found within the North Touak-Cape Dyer volcanic belt on Cumberland Peninsula, Baffin Island. This has been accomplished through both fieldwork and lab work involving mainly petrological, and geochemical analysis. Other objectives were to interpret these rocks with respect to their petrogenesis and tectonic setting, in order to better understand the geologic history of the Cumberland Peninsula, to attempt to correlate the rocks on a regional scale, to assess their metallogenic potential, and to refine the definition of Karasjok-type komatiites. All of these objectives have received consideration and interpretations have been presented. Future work on the Cumberland Peninsula will help to refine these interpretations and provide a clearer picture of the geology present.

6.1 Totnes Road formation and Karasjok-type Komatiites

The green-weathering volcanic rocks were found to be Mg-rich and thus represent a suite of komatiitic basalts and komatiites with some Fe-rich tholeiites (black-weathering volcanic rocks). They possess numerous unusual features for komatiites including a dominantly fragmental nature, with no spinifex texture observed, an interpreted young eruption age of > 2.0 Ga through ancient continental crustal material, and geochemical enrichment in the high-field strength elements. Given the textural and geochemical similarities between samples from throughout the volcanic belt, all of the volcanic rocks are considered co-genetic and thus represent one major period of plume-related volcanic activity. The fragmental nature of the rocks may be explained by a combination of steam and magmatic explosivity, the latter process requires volatiles to be present within the magma, which is unusual for ultramafic magmas. However it is very likely that the magma could have been contaminated upon passing through the older continental crust in the area and water may have been incorporated into the magma at this time. The dominance of a fragmental texture also likely explains the lack of spinifex texture,

as spinifex requires an effusive, flow-forming, eruption style. The unusual geochemical characteristics of the Totnes Road formation can be explained by incorporation of recycled garnet-bearing eclogitic material into the source of the volcanic rocks.

The combination of the above-mentioned unusual characteristics places the Totnes Road formation within the uncommon and poorly understood Karasjok-type komatiite sub-type. Karasjok-type komatiites have been described from only five localities worldwide at the time of writing this thesis and most of the available literature on them provides only a baseline description. All Karasjok-type komatiites share a fragmental nature, lack spinifex texture, are enriched in the HFSE, notably Ti, possess negative Zr-Hf anomalies and moderate to strongly fractionated REE patterns, young eruption ages, and sit atop older crustal material. If the worldwide consensus is that Karasjok-type komatiites truly belong in the komatiite family, then the current upper limit of 1 wt% TiO_2 for komatiites should be raised to 2 wt% to allow for the proper classification of this sub-type.

Ultramafic volcanic sequences can be prospective for Ni-Cu-PGE type mineralization, however to date no mineralized areas have been mapped and there is no geochemical indicator that these elements have been stripped from barren zones to be deposited as ore elsewhere.

6.2 Regional Correlations of the Totnes Road formation

An important goal of the CPIG project as a whole was to provide as much information as possible regarding regional correlations of the Hoare Bay group and its underlying Archean basement. Prior to CPIG, one interpretation was that the Hoare Bay group was correlative with the Piling Group (St-Onge et al., 2009). However, the volcanic rocks of the Piling Group, the Bravo Lake Formation (Johns et al., 2006), are chemically distinct, with the Bravo Lake Formation being composed of basalts with no ultramafic components. Therefore the search for a possible correlation was expanded to include other mafic-ultramafic occurrences within northeast Canada and west Greenland.

Rocks from the Ussuit locality in East Greenland (Kalsbeek and Manatschal, 1999) and from the Chukotat and Povungnituk Groups of northern Quebec (St-Onge et al., 2000) are ultramafic in nature, hinting at a plume source, however their trace-element signatures do not show any relation to those from the Totnes Road formation.

The trace element signature of a komatiite from the Schooner Harbour sequence of southern Baffin Island (Sanborn-Barrie et al., 2008) is almost identical in both pattern and concentration to the Totnes Road formation and basaltic samples from the Schooner Harbour sequence show remarkable similarity in both pattern and concentrations to the Bravo Lake formation. Interestingly, the patterns from the Totnes Road formation and the komatiitic sample from the Schooner Harbour sequence and the basaltic samples from the latter and the Bravo Lake formation are nearly identical. It may be possible that the Bravo Lake Formation, Totnes Road formation, and the Schooner Harbour sequence were all sourced from the same source, likely a mantle plume. The more komatiitic rocks having been sourced from the hotter, uncontaminated plume axis and the basaltic rocks from the plume head, which has experienced the most contact with the surrounding crustal rocks and thus is likely cooler and more contaminated (Campbell et al., 1990). Further geochemical and geochronological work will be needed to fully assess the validity of this hypothesis.

6.3 Clephane Bay formation

The Clephane Bay formation has been defined to include the thin, discontinuous outcrops of silicate facies iron formation, chert, pyritic-graphitic schist, and semi-massive sulphide boulders that overlie the Totnes Road formation. At any location where the formation crops out one, two, or all of the above-mentioned lithologies may be present within a gossanous zone that clearly outlines the formations location.

The variability of the chemical sedimentary rocks raised the question of whether or not they were all correlative throughout the volcanic belt. Major element geochemistry indicated that the lithological variability was likely due to the mixing of both hydrothermal and detrital sources, as Fe and Al concentrations were variable between different units. Trace element

geochemistry, specifically the REE, showed near identical patterns on chondrite-normalized plots, which indicates that the formation was deposited in the same basin with the same hydrothermal and detrital sources. Therefore, the Clephane Bay formation is correlative throughout the North Touak-Cape Dyer volcanic belt and represents one major period of hydrothermal activity within one basin. It is very likely that the waning heat from the plume that sourced the Totnes Road formation drove this hydrothermal activity.

Given the abundance of Fe and lack of high-temperature economic minerals such as Cu-, Zn- or Pb-bearing sulphides it appears that the Clephane Bay formation represents relatively low temperature hydrothermal activity and thus is likely not economically prospective. However, the formation covers a vast area and not all of it was mapped in detail and therefore a high-temperature vent complex may exist somewhere and the lithologies mapped to date may merely represent the more distal portions of the system.

6.4 Evolution of the Cape Dyer-North Touak volcanic belt

The Archean basement rocks of the Cumberland Peninsula record ages of 2.7-2.99 Ga (Rayner et al., 2012 in press, Sanborn-Barrie et al., 2011a) and the Hoare Bay group is a Paleoproterozoic supracrustal sequence that sits atop this basement. The exact nature of the relationship between the basement and cover rocks, autochthonous or allochthonous, has yet to be unequivocally determined. The age of the entire supracrustal package is bracketed between <1.99-1.96 Ga, the youngest Paleoproterozoic detritus found in the Hoare Bay group, and ca. 1890 Ma, the age of the Qikiqtarjuaq plutonic suite, which is intrusive into the Hoare Bay group (Rayner et al., 2012, in press; Wodicka, personal communication). Therefore the Hoare Bay group was deposited within this ca. 70-100 Ma period. The time of eruption of the volcanic rocks is unknown primarily due to the lack of datable material in these rocks (Wodicka and Sanborn-Barrie, personal communication).

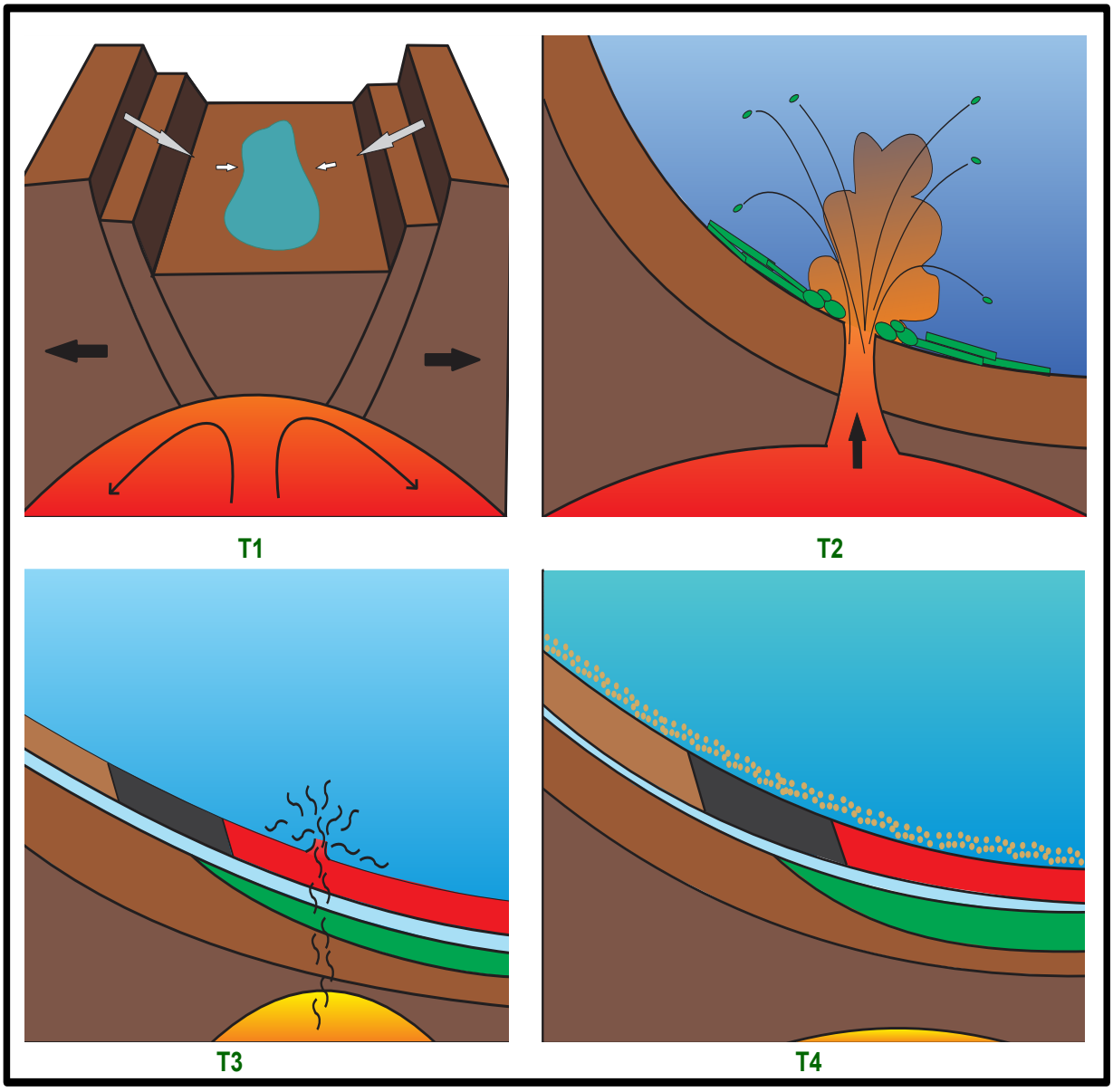

Figure 6-1. A schematic diagram illustrating the interpreted evolution of the Hoare Bay group. In time 1 (T1) rifting is initiated in continental crust due to the impingement of a mantle plume, possibly causes the observed spike in ca. 2.0 Ga detritus. In T2 subaqueous mafic-ultramafic volcanic activity takes place due to the continued impingement of the mantle plume. In T3 a variety of hydrothermal sediments are deposited due to residual heat from the mantle plume causing the circulation of hydrothermal fluids within the basin. In T4 clastic sedimentation briefly returns before deposition ceases.

As stated in Chapter 2, the occurrence of quartzite and marble in the western, and lowermost, portion of the supracrustal sequence is suggestive of a shelf succession, whereas the North Touak-Cape Dyer volcanic belt to the east is suggestive of a more basinal succession. The presence of ultramafic volcanic rocks and sills insinuates the presence of a mantle plume underlying the Cumberland Peninsula at the time of eruption. Throughout the Hoare Bay group there is a large spike in 2.0 Ga detritus (Sanborn-Barrie, personal communication) that suggests a large amount of deposition occurring <2 Ga. This large increase in the amount of detritus being deposited could be due to rifting caused by the arrival and impingement of a mantle plume. The volcanic rocks and sills would have been emplaced during this time. The chemical sediments were sourced by hydrothermal activity in the basin caused by high heat flow as the volcanic activity waned and the plume heat started to abate. The return to clastic sedimentation must have been rapid as detrital zircons from the upper clastic package, from King Alberts Peak, located just north of Sunneshine Fiord, have a distinct age peak at 1990 Ma (Wodicka, peronsal communication). Deposition of the entire Hoare Bay group had ceased by ca. 1890 Ma, the time of emplacement of the Qikiqtarjuaq suite (Rayner et al., 2012, in press). Therefore, an initial interpretation would be that rifting occurred due to impingement of a mantle plume at a continental margin affecting both shelf and basinal successions. Rifting would cause crustal thinning which is the most likely cause for the lack of a negative Nb anomaly within in the Totnes Road formation. This mantle plume produced mafic-ultramafic volcanic rocks as well as ultramafic sills and residual heat from it led to hydrothermal activity in the basin causing the deposition of chemical sedimentary rocks. The return to clastic sedimentation was rapid and brief, as deposition of the entire supracrustal package lasted only ~100 Ma.

REFERENCES CITED

Anders, E., and Grevesse, N., 1989. Abundances of the elements: Meteoritic and solar; Geochimica et Cosmochimica Acta, v. 53, p. 197-214.

Anhaeusser, C.R., 1975. Precambrian tectonic environments; Annual Review Earth and Planetary Sciences, v. 3, p. 31-53.

Arndt, N.A., 2008. Komatiite; Cambridge University Press.

Arndt, N.A., Francis, D., and Hynes, A.J., 1979. The field characteristics and petrology of Archean and Proterozoic komatiites; Canadian Mineralogist, v. 17, p. 147-163.

Arndt, N.T. and Nisbet, E.G., 1982. What is a komatiite? In: N.T. Arndt and E.G. Nisbet (eds.) Komatiites, pp.19-27. London: George Allen and Unwin.

Barley, M.E., Kerrich, R., Reudavy, I., Xie, Q., 2000. Late Archaean Ti-rich, Al-depleted komatites and komatiitic volcaniclastic rocks from the Murchison Terrane in Western Australia; Australian Journal of Earth Sciences, v. 47, p. 873-883.

Bickle, M., 1993. Plume origin for komatiites; Nature, v. 365, p.390-391.

Barnes, S. & Often, M. 1990., Ti-rich komatiites from northern Norway; Contributions to Mineralogy and Petrology, v. 105, p. 42-54.

Bekker, A., Slack, J.F., Planavsky, N., Krapež, B., Hofmann, A., Konhauser, K.O., and Rouxel, O.J., 2010. Iron formation: The sedimentary product of a complex interplay among mantle, tectonic, oceanic, and biospheric processes; Economic Geology, v. 105, p. 467-508.

Beswick, A.E., 1982. Some geochemical aspects of alteration, and genetic relations in komatiitic suites; *in* Komatiites, (ed.) N.T. Arndt and E.G. Nisbet; George Allen & Unwin (Publishers) Ltd, p. 283-308.

Brostöm, K. 1973. The origin and fate of ferromanganoan active ridge sediments; Stockholm Contributions to Geology, v. 27, p. 147-243.

Broström, K., and Peterson, M.N.A. 1969. Origin of aluminum-poor ferromanganoan sediments in areas of high heat flow on the East Pacific Rise; Marine Geology, v. 7, p. 427-47.

Campbell, I. H., Griffiths, R.W., and Hill, R.I. 1989. Melting in an Archean mantle plume: heads it's basalts, tails it's komatiites; Nature, vol. 338, p. 697-698.

Cann, J.R., 1970. Rb, Sr, Y, Zr, and Nb in some ocean floor basaltic rocks; Earth and Planetary Science Letters, v. 10, p. 7-11.

Capdevila, R., Arndt, N., Letendre, J., Sauvages., 1999. Diamonds in volcaniclastic komatiite from French Guiana; Nature, v. 399, p. 456-458.

Chavagnac, V. 2004., A geochemical and Nd isotopic study of the Barberton komatiites (South Africa): Implication for the Archean mantle; Lithos, v. 75, p. 253-281.

Condie, K.C., 2001. Mantle plumes and their record in earth history; Cambridge University Press.

Connelly, J.N., Thrane, K., Krawiec, A.W., and Garde, A.A., 2006. Linking the Palaeoproterozoic Nagssugtoqidian and Rinkian orogens through the Disko Bugt region of West Greenland; Journal of the Geological Society of London, v. 163, p. 319-335.

Corrigan, D., Pehrsson, S., Wodicka, N., de Kemp, E. 2009., The Palaeoproterozoic Trans-Hudson Orogen: a prototype of modern accretionary processes; Geological Society of London, Special Publications, v. 327, p. 457-479.

Corrigan, D., Scott, D. J., St-Onge, M. R., 2001. Geology of the northern margin of the Trans-Hudson Orogen (Foxe Fold Belt), central Baffin Island, Nunavut; Geological Survey of Canada, Current Research 2001-C23, 2001; 27 pages

Coyle, M., 2009. Residual total and first vertical derivative of the magnetic field, Cumberland Peninsula aeromagnetic survey, part of NTS 16 D North, Nunavut; Geological Survey of Canada, Open File 6086 -6103 , scale 1:100,000.

Cronan, D. 1976. Basal metalliferous sediments from the eastern Pacific; Geological Society of America, Bulletin, v. 87, p. 928-934.

Dasgupta, R., Jackson, M.G., and Lee, C.A., 2010. Major element chemistry of ocean island basalts – Conditions of mantle melting and heterogeneity of mantle source, v. 289, p. 377-392.

Dubé, B., and Gosselin, P., 2007. Grenstone-hosted quartz-carbonate being deposits, *in* Goodfellow, W.D., ed., Mineral Deposits of Canada: A synthesis of major deposit-types, district metallogeny, the evolution of geological provinces, and exploration methods; Geological Association of Canada, Mineral Deposits Division, Special Publication No.5, p. 49-73.

Dyke, A. a), in press, Surficial geology of Hoare Bay north, Geological Survey of Canada, Canadian Geoscience Map 17 (preliminary version), 1:100 000

Dyke, A. b), in press, Surficial geology of Pangnirtung south, Geological Survey of Canada, Canadian Geoscience Map 19 (preliminary version) 1:100 000

Dyke, A. c), in press, Surficial geology of Cape Dyer south, Geological Survey of Canada, Canadian Geoscience Map 20 (preliminary version) 1:100 000

Elkins-Tanton, L.T., Draper, D.S., Agee, C.B., Jewell, J., Thorpe, A., Hess, P.C., 2006. The last lavas erupted during the main phase of the Siberian flood volcanic province: results from experimental petrology; Contributions to Mineral Petrology, v. 153, p. 191-209.

Ernst, R., and Bleeker, W., 2010. Large igneous province (LIPS), giant dyke swarms, and mantle plumes: significance for breakup events within Canada and adjacent regions from 2.5 Ga to the Present; Canadian Journal of Earth Sciences, v. 47, p. 695-739.

Evans, K.A., Phillips, G.N., Powell, R. 2006. Rock-buffering of auriferous fluids in altered rocks associated with the Golden Mile-style mineralization, Kalgoorlie gold field, Western Australia; Economic Geology, v. 101, p. 805-817.

Fan, J. & Kerrich, R., 1997. Geochemical characteristics of aluminum depleted and undepleted komatiites and HREE-enriched low-Ti tholeiites, western Abitibi greenstone belt: A heterogeneous mantle plume-convergent margin environment; Geochimica et Cosmochimica Acta, v. 61, p. 4723-4744.

Fisher, R.V., 1966. Rocks composed of volcanic fragments and their classification; Earth-Science Reviews, v. 1., p. 287-298.

Fowler, A.D., Berger, B., Shore, M., Jones, M.I. and Ropchan, J, 2002. Supercooled rocks: development and significance of varioles, spherulites, dendrites and spinifex in Archean volcanic rocks, Abitibi Greenstone Belt Canada; Precambrian Research, v.115, p. 311-328

Fowler, A.D., Jensen, L.S., Peloquin, S.A. 1986. Varioles in Archean basalts: products of spherultic crystallization.; Canadian Mineralogist, v. 25, p. 275-289.

Gammon, P., Dyke, A., Sanborn-Barrie, M., Young, M., 2011. Geochemistry and physical properties of till samples collected in 2009 from Cumberland Peninsula, Nunavut; Geological Survey of Canada, Open file 6793, doi:10.4095/287453.

Gangopadhyay, A., Walker, R.J., Hanski, E., Solheid, P.A., 2006. Origin of Paleoproterozoic komatiites at Jeesiörova, Kittilä Greenstone complex, Finnish Lapland; Journal of Petrology, v. 47, p. 773-789.

Gélinas, L. Trzcienski, W.E., Brooks, C. 1977., Archean variolites – quenched immiscible liquids; Canadian Journal of Earth Sciences, v. 13, p. 210-230.

Gruau, G., Tourpin, S., Fourcade, S., Blais, S., 1992. Loss of isotopic (Nd, O) and chemical (REE) memory during metamorphism of komatiites: new evidence from eastern Finland; Contributions to Mineralogy and Petrology, v. 112, p. 66-82.

Hanski, H., Huhma, H., Rastas, P., Kamenetsky, V.S., 2001. The Palaeoproterozoic komatiite-picrite association of Finnish Lapland; Journal of Petrology, v. 42, p. 855-876.

Henderson, P., 1980. Rare earth element partition between sphene, apatite, and other coexisting mineral of the Kangerdlugssuaq Intrusion, E. Greenland; Contributions to Mineralogy and Petrology, v. 72, p. 81-85.

Henriksen, N., Higgins, A.K., Kalsbeek, F., and Pulvertaft, C.R., 2009. Greenland from Archean to Quaternary; Geological Survey of Denmark and Greenland Bulletin, v. 18, 126 pp.

Herzberg, C., 1995. Generation of plume magmas through time: an experimental perspective; Chemical Geology, v. 126, p. 1-16.

Hofmann, A.W., and White, W.M., 1982. Mantle plumes from ancient oceanic crust; Earth and Planetary Science Letters, v. 57, p. 421-436.

Jackson, G.D., Taylor, F.C., 1972. Correlation of major Aphebian rock units in the Northeastern Canadian Shield; Canadian Journal of Earth Sciences, v. 9, p. 1650-1670

Jackson, M.G., Hart, S.R., Saal, A.E., Shimizu, N., Kurz, M.D., Blusztajn, J.S., Skovgaard, A.C., 2008. Globally elevated titanium, tantalum, and niobium (TITAN) in ocean island basalts with high $^{3}He/^{4}He$; Geochemistry Geophysics Geosystems, v. 9, Q04027

James, H.L. 1954. Sedimentary facies of iron formation; Economic Geology, v. 49, p. 235-293.

Jenner G. A., Longerich H. P., Jackson S. E., and Fryer B. J., (1990). ICP-MS - A powerful tool for high precision trace-element analysis in earth sciences: Evidence from analysis of selected USGS reference samples; Chemical Geology, v.83, p. 133-148.

John, T., Scherer, E.E., Haase, K., Schenk, V., 2004. Trace element fractionation during fluid-induced eclogitization in a subducting slab: trace element and Lu-Hf-Sm-Nd isotope systematics; Earth and Planetary Science Letters, v. 227, p. 441-456.

Johns, S.M., Helmstaedt, H.H., Kyser, T.K., 2006. Paleoproterozoic submarine intrabasinal rifting, Baffin Island, Nunavut, Canada: volcanic structure and geochemistry of the Bravo Lake Fromation; Canadian Journal of Earth Sciences, v. 43, p. 593-616.

Kalfoun, F., Ionov, D. Merlet, C., 2002. HFSE residence and Nb/Ta ratios in metasomatised, rutile-bearing mantle peridotites; Earth and Planetary Science Letters, v. 199, p. 49-65.

Kalsbeek, F., and Manatschal, G., 1999. Geochemistry and tectonic significance of peridotitic and metakomatiitic rocks from the Ussuit area, Nagssugtoqidian orogen, West Greenland; Precambrian Research, v. 94, p. 101-120.

Keim, R.D., 2010. Stratigraphy, petrology, and geochemistry of the Totnes Road volcanic rocks, Cumberland Peninsula, Baffin Island, unpub. B.Sc. thesis report, University of Saskatchewan.

Keim, R.D., Sanborn-Barrie, M., Ansdell, K., Young, M., 2011. Totnes Road metavolcanic rocks: a fragmental, Ti-enriched komatiitic volcanic suite on Cumberland Peninsula, Baffin Island, Nunavut; Geological Survey of Canada, Current Research 2011-13, 18 p. doi:10.4095/289072.

Kerr, A.C., and Arndt, N.T., 2001. A note of the IUGS reclassification of the high-Mg and picritic volcanic rocks; Journal of Petrology, v. 42, p. 2169-2171.

Kokelaar, P., 1986. Magma-water interactions in subaqueous and emergent basaltic volcanism; Bulletin of Volcanology, v. 48, p. 275-289.

Lahaye, Y., Arndt, N., Byerly, G., Chauvel, C., Fourcade, S., Gruau, G., 1995. The influence of alteration on the trace-element and Nd isotopic compositions of komatiites; Chemical Geology, v., 126, p. 43-64.

Le Bas., M.J., 2000. IUGS reclassification of the high-Mg and picritic volcanic rocks; Journal of Petrology, v. 41, p. 1467-1470.

Le Bas, M.J., 2001. Reply to comment by Kerr and Arndt; Journal of Petrology, v. 42, p. 2173-2174.

Lydon, J.W., Paakki, J., Anderson, H.E. and Reardon, N.C.. 2000a. An overview of the geology and geochemistry of the Sullivan Deposit; Chapter 27, *in* Lydon, J.W., Höy, T., Slack, J.F., and Knapp, M., eds., The Geological

Environment of the Sullivan Pb-Zn-Ag Deposit, British Columbia: Mineral Deposits Division of the Geological Association of Canada, Special Publication 1, p.505-522.

Marchig, V., Gundlach, H., Möller, P., Schley, F. 1982. Some geochemical indicators for discrimination between diagenetic and hydrothermal metalliferous sediments; Marine Geology, v. 50, p. 241-256.

Marshall, B., and Gilligan, L.B. 1989. Durchbewegung structure, piercement cusps, and piercement veins in massive sulfide deposits: formation and interpretation: Economic Geology, v. 84, p. 2311-2319.

Mackay, C., 2011. Petrographic and geochemical study of the origin of "spotted" dykes and their relationship to the North Touak-Cape Dyer volcanic belt: Cumberland Peninsula, Baffin Island, unpub. B.Sc. thesis report, University of Saskatchewan.

Nesbitt, R.W., 1971. Skeletal crystal forms in the ultramafic rocks of the Yilgarn Block, Western Australia: Evidence for an Archaean ultramafic liquid; Geological Society of Australia, v. 3, p. 331-347.

Nesbit, R.W., Sun, S.S., and Purvis, A.C., 1979. Komatiites: geochemistry and genesis; Canadian Mineralogist, v. 17, p. 165-186.

Niu, Y., and O'Hara, M.J., 2003. Origin of ocean island basalts: A new perspective from petrology, geochemistry, and mineral physics considerations; Journal of Geophysical Research, v. 108(B4).

Niu, Y., Wilson, M., Humphreys, E.R., O'Hara, M.J., 2011. The origin of intra-plate ocean island basalts (OIB): The lid effect and its geodynamic implications; Journal of Petrology, v. 52, p. 1443-1468.

North American commission on stratigraphic nomenclature., 2005. North American stratigraphic code; AAPG Bulletin, v.89, p. 1547-1591.

Pearce, J.A., 1996.A user's guide to basalt discrimination diagrams, *in* (ed) D.A. Wyman, Trace element geochemistry of volcanic rocks: applications for massive sulphide exploration; Geological Association of Canada, Short Course Notes, v. 12, p. 79-113.

Pearce, J.A., 2008. Geochemical fingerprinting of oceanic basalts with applications to ophiolite classification and the search from Archean oceanic crust; Lithos, v. 100, p. 14-48.

Pearce, T.H., 1968. A contribution to the theory of variation diagrams; Contributions to Mineralogy and Petrology, v. 19, p. 142-157.

Peter, J.M. 2003. Ancient iron formations: their genesis and use in the exploration for stratiform base metal sulphide deposits, with examples from the Bathurst Mining Camp; in Lentz, D.R., ed., Geochemistry of Sediments and Sedimentary Rocks: Evolutionary Considerations to Mineral Deposit-Forming Environments: Geological Association of Canada, GeoText 4, p. 145-176.

Petit, C., 2010, Continental Hearts: Science News, v. 178, p.22

Pilet, S., Hernandez, J., Sylvester, P., Poujol, M., 2005. The metasomatic alternative for ocean island basalt chemical heterogeneity; Earth and Planetary Science Letters, v. 236, p. 148-166.

Prytulakm J., and Elliott, T., 2007. TiO_2 enrichment in ocean island basalts; Earth and Planetary Science Letters, v. 263, p. 388-403.

Pyke, D.R., Naldrett, A.J., and Eckstrand, O.R., 1973. Archean ultramafic flows in Munro Township, Ontario; Geological Society of America Bulletin, v. 84, p. 955-978.

Rayner, N.M, Sanborn-Barrie, M., Young, M.D., and Whalen, J.B., 2012. U-Pb ages of Archean basement and Paleoproterozoic plutonic rocks, southern Cumberland Peninsula, eastern Baffin Island, Nunavut; Geological Survey of Canada, Current Research, 2012-8, 24 p. doi: 10.4095/291401.

Said, N., & Kerrich, R., 2009. Geochemistry of coexisting depleted and enriched Paringa Basalts, in the 2.7 Ga Kalgoorlie Terrane, Yilgarn Craton, Western Australia: Evidence for a heterogeneous mantle plume event; Precambrian Research, v. 174, p. 287-309.

Sanborn-Barrie, M., St-Onge, M.R., Young, M.D., and James, D.T., 2008. Bedrock geology of southwestern Baffin Island, Nunavut: expanding the tectonostratigraphic framework with relevance to mineral resources; Geological Survey of Canada Current Research 2008-6, 16 p.

Sanborn-Barrie, M., & Young, M. 2011. Bulk compositional data for sulfidic and gossanous rocks from Cumberland Peninsula, Baffin Island, Nunavut. Geological Survey of Canada, Open File 6916. doi:10.4095/288710

Sanborn-Barrie, M. and Young, M., 2012*a*. Geology, Circle Lake, Nunavut; Geological Survey of Canada, Canadian Geoscience Map 5 (preliminary), scale 1:100 000

Sanborn-Barrie, M. and Young, M, 2012*b*. Geology, Durban Harbour, Nunavut; Geological Survey of Canada, Canadian Geoscience Map 37 (preliminary), scale 1:100 000

Sanborn-Barrie, M. and Young, M., 2012*c*. Geology, Padle Fiord, Nunavut; Geological Survey of Canada, Canadian Geoscience Map 38 (preliminary), scale 1:100 000

Sanborn-Barrie, M., Young, M., Keim, R. and Hamilton, B., 2012*a*. Geology, Sunneshine Fiord, Nunavut; Geological Survey of Canada, Canadian Geoscience Map 6 (preliminary), scale 1:100 000

Sanborn-Barrie, M., Young, M and Whalen J.B., 2012*b*. Geology, Qikiqtarjuaq, Nunavut; Geological Survey of Canada, Canadian Geoscience Map 39 (preliminary), scale 1:100 000

Sanborn-Barrie, M, Young, M., Whalen, J., James, D. and St-Onge, M.R.., 2011c. Geology, Touak Fiord, Nunavut; Geological Survey of Canada, Canadian Geoscience Map 3 (preliminary version) scale 1:100,000 doi:10.4095/288209

Sanborn-Barrie, M, Young, M., Whalen, J. and James, D., 2011a. Geology, Ujuktuk Fiord, Nunavut; Geological Survey of Canada, Canadian Geoscience Map 1 (preliminary version) scale 1:100,000 doi:10.4095/288206

Sanborn-Barrie, M, Young, M., and Whalen, J., 2011b. Geology, Kingnait Fiord, Nunavut; Geological Survey of Canada, Canadian Geoscience Map 2 (preliminary version) scale 1:100,000

Sanborn-Barrie, M., Young, M., Whalen, J., St-Onge, M., James, D., Rayner, N., Coyle, M., Lynds, T., and Hilary, B in Palmer, E. (complier), 2010. A new bedrock geology map of the Cumberland Peninsula, Nunavut: An initial step in evaluating the mineral potential of eastern Baffin Island. 38th Annual Yellowknife Geoscience Forum

Abstracts; Northwest Territories Geoscience Office, Yellowknife, NT. YKGSF Abstracts Volume 2010.

Schaefer, S.J. & Morton, P., 1991. Two komatiitic pyroclastic units, Superior Province, northwestern Ontario: their geology, petrography, and correlation; Canadian Journal of Earth Sciences, v. 28, p. 1455-1470.

Scott, D.J., St-Onge, M.R., and Corrigan, D., 2002. Geology of the Paleoproterozoic Piling Group and underlying Archean gneiss, central Baffin Island, Nunavut; Geological Survey of Canada Current Research 2002-C17, 10 p.

Sobolev, A.V., Sobolev, S.V., Kuzmin, D.V., Malitch, K.N., and Petrunin, A.G., 2009. Siberian meimechites: origin and relation to flood basalts and kimberlites; Russian Geology and Geophysics, v. 50, p. 999-1033.

Sohn et al., 2008. Explosive volcanism on the ultraslow-spreading Gakkel ridge, Arctic Ocean; Nature, v. 453, p. 1236-1238.

Stone, W.E., Crocket, J.H., Dickin, A.P., and Flett, M.E., 1995. Origin of Archean ferropicrites: geochemical constraints from the Boston Creek Flow, Abitibi greenstone belt, Ontario, Canada; Chemical Geology, v. 121, 51-71.

Stone, W.E., Jensen, L.S., and Church, W.R., 1987. Petrography and geochemistry of an unusual Fe-rich basaltic komatiite form Boston Township, northeastern Ontario; Canadian Journal of Earth Sciences, v. 24, p. 2537-2550.

St-Onge, M.R., Jackson, G.D., Henderson, I., 2006a. Geology, Baffin Island (south 70°N and east of 80°W), Nunavut; Geological Survey of Canada, Open File 4931, doi:10.4095/222520.

St-Onge, M.R., Lucas, S.B., Parrish, R.R., 1992. Terrane accretion in the internal zone of the Ungava orogen, northern Quebec. Part 1: Tectonostratigraphic assemblages and their tectonic implications; Canadian Journal of Earth Sciences, v. 29, p. 746-764.

St-Onge, M.R., Scott, D.J., and Lucas, S.B., 2000; Early partitioning of Quebec: Microcontinent formation in the Paleoproterozoic; Geology, v. 28, p. 323-326.

St-Onge, M.R., Searle, M.P., Wodick, N., 2006b. Trans-Hudson Orogen of North America and Himalaya-Karakoram-Tibetan Orogen of Asia: structural and thermal characteristics of the lower and upper plates; Tectonics, v. 25.

St-Onge, M.R., Van Gool, J., Garde, A.A., Scott, D.J., 2009. Correlation of Archaean and Palaeoproterozoic units between northeastern Canada and western Greenland: constraining the pre-collisional upper plate accretionary history of the Trans-Hudson orogen; Geological Society of London, Special Publications, v. 318, p. 193-235.

Sun, S.S. & McDonough, W.F., 1989. Chemical and isotopic systematics of oceanic basalts: implications for mantle composition and processes, *in* Saunders, A.D. & Norry, M.J., Magmatism in the ocean basins; Geological Society of London, Special Publications, v. 42, p. 313-345.

Sun, S.S., & Nesbitt, R.W., 1978. Petrogenesis of Archaean Ultrabasic and Basic Volcanics: Evidence From Rare Earth Elements; Contributions to Mineralogy and Petrology, v. 65, p. 301-325.

Tomlinson, K.Y., Davis, D.W., Percival, J.A., Hughes, D.J., Thurston, P.C., 2002. Mafic to felsic magmatism and crustal recycling in the Obonga Lake greenstone belt, western Superior Province: evidence from geochemistry, Nd isotopes and U-Pb geochronology; Precambrian Research, v. 114, p. 295-325.

Tomlinson, K.Y., Hughes, D.J., Thurston, P.C., Hall, R.P., 1999. Plume magmatism and crustal growth at 2.9 to 3.0 Ga in the Steep Rock and Lumby Lake area, Western Superior Province; Lithos, v. 46, p. 103-136.

van Westrenen, W., Blundy, J.D., Wood, B. J., 2001. High field strength element/rare earth element fractionation during partial melting in the presence of garnet: Implications for identification of mantle heterogeneities; Geochemistry Geophysics Geosystems, v. 2.

Viljoen, M.J., & Viljoen, R.P., 1969. The geology and geochemistry of the lower ultramafic unit of the Onverwacht Group and a proposed new class of igneous rocks; Geological Society of South Africa, Special Publication, v. 21, p. 55-85.

Viljoen, M.J., Viljoen, R.P., Smith, H.S., Erlank, A.J., 1983. Geological, textural and geochemical features of komatiitic flows from the Komati Formation; Geological Society of South Africa, Special Publication, v. 9, p. 1-20.

Vuorinen, J.H., and Hålenius, U., 2005. Nb-, Zr- and LREE-rich titantite from the Alnö alkaline complex: crystal chemistry and its importance as a petrogenetic indicators; Lithos, v. 83, p. 128-142.

Wagner, T.P. & Grove, T.L., 1997. Experimental constraints on the origin of lunar high-Ti ultramafic glasses; Geochimica et Cosmochimica Acta, v.61, p. 1315-1327. Weaver, B.L., 1991. The origin of ocean island basalt end-member compositions: trace element and isotopic constraints; Earth and Planetary Science Letters, v. 104, p. 381-397.

Weaver, B.L., 1991. The origin of ocean island basalt end-member compositions: trace element and isotopic constraints; Earth and Planetary Science Letters, v. 104, p. 381-397.

White, W.M., 2010. Oceanic island baslats and mantle plumes: The geochemical perspective; Annual Review Earth and Planetary Science, v. 38, p. 133-160.

Winchester, J.A., & Floyd, P.A., 1976. Geochemical magma type discrimination application to altered and metamorphosed basic igneous rocks; Earth and Planetary Science Letters, v. 28, [. 459-469.

Wood, D.,A., Joron, J.L., and Treuil, M., 1979. A re-appraisal of the use of trace elements to classify and discriminate between magma series erupted in different tectonic settings; Earth and Planetary Science Letters, v. 45, p. 326-336.

Xie, Q., Kerrich, R., and Fan, J., 1993. HFSE/REE fractionations recorded in three komatiite-basalt sequences, Archean Abitibi greenstone belt: Implications for multiple plume sources and depths; Geochimica et Cosmochimica Acta, v. 57, p. 4111-4118.

Young, M.D., Sandeman, H., Berniolles, F., and Gertzbein, P.M., 2004. A preliminary stratigraphic and structural geology framework for the Archean Mary River Group, northern Baffin Island (NTS 37G), Nunavut; Geological Survey of Canada, Current Research 2004-C1, 14 p.

Appendix 1. Samples of volcanic rocks

Sample Number	Latitude	Longitude	Lithology	Use
09SRB-R098B-2	66.394	-62.493	Volcanic Rock	g/c & t/s
09SRB-R098B-3	66.394	-62.493	Volcanic Rock	g/c & t/s
09SRB-M105A-1	66.394	-62.495	Volcanic Rock	g/c & t/s
09SRB-R097E-1	66.394	-62.491	Volcanic Rock	g/c & t/s
09SRB-R097C	66.394	-62.491	Volcanic Rock	g/c & t/s
09SRB-R097C-1	66.394	-62.491	Volcanic Rock	g/c & t/s
09SRB-R097C2	66.394	-62.491	Volcanic Rock	g/c & t/s
10SRB-R221	66.393	-62.467	Volcanic Rock	g/c & t/s
09SRB-R098B-4	66.394	-62.493	Volcanic Rock	g/c & t/s
09SRB-R098B-5	66.394	-62.493	Volcanic Rock	g/c & t/s
09SRB-M105A-2	66.394	-62.495	Volcanic Rock	g/c & t/s
09SRB-R097F-4	66.394	-62.491	Volcanic Rock	g/c & t/s
09SRB-R097F1-0	66.394	-62.491	Volcanic Rock	g/c & t/s
09SRB-R097F1-1	66.394	-62.491	Volcanic Rock	g/c & t/s
09SRB-H68A3	66.053	-63.361	Volcanic Rock	g/c & t/s
10SRB-G52B	66.055	-63.345	Volcanic Rock	g/c & t/s
10SRB-G52A	66.055	-63.345	Volcanic Rock	g/c & t/s
10SRB-M273C-1	66.245	-62.901	Volcanic Rock	g/c & t/s
09SRB-C119A	66.237	-62.853	Volcanic Rock	g/c & t/s
09SRB-T75D1	66.220	-62.867	Volcanic Rock	g/c & t/s
09SRB-C118A	66.218	-62.861	Volcanic Rock	g/c & t/s
10SRB-Y218B	66.383	-62.769	Volcanic Rock	g/c & t/s
10SRB-Y218A	66.383	-62.769	Volcanic Rock	g/c & t/s
10SRB-Y218C	66.383	-62.769	Volcanic Rock	g/c & t/s
10SRB-G101A-1	66.458	-62.624	Volcanic Rock	g/c & t/s
10SRB-R303G-1	66.481	-62.638	Volcanic Rock	g/c & t/s
10SRB-Y222	66.431	-62.675	Volcanic Rock	g/c & t/s
10SRB-R186C	66.480	-62.098	Volcanic Rock	g/c & t/s
10SRB-Y188B	66.499	-62.032	Volcanic Rock	g/c & t/s
10SRB-H270C	66.590	-61.944	Volcanic Rock	g/c & t/s
10SRB-H271	66.590	-61.928	Volcanic Rock	g/c & t/s
10SRB-R275A	66.588	-61.899	Volcanic Rock	g/c & t/s
10SRB-R275D	66.588	-61.899	Volcanic Rock	g/c & t/s
10SRB-H272A	66.587	-61.893	Volcanic Rock	g/c & t/s
10SRB-H242	66.613	-61.873	Volcanic Rock	g/c & t/s
10SRB-R181E2	66.710	-62.114	Volcanic Rock	g/c & t/s
10SRB-R162	66.585	-61.427	Volcanic Rock	g/c & t/s
10SRB-Y227B	66.773	-61.724	Volcanic Rock	g/c & t/s
10SRB-Y227A	66.773	-61.724	Volcanic Rock	g/c & t/s

Appendix 1 cont. Samples of volcanic rocks

10SRB-R284B	66.745	-63.281	Volcanic Rock	g/c & t/s
10SRB-Y205	66.647	-62.763	Volcanic Rock	g/c & t/s
10SRB-H320	66.579	-61.366	Volcanic Rock	g/c & t/s
10SRB-Y221A	66.330	-62.202	Volcanic Rock	t/s
10SRB-H316	66.286	-62.362	Volcanic Rock	t/s
10SRB-R190A	66.456	-62.115	Volcanic Rock	t/s
10SRB-Y189A	66.246	-62.022	Volcanic Rock	t/s
10SRB-R190B2	66.456	-62.115	Volcanic Rock	t/s
10SRB-R249A	66.391	-62.492	Volcanic Rock	t/s
10SRB-R303C-1	66.481	-62.638	Volcanic Rock	t/s
10SRB-R275C	66.588	-61.899	Volcanic Rock	t/s
10SRB-R193	66.230	-62.905	Volcanic Rock	t/s
10SRB-R200B	66.055	-63.347	Volcanic Rock	t/s
10SRB-R305B-2	66.455	-62.619	Volcanic Rock	t/s
09SRB-Y55C	66.109	-63.120	Volcanic Rock	t/s
09SRB-R81A4	65.878	-63.909	Volcanic Rock	t/s
10SRB-R275B	66.588	-61.899	Volcanic Rock	t/s
10SRB-M273C-2	66.245	-62.901	Volcanic Rock	t/s
10SRB-R226	66.394	-62.476	Volcanic Rock	t/s
10SRB-R231	66.392	-62.499	Volcanic Rock	h/s
10SRB-R197A1	66.220	-62.865	Volcanic Rock	h/s
10SRB-R198A	66.218	-62.860	Volcanic Rock	h/s
10SRB-R198B	66.218	-62.860	Volcanic Rock	h/s
09SRB-M112A	66.066	-63.270	Volcanic Rock	h/s
09SRB-M112B	66.066	-63.270	Volcanic Rock	h/s
09SRB-R096C	66.058	-63.254	Volcanic Rock	h/s
09SRB-R97D	66.394	-62.491	Volcanic Rock	h/s
10SRB-R248	66.393	-62.493	Volcanic Rock	h/s
10SRB-R198C	66.218	-62.860	Volcanic Rock	h/s
10SRB-R190B1	66.456	-62.115	Volcanic Rock	h/s
10SRB-R222B	66.394	-62.469	Volcanic Rock	h/s
g/c, geochemistry; t/s, thin section; h/s, hand sample				

Appendix 2. Samples of sedimentary rocks

Sample Number	Latitude	Longitude	Lithology	Use
10SRB-R192B	66.453	-62.114	Clastic Sedimentary Rock	h/s
10SRB-R192C	66.453	-62.114	Clastic Sedimentary Rock	h/s
10SRB-R218	66.393	-62.469	Clastic Sedimentary Rock	h/s
10SRB-R224	66.394	-62.475	Clastic Sedimentary Rock	h/s
10SRB-R232	66.394	-62.499	Clastic Sedimentary Rock	h/s
10SRB-R240B	66.395	-62.498	Clastic Sedimentary Rock	h/s
10SRB-R245	66.396	-62.510	Clastic Sedimentary Rock	h/s
10SRB-R249C	66.391	-62.492	Clastic Sedimentary Rock	t/s
10SRB-R235	66.394	-62.489	Clastic Sedimentary Rock	t/s
10SRB-R240	66.395	-62.498	Clastic Sedimentary Rock	t/s
10SRB-R222A	66.394	-62.469	Clastic Sedimentary Rock	t/s
10SRB-R225	66.394	-62.475	Clastic Sedimentary Rock	t/s
09SRB-M117B	66.394	-62.496	Clastic Sedimentary Rock	t/s
10SRB-R236	66.395	-62.487	Clastic Sedimentary Rock	g/c & t/s
10SRB-R215B	66.389	-62.483	Clastic Sedimentary Rock	g/c & t/s
10SRB-R188	66.456	-62.117	Chemical Sedimentary Rock	g/c & t/s
10SRB-R216	66.390	-62.476	Chemical Sedimentary Rock	g/c & t/s
10SRB-R192A	66.453	-62.114	Chemical Sedimentary Rock	g/c & t/s
09SRB-Y76A	66.391	-62.471	Chemical Sedimentary Rock	g/c & t/s
10SRB-R201A-1	66.053	-63.346	Chemical Sedimentary Rock	g/c & t/s
10SRB-R203	66.395	-62.521	Chemical Sedimentary Rock	g/c & t/s
10SRB-R202B-4	66.397	-62.525	Chemical Sedimentary Rock	g/c & t/s
10SRB-R206	66.394	-62.515	Chemical Sedimentary Rock	g/c & t/s
10SRB-R191	66.453	-62.115	Chemical Sedimentary Rock	g/c & t/s
10SRB-R303E	66.481	-62.638	Chemical Sedimentary Rock	g/c & t/s
10SRB-R249B	66.391	-62.492	Chemical Sedimentary Rock	g/c & t/s
10SRB-R250	66.390	-62.486	Chemical Sedimentary Rock	g/c & t/s
10SRB-R201A-2	66.053	-63.346	Chemical Sedimentary Rock	g/c & t/s

Appendix 2 cont. Samples of sedimentary rocks

10SRB-R241	66.394	-62.501	Chemical Sedimentary Rock	t/s
10SRB-R202B-1	66.397	-62.525	Chemical Sedimentary Rock	t/s
10SRB-R217	66.393	-62.472	Chemical Sedimentary Rock	t/s
10SRB-R202B-3	66.397	-62.525	Chemical Sedimentary Rock	t/s
10SRB-R254	66.391	-62.484	Chemical Sedimentary Rock	t/s
10SRB-Y206	66.246	-62.896	Chemical Sedimentary Rock	t/s
09SRB-Y103B-2	66.393	-62.504	Chemical Sedimentary Rock	t/s
10SRB-R196A	66.220	-62.867	Chemical Sedimentary Rock	t/s
10SRB-R219	66.392	-62.467	Chemical Sedimentary Rock	t/s
09SRB-T11B	65.574	-64.324	Chemical Sedimentary Rock	t/s
09SRB-T75A	66.220	-62.867	Chemical Sedimentary Rock	t/s
10SRB-R189A-2	66.456	-62.117	Chemical Sedimentary Rock	t/s
09SRB-Y16B	65.766	-64.760	Chemical Sedimentary Rock	t/s
10SRB-H170	66.819	-63.883	Chemical Sedimentary Rock	t/s
10SRB-G101D	66.458	-62.624	Chemical Sedimentary Rock	t/s
10SRB-M176B	66.383	-61.530	Chemical Sedimentary Rock	h/s
10SRB-R202B-2	66.397	-62.525	Chemical Sedimentary Rock	h/s
10SRB-R215A	66.389	-62.483	Chemical Sedimentary Rock	h/s
10SRB-H275C	66.703	-63.957	Chemical Sedimentary Rock	h/s
10SRB-H172A	66.818	-63.215	Chemical Sedimentary Rock	h/s
10SRB-R149B	66.922	-62.759	Chemical Sedimentary Rock	h/s
10SRB-H171E	66.816	-63.212	Chemical Sedimentary Rock	h/s
10SRB-H282B	66.926	-62.142	Chemical Sedimentary Rock	h/s
10SRB-C186A	66.708	-63.593	Chemical Sedimentary Rock	h/s
10SRB-H316D	66.286	-62.362	Chemical Sedimentary Rock	h/s
10SRB-R189B	66.456	-62.117	Chemical Sedimentary Rock	h/s
10SRB-H282A	66.926	-62.142	Chemical Sedimentary Rock	h/s
10SRB-Y174C	66.527	-62.971	Chemical Sedimentary Rock	h/s
g/c, geochemistry; t/s, thin section; h/s, hand sample				